



**Università
di Genova**



Integrata

DEPARTMENT OF EXPERIMENTAL MEDICINE

PhD COURSE IN EXPERIMENTAL MEDICINE

Curriculum of Biochemistry

**SIRTUIN 2 AND SIRTUIN 6 MODULATORS
AS CANCER THERAPEUTICS**

Candidate

Elena Abbotto

Tutor

Prof. Santina Bruzzone

PhD Program Coordinator

Prof. Ernesto Fedele

Academic Year 2021-2022

XXXIV Cycle

TABLE OF CONTENTS

ABSTRACT.....	5
LIST OF ABBREVIATIONS.....	7
INTRODUCTION.....	12
1. Sirtuins.....	12
2. Sirtuins and pharmacological approaches: SIRT-2 and SIRT-6 modulators.....	16
2.1 Sirtuin 2 modulators and their application in cancer.....	16
2.2 Sirtuin 6 modulators and their application in cancer.....	18
2.3 Methods to identify novel sirtuin modulators.....	21
2.3.1 Computer-aided drug design.....	21
2.3.2 The HPLC-based enzymatic assay.....	23
3. Skin, cutaneous squamous cell carcinoma and sirtuins.....	24
3.1 Skin anatomy and keratinocyte differentiation in healthy human skin.....	24
3.2 Skin cancers and cSCC.....	26
3.2.1 Overview of skin cancers and cSCC.....	26
3.2.2 Molecular markers of cSCC.....	27
3.2.3 cSCC in animal studies: the two-stage skin carcinogenesis mouse model..	28
4. Sirtuins in skin and skin cancer.....	30
4.1 Sirtuins in cSCC.....	32
4.2 Sirtuin 6 overview and its role in cSCC.....	33
5. Microemulsions for topical application.....	38
5.1 Topical drug administration.....	38
5.2 Colloidal systems, emulsions and microemulsions for topical use.....	39
5.2.1 Colloidal systems for topical use.....	39
5.2.2 Emulsions, microemulsions and nanoemulsions for topical use.....	41
5.3 Microemulsions as carriers for lipophilic drugs.....	43
SUMMARY of the undertaken TASKS to reach our AIMS.....	44
1. Development of HPLC-based methods to identify SIRTs modulators.....	44
2. Discovery of novel sirtuin inhibitors.....	44
3. Development of a stable O/W ME containing SIRT-6 modulators for topical application.....	44
4. <i>In vivo</i> evaluation of SIRT-6 pharmacological modulation in a skin cancer mouse model.....	44
5. Is SIRT-2 involved in cSCC?.....	45
RESULTS AND DISCUSSION.....	46
1. Development of HPLC-based methods to identify SIRTs modulators.....	46

2.	Discovery of novel sirtuin inhibitors.....	47
	Investigation of novel SIRT-6 inhibitors.....	47
	Discovery of novel SIRT-2 inhibitors.....	53
3.	Development of a stable O/W ME containing SIRT-6 modulators for topical application.....	57
4.	Skin cancer progression delayed by a SIRT-6 inhibitor in an <i>in vivo</i> cSCC mouse model.....	60
5.	Is SIRT-2 involved in cSCC?.....	67
	CONCLUSIONS.....	69
	MATERIALS AND METHODS.....	71
	MATERIALS.....	71
	<i>Preparation of the compounds.</i>	71
	<i>SIRT-1, -2, -6 fluorescent and chemiluminescent kit.</i>	72
	<i>Reagents for peptide synthesis.</i>	72
	<i>Reagents for enzymatic reactions.</i>	72
	<i>Reagents for MDL-800 synthesis.</i>	72
	<i>Reagents for the preparation of the formulations.</i>	72
	<i>Cell culture material.</i>	72
	<i>Materials for viral transfection.</i>	72
	<i>Animals.</i>	73
	<i>Materials for the skin carcinogenesis protocol and for the topical treatments.</i>	73
	<i>Materials for protein extraction from cells.</i>	73
	<i>Materials for mRNA extraction from skin tissues, retro transcription, and RT-PCR.</i> ..	73
	<i>mRNA and tissue lysates of DS at different stages of skin carcinogenesis.</i>	73
	<i>Antibodies for Western Blot and for Immunofluorescence.</i>	73
	<i>Oligonucleotides used for RT-PCR.</i>	74
	METHODS.....	74
	<i>CADD for SIRT-6 inhibitor identification.</i>	74
	<i>CADD for SIRT-2 inhibitors identification.</i>	75
	<i>Drug profile prediction of the putative SIRT-6 inhibitors.</i>	75
	<i>H3K9Ac and H3K9Palm peptide synthesis.</i>	76
	<i>Recombinant SIRT-6 synthesis.</i>	76
	<i>Screening of different reaction conditions to evaluate the deacetylation of SIRT -2.</i>	76
	<i>Screening of different reaction conditions to evaluate the deacetylation of SIRT -1 and -3.</i>	76
	<i>Reaction conditions to assay SIRT-6 depalmitoylation.</i>	77
	<i>Screening of different SIRT-6 activators to assay SIRT-6 deacetylation.</i>	77

<i>Screening of different HPLC settings to evaluate the deacetylation/deacylation of sirtuins.</i>	78
<i>Screening of different protocols to block the enzymatic reactions in the HPLC-based assay.</i>	78
<i>Stability studies of the peptides H3K9, H3K9Ac and H3K9Palm in the quenching solvent.</i>	79
<i>Screening of putative sirtuins' modulators by HPLC-based enzymatic assays.</i>	79
<i>Determination of the IC₅₀ of the SIRT-2 inhibitors by HPLC-based enzymatic assay.</i>	80
<i>MDL-800 chemical synthesis.</i>	80
<i>Evaluation of solubility properties of S6 and MDL-800.</i>	81
<i>Preparation of lipogels.</i>	81
<i>Preparation of O/W emulsions and MEs.</i>	82
<i>Stability studies of lipogels.</i>	83
<i>Stability studies of emulsions and MEs.</i>	83
<i>Plan of the dose of S6 and MDL-800 to apply in the in vivo studies.</i>	83
<i>Preparation of ME-25 loaded with S6 or MDL-800 or vehicle.</i>	83
<i>Stability studies of drug-loaded MEs.</i>	84
<i>Preparation of bulk quantities of drug-loaded MEs.</i>	84
<i>Cell culture.</i>	85
<i>Constructs and viral infection: SIRT-6 silencing in SCC13 cells.</i>	85
<i>Cell viability assay.</i>	85
<i>Co-treatment of SCC13 with sirtuins' modulators and 5-FU or Celecoxib.</i>	85
<i>Cell treatment with the sirtuins' modulators for WB analyses.</i>	86
<i>Cutaneous chemical carcinogenesis and topical treatment with MEs.</i>	86
<i>Animal sacrifice and tissue collection.</i>	87
<i>Animal study approval.</i>	87
<i>Protein extraction from cells or DS tissues.</i>	87
<i>Western Blot analysis.</i>	88
<i>mRNA extraction from DS tissues and real-time PCR.</i>	88
<i>Histology and Immunostaining of DS tissues.</i>	88
ACKNOWLEDGMENTS	89
REFERENCES	90

ABSTRACT

Sirtuins (SIRT) are a family of 7 NAD⁺-dependant enzymes with a deacetylase, deacylase and/or ADP-ribosyl transferase activity. They are involved in several physiological and pathological processes, including metabolism, inflammation and cancer. SIRT-2 and SIRT-6 have been linked to carcinogenesis either as tumour promoters or suppressors and their pharmacological modulation can be considered a promising strategy to modify cancer initiation and progression. Known SIRT-2 and SIRT-6 inhibitors face several issues, such as water solubility and selectivity for the intended sirtuin over the other isoforms. Therefore, it is still crucial to seek novel SIRT-2 and SIRT-6 inhibitors, that are potent and selective.

In cancer, sirtuins often possess a dual function in tumorigenesis, behaving as oncopromoter or oncosuppressor, depending on the sirtuin and on the cancer type. In cutaneous squamous cell carcinoma (cSCC), both SIRT-2 and SIRT-6 present a controversial role. Further work therefore is still needed to clarify their functions in this type of cancer.

The main goals of my PhD work were:

- The discovery of novel SIRT-2 and SIRT-6 inhibitors;
- The comparison of the pharmacological effects of the inhibition and activation of SIRT-6 in a skin cancer mouse model.

In this thesis, the following stages of the PhD research are described: the development of an HPLC-based method for the evaluation of the enzymatic activity of different sirtuins; the screening of compounds for the discovery of novel SIRT-2 and SIRT-6 inhibitors, and the evaluation of their biological effects on recombinant sirtuins, and subsequently on SCC cells; the development of a stable formulation containing a SIRT-6 inhibitor or a SIRT-6 activator for topical use; the evaluation of the effects of SIRT-6 pharmacological modulation by topical application in a 2-step carcinogenesis mouse model.

Our results indicate that thiazoles, pyrazolopyrimidines and benzimidazoles represent good scaffolds for the development of SIRT-2 inhibitors, with the discovery of several SIRT-2 and dual SIRT-1/SIRT-2 inhibitors. A selection of these compounds had also a cytotoxic effect on cSCC cells, with minor effects on healthy keratinocytes, hinting the oncogenic role of SIRT-2 in this type of cancer.

In addition, few compounds with a quinazoline-2,4(1H,3H)-dione structure were identified as novel SIRT-6 inhibitors. These proved to be cell-membrane permeable and induced keratinocyte differentiation in cSCC cells, reproducing the pro-differentiating effects of SIRT-6 silencing on keratinocytes, observed by Lefort and colleagues.

Last, by inhibiting pharmacologically SIRT-6 in a 7,12-dimethylbenz[*a*]anthracene (DMBA) - 12-*O*-tetradecanoylphorbol-13-acetate (TPA) induced skin cancer mouse model, skin cancer progression was delayed. In particular, by applying topically a SIRT-6 inhibitor (compound 2,4-Dioxo-N-(4-(pyridin-3-yloxy)phenyl)-1,2,3,4-tetrahydroquinazoline-6-sulfonamide, renamed in this thesis "S6") with a preventive approach at the promotion stage, epithelial-mesenchymal transition (EMT), and thus carcinogenesis, resulted less advanced compared to untreated mice.

LIST OF ABBREVIATIONS

2-OAADPr	2-O-acetyl/acyl-ADP-ribose
3D	Three-dimensional
5-FU	5-Fluorouracil
aa	Amino acids
Ac	Acetyl
AcCN	Acetonitrile
ACECS	Acetyl-CoA synthetase, cytoplasmic
ACLY	ATP citrate lyase
AcOH	Acetic acid
AD	Alzheimer's disease
ADME	Absorption-distribution-metabolism-excretion
ALS	Amyotrophic lateral sclerosis
AK	Actinic Keratosis
AKT	Protein kinase B
AML	Acute myeloid leukaemia
AMPK	Adenosine monophosphate-activated protein kinase
APC/C	Anaphase-promoting complex/cyclosome
API	Active pharmaceutical ingredient
ATG	Autophagy protein
BCC	Basal cell carcinoma
BPE	Bovine pituitary extract
BSA	Bovine serum albumin
BUBR1	BUB1-related kinase
CADD	Computer aided drug design
CD	Clusters of differentiation
CD44ICD	Intra-cytoplasmic domain of CD44
CDC20	Cell division cycle 20
CDK9	Cyclin-dependent kinase 9
CDKN1A	Cyclin dependent kinase inhibitor 1A
cDNA	Complementary DNA
circRNA	Circular RNA
cKO	Conditional knock out
CNS	Central nervous system
CPS1	Carbamoyl-phosphate synthase 1
CRC	Colorectal cancer
CRCT	Cysteine-rich carboxy-terminal
CREB	Cyclic AMP-responsive element-binding
COX-2	Cyclooxygenase-2
CSC	Cancer stem cell
cSCC	Cutaneous squamous cell carcinoma
CUL4B	Cullin 4B
CYPD	Cyclophilin D
DCAF1	DDB1- and CUL4-associated factor 1
DDB1	DNA damage-binding protein 1
DLBCL	Diffuse large B cell lymphoma
DMBA	7,12-dimethylbenz[<i>a</i>]anthracene
DMSO	Dimethyl sulfoxide

DNA-PK	DNA-dependent protein kinase
DS	Dorsal skin
EC ₅₀	Half maximal effective concentration
ECL	Enhanced chemiluminescence
ECM	Extracellular matrix
EGF 1-53	Epidermal growth factor 1-53
EMA	European medicines agency
EMT	Epithelial–mesenchymal transition
eNOS	Endothelial nitric oxide synthase
ESR	Early-stage researcher
EtOH	Ethanol
FA	Fatty acid
FDA	Food and drug administration
FoA	Formic Acid
FLG	Filaggrin
FLR	Fluorescence
FOX	Forkhead box
FXR	Farnesoid X receptor
FU	Farmacopea Ufficiale
G3BP	RasGAP SH3 domain-binding protein
G6PD	Glucose-6-phosphate 1-dehydrogenase
GABPβ1	GA-binding protein subunit β1
GAPDH	Glyceraldehyde-3-phosphate dehydrogenase
GCN5	General control nonrepressed protein 5
GDH	Glutamate dehydrogenase
GLUT1	Glucose transporter 1
GOT2	Glutamate oxaloacetate transaminase 2
GSH	Glutathione
GSSG	Glutathione disulfide
H&E	Haematoxylin and Eosin
H ₂ O	Water
H1K	Histone 1 Lysine
H3	Histone 3
H3K	Histone 3 Lysine
H4K	Histone 4 Lysine
HCl	Hydrochloric acid
HD	Huntington's disease
HDAC	Histone deacetylase
hERG	Human Ether-à-go-go-Related Gene
HIA	Human intestinal absorption
HIF	Hypoxia-inducible factor
HMGCS2	3-hydroxy-3-methylglutaryl-CoA synthase 2
HNF4α	Hepatocyte nuclear factor 4α
HNSCC	Head and neck squamous cell carcinoma
HPLC	High performance liquid chromatography
IC ₅₀	Half maximal inhibitory concentration
IDE	Insulin-degrading enzyme
IDH2	Isocitrate dehydrogenase 2
IGF-1	insulin-like growth factor 1
INV	Involucrin

IPM	Isopropyl myristate
ITPK1	Inositol-tetrakisphosphate 1-kinase
KAP1	Kruppel-associated box-associated protein-1
KRT	Keratin
LBDD	Ligand-based drug design
LC3-II	LC3-phosphatidylethanolamine conjugate
LCAD	Long-chain-specific acyl-CoA dehydrogenase
LDH	Lactate dehydrogenase
LKB1	Liver kinase B1
LXR	Liver X receptor
LOR	Loricrin
MA	Myristic acid
MCD	Malonyl-CoA decarboxylase
ME	Microemulsion
MeOH	Methanol
MgCl ₂	Magnesium chloride
miRNA	Micro RNA
MM	Multiple myeloma
MMP	Matrix metalloproteinases
MRPL10	Mitochondrial ribosomal protein L10
MS	Multiple sclerosis
MYBBP1A	MYB-binding protein 1a
MYC	Myelocytomatosis
MYOD	Myoblast determination protein
MW	Molecular weight
NAD ⁺	Nicotinamide adenine dinucleotide
NAM	Nicotinamide
NBS1	Nijmegen breakage syndrome 1
ND	Neurodegenerative disease
NDUFA9	NADH dehydrogenase (ubiquinone) 1 α subcomplex subunit 9
NE	Nanoemulsion
NF- κ B	Nuclear factor- κ B
NHEK	Normal human epidermal keratinocytes
NHLH2	Nescient helix-loop-helix 2
NKX2-1	NK2 homeobox 1
NMSC	Nonmelanoma skin cancer
NSCL	Non-small cell lung
O/N	Overnight
O/W	Oil-in-water
O:W	Oil-Water
OPA1	Optic atrophy 1
OTC	Ornithine carbamoyltransferase
P-gp	permeability glycoprotein
PA	Palmitic acid
PAF53	RNA Pol I-associated factor 53
Palm	Palmitic
PAR3	Partitioning defective 3 homologue
PARP	Poly-ADP-ribose polymerase
PBS	Phosphate-buffered saline
PCAF	P300/CBP-associated factor

PD	Parkinson's disease
PDAC	Pancreatic ductal adenocarcinoma
PDH	Pyruvate dehydrogenase
PDP1	PDH phosphatase 1
PDT	Photo dynamic therapy
PEG	Polyethylene glycol
PEPCK1	Phosphoenolpyruvate carboxykinase 1
PGAM	Phosphoglycerate mutase
PGC1 α	PPAR γ co-activator 1 α
PKC	Protein kinase C
PMSF	Phenylmethylsulfonyl fluoride
POL I	Polymerase I
PPAR	Peroxisome proliferator-activated receptor
PPB	Plasma protein binding
PPP	Pentose phosphate pathway
PRLR	Prolactin receptor
PTM	Post-translational modification
PTP1B	Protein-tyrosine phosphatase 1B
RAR β	Retinoic acid receptor- β
ROS	Reactive oxygen species
RB	Retinoblastoma
RT	Room temperature
RT-PCR	Real-time PCR
S6K1	S6 kinase 1
SAR	Structure-activity relationship
SBDD	Structure-based drug design
SCC	Squamous cell carcinoma
SDH	Succinate dehydrogenase
Sir2	Silence information regulator 2
SIRT	Sirtuin (the protein)
Sirt	Sirtuin (the gene)
SKP2	S-phase kinase-associated protein 2
SLC25A5	Solute carrier family 25 member 5
SNF2H	Sucrose nonfermenting 2 homolog
SOD	Superoxide dismutase
SRB	Sulphorhodamine
SREBP	Sterol regulatory element-binding protein
STAT3	Signal transducer and activator of transcription 3
SUV39H1	Suppressor of variegation 3–9 homologue 1
T2D	Type 2 diabetes
TBS	Tris-buffered saline
TFA	Trifluoroacetic acid
TFAM	Transcription factor A, mitochondrial
TFIIIC2	General transcription factor IIIC polypeptide 2
TG1	Transglutaminase 1
TNF	Tumour necrosis factor
TOPBP1	DNA topoisomerase 2-binding protein 1
TPA	12- <i>O</i> -tetradecanoylphorbol-13-acetate
TSC2	Tuberous sclerosis 2
UCP2	Mitochondrial uncoupling protein 2

USP10	Ubiquitin-specific processing protease 10
UV	Ultraviolet
UVR	Ultraviolet radiation
V	Volume
VLCAD	Very long-chain-specific acyl-CoA dehydrogenase
VS	Virtual screening
W/O	Water-in-oil
WB	Western blot
WRN	Werner syndrome ATP-dependent helicase
WT	Wild type
XPA	Xeroderma pigmentosum complementation group A

INTRODUCTION

1. Sirtuins

Sirtuins (SIRT) are a family of evolutionary conserved enzymes that depend on nicotinamide adenine dinucleotide (NAD⁺) (1) and are homologues of the Silence information regulator 2 (Sir2) enzyme, thus being known also as Sir2-like proteins (2). In mammals the 7 known sirtuins, named SIRT-1 to SIRT-7, are classified as class III histone deacetylases (HDACs) (3, 4). Their substrates however have been reported to be also non-histone proteins, such as cytoskeletal proteins, signalling molecules, transcription factors, chaperones, p53 and DNA repair proteins (Table 2) (5). Sirtuins, moreover, possess often other enzymatic activities apart from the deacetylation one, such as deacylation and mono-ADP-ribosylation (Figure 2 and Table 1) (6). Each sirtuin has a particular preference for one activity over the others, as well as for specific substrates. In particular, SIRT-1, -2 and -3 are strong deacetylases and also deacylases; SIRT-6 displays a weak deacetylase activity and a strong deacylase one; SIRT-4 and SIRT-5 possess strong lipoamidase and desuccinylase activity, respectively; and SIRT-7, which is less characterized than the other sirtuins, is known to be a weak deacetylase (7). The ADP-ribosylation activity of all sirtuins, instead, has been less investigated, having been reported so far solely for SIRT-4 and SIRT-6 (8) (9, 10). Structurally, the 7 isoforms share a central catalytic domain of about 270 amino acids, where a Rossmann fold and a smaller domain with the NAD⁺-binding module and a zinc-binding one, create the enzymatic active site; the 7 sirtuins then differ in the N-terminal and C-terminal domains (Figure 1) (11). The crystal structures of the 7 sirtuins chosen on the basis of resolution values (< 2.00 Å) are represented in Figure 1.

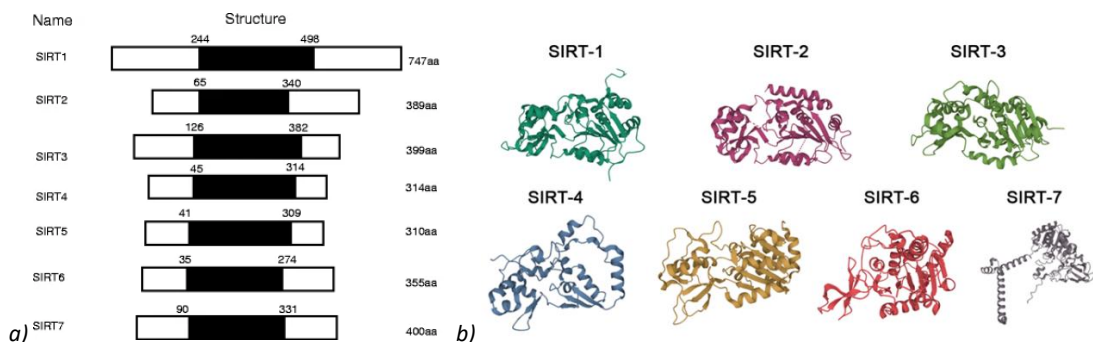


Figure 1. a) Schematic representation of the 7 human sirtuins, with catalytic core domain in black and N and C terminus in white. Abbreviation: aa, amino acids. Figure is adapted from (12). b) Crystal structures of the 7 human sirtuins. The PDB identifiers are 4KXQ, 4Y6O, 4BN4, 6LJK, 6HOY, for SIRT-1, SIRT-2, SIRT-3, SIRT-5 and SIRT-6, respectively. SIRT-4 and SIRT-7 AlphaFold-predicted structures AF-A0A347ZJG7-F1 and AF-Q9NRC8-F1 respectively, are reported in the figure, since no crystal structures are currently known for these two isoforms.

Sirtuins are characterized by diverse subcellular localizations (13), unique substrate specificity (5), distinct enzymatic activities (5) and different tissue abundance (14), and this confers to each isoform specific functions (Table 1 and Table 2).

SIRT-1 is the best characterized isoform of the sirtuin class of enzymes: it is located in the nucleus and it regulates gene stability, stress response and apoptosis (15-17). SIRT-2 is localized in the cytoplasm, although it can shuttle to the nucleus to participate to several physiological and pathological functions (18). It plays a role in several processes, including cell cycle regulation and metabolism (19, 20). SIRT-3 is located in the mitochondria and has been shown to act on several metabolic and respiratory enzymes regulating their functions

(21). In addition, SIRT-3 can regulate the production and clearance of reactive oxygen species (ROS), by deacetylating numerous mitochondrial enzymes (22-24). SIRT-4 is located in the mitochondrial matrix, where it controls several pathways by modifying the activation status of different proteins (25). SIRT-5 is located in the mitochondria as well, and controls several physiological pathways, including the promotion of ammonia detoxification, fatty acid β -oxidation and ketone body production and the regulation of energy production (26). SIRT-6 is a nuclear sirtuin and its role in the regulation of different processes is being increasingly recognized, covering many different functions, including energy metabolism derived both from glucose and lipids, DNA repair, aging, inflammation and immunity (27). SIRT-7 is localized in the nucleus, where it is involved in the activity of RNA polymerase I and it is important for cell viability (28, 29). Very few reports are available for this sirtuin. The interest in SIRT-7 has increased in the last decade, but research still needs to be accomplished to understand its role in the aetiology of pathologies.

Table 1. Cellular localizations of the 7 sirtuins and overview of the tissues in which they are highly expressed (13).

Sirtuin	Cellular localization	High expression tissues
SIRT-1	Nucleus, Cytoplasm (less abundant)	Brain, skeletal muscle, heart, kidney and uterus
SIRT-2	Cytoplasm, Nucleus (less abundant)	Brain
SIRT-3	Mitochondria	Brain, heart, liver, kidney and brown adipose tissue
SIRT-4	Mitochondria	Pancreatic β -cells, brain, liver, kidney, heart
SIRT-5	Mitochondria	Brain, testis, heart, muscle, lymphoblast
SIRT-6	Nucleus	Muscle, brain, heart, ovary and bone cells
SIRT-7	Nucleus (nucleolus)	Peripheral blood cells

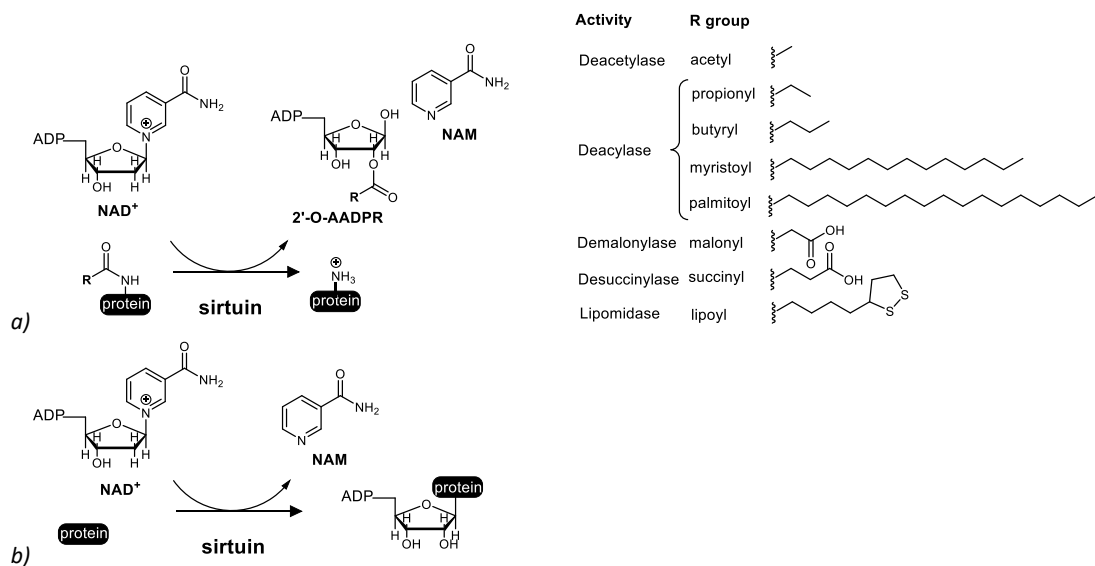


Figure 2. Schematic representation of the NAD^+ -dependent reactions of sirtuins. a) The R group of the post-translational modification (PTM) present on the substrate determines the enzymatic activity of the sirtuin. In the figure the R groups that define the deacetylase, deacylase, demalonylase, desuccinylase or lipoamidase activity are depicted. SIRTs use NAD^+ as a substrate to remove acetyl/acyl groups from a target protein, yielding the deacetylated/deacylated substrate, nicotinamide (NAM) and 2'-O-acetyl/acyl-ADP ribose (2-OAADPr). b) In the mono-ADP-ribosyl transferase activity, the NAD^+ ADP ribose moiety is added to the protein and NAM and the ADP-ribosylated substrate are released.

Table 2. Enzymatic activities, preferred substrates and main functions of the 7 sirtuins (7-10, 27, 30-32). Table adapted from (5).

Sirtuin	Enzymatic activity	Substrates and/or targets	Functions
SIRT-1	Deacetylase, Deacylase	H3K9, H3K56, H4K16, H1K26, SUV39H1, p300, PCAF	Chromatin regulation and transcription
		HDAC1, PARP1, p53, KU70, NBS1, E2F1, RB, XPA, WRN, survivin, β -catenin, MYC, NF- κ B, TOPBP1	DNA repair and cell survival
		PGC1 α , FOXO1, FOXO3A, FOXA2, CRCT1, CRCT2, PPAR α , PPAR γ , LXR, FXR, RAR β , SREBP1C, SREBP2, HNF4 α , HIF1 α , HIF2 α , CREB, NKX2-1, STAT3, TFAM, MYOD, NHLH2, UCP2, TSC2, eNOS, LKB1, SMAD7, AKT, ATG5, ATG7, ATG8, 14-3-3 ζ , PGAM1, ACECS1, PTP1B, S6K1	Metabolism
SIRT-2	Deacetylase, Deacylase	In cytoplasm: Tubulin, keratin 8, PAR3, PRLR	Differentiation
		In cytoplasm: G6PD, LDH, PEPCK1, ACLY, MEK1, ITPK1, S6K1, PGAM	Metabolism
		In nucleus: FOXO1, FOXO3A, p300, NF- κ B, HIF1 α	
SIRT-3	Deacetylase, Deacylase	LCAD, VLCAD, HMGCS2, NDUFA9, SKP2, SDHA, ACECS2, GDH, IDH2, MRPL10, PDP1, SOD2, OTC, CYPD, OPA1, PDH, FOXO3 and GOT2	Metabolism
		SIRT-4	Mono-ADP-ribosyl transferase, Lipoamidase
SIRT-5	Desuccinylase, Demalonylase	CPS1, HMGCS2, PDH, SDH, SOD1, GAPDH	Metabolism
SIRT-6	Deacetylase, Deacylase, Mono-ADP-ribosyl transferase	H3K9, H3K56, GCN5, SNF2H, G3BP, FOXO3, PARP1, KAP1, H3K18, H3K27	Chromatin and DNA repair
		MYC, HIF1 α , NF- κ B, TNF, SREBP1, SREBP2, USP10	Metabolism
SIRT-7	Deacetylase	MYC, H3K18, PAF53, HIF1 α , HIF2 α , ELK4, RNA Pol I, MYBBP1A, TFIIC2, p53	Transcription
		mTOR, DCAF1, DDB1, CUL4B, GABP β 1	Metabolism

Given their involvement in different biological pathways, ranging from transcription to metabolism, to genome stability (Table 2) (5), their dysregulation is implicated in many diseases, such as cancer, neurodegenerative disorders, diabetes and cardio-vascular and autoimmune diseases (33-37).

In cancer, sirtuins often possess often a dual function in tumorigenesis, behaving as oncopromoter or oncosuppressor, depending on the sirtuin and on the cancer type (Table 3) (38, 39). In addition, often one same sirtuin presents controversial roles within the same cancer type, with independent studies reporting that both activators/overexpression or inhibitors/knock down have both anti-cancer effects (39). On the one hand, the possibility that sirtuins act as tumour suppressors is mainly corroborated by their role in maintaining genome stability through chromatin regulation and DNA repair (39). On the other hand, some sirtuins were found to be overexpressed in certain tumours, and were also shown to promote angiogenesis (39). Moreover, sirtuins affects metabolism, thus acquiring pro-tumorigenic or oncosuppressive functions. For instance, one reason to consider SIRT-6 as an oncosuppressor, is represented by the shift from aerobic respiration to glycolysis observed in SIRT6-deficient cells resembling the Warburg effect, typical of cancer cells (39). However, the number of pathways affected by the different sirtuins is so wide, that in different cancer

context the final outcome of sirtuins' contribution can be dual (39). Of note, changes in sirtuins expression are often a consequence and not a cause of different oncogenic pathways (39).

Sirtuins are also involved in many neurodegenerative diseases (NDs), among which Alzheimer's disease (AD), Parkinson's disease (PD), Huntington's disease (HD), amyotrophic lateral sclerosis (ALS) and multiple sclerosis (MS) are the most common. The 7 sirtuins do not possess the same function in neuro-degenerative diseases, with some that are downregulated and others that are upregulated in disease progression (37).

Table 3. Overview of the role of the 7 sirtuins in different cancer types. Abbreviations: TS, tumour suppressor. TP, tumour promotor. The expression of different SIRTs in skin cancers is further described in Introduction, paragraph 4. Table adapted from (5, 44).

Cancer type\Sirtuin	SIRT-1	SIRT-2	SIRT-3	SIRT-4	SIRT-5	SIRT-6	SIRT-7
Breast cancer	TS	TS	-	TS	-	TP	-
Liver cancer	TS/ TP	TS	TS	-	-	TS	-
Glioblastoma	TS	TS	TS	-	-	-	-
Bladder carcinoma	TS	-	-	-	-	-	-
Prostate cancer	TS	TS	TS	-	-	TP	TP
Ovarian cancer	TS	-	TS	-	-	TS	TP
Colon cancer	TS/TP	-	-	-	-	TS	TP
Oral squamous cell carcinoma	TS	-	TP	-	-	-	-
Thyroid cancer	TP	-	-	-	-	-	-
Leukaemia	-	-	-	TS	-	-	-
Acute myeloid leukaemia (AML)	TP	-	-	-	-	-	-
Chronic myeloid leukaemia	TP	-	-	-	-	-	-
Clear-cell renal cell carcinoma	-	TS	TS	-	-	-	-
Anaplastic oligodendroglioma	-	TS	-	-	-	-	-
Medulloblastoma	-	-	TS	-	-	-	-
Lung cancer	-	-	TS	TS	-	TP/TS	-
Non-small cell lung cancer (NSCLC)	-	-	-	-	TP	-	-
Testicular cancer	-	-	TS	-	-	-	-
Head and neck squamous cell cancer (HNSCC)	-	-	TS	-	-	-	-
Pancreatic cancer	-	-	TS	-	-	TS	-
Brain cancer	-	-	TP	-	-	-	-
Gastric cancer	-	-	-	TS	-	-	-
Bladder cancer	-	-	-	TS	-	-	-
Uterine cancer	-	-	-	-	-	-	TP
Kidney cancer	-	-	-	-	-	-	TP

In type 2 diabetes (T2D) some studies have been carried in the past decades to define the role of SIRTs (34). Briefly, SIRT-1 regulates glucose/lipid metabolism; in particular, among other T2D-related mechanisms, it positively regulates insulin secretion and protects pancreatic β -cells from oxidative stress and inflammation (40). Conversely, the function of SIRT-2 in insulin signalling is still controversial, with some studies reporting that its overexpression improves insulin sensitivity, and with others demonstrating the opposite (41). SIRT-6 was reported to be involved in several metabolic pathways, by negatively regulating glucose uptake, and therefore by repressing hypoxia inducible factor-1 α (HIF- 1 α) (42, 43).

2. Sirtuins and pharmacological approaches: SIRT-2 and SIRT-6 modulators

It is widely accepted that pharmacological modulation of the enzymatic activity of sirtuins is a promising strategy to modify disease initiation and/or progression. The most studied SIRTs in cancer are SIRT-1, -2, -3 and -6, with modulators that either exhibit an anti-proliferative effect, induce apoptosis, or sensitize cancer cells to existing chemotherapeutics *in vitro*, or that block tumour growth *in vivo* (45). In neurodegenerative diseases, sirtuins' modulators proved to be effective in reducing the symptoms and in some cases also in preventing neurodegeneration progression (AD, PD, ALS) or inflammatory relapses (MS) (45). NDs are characterized by neuronal cell death, which leads to progressive loss of mobility, coordination, sensation and memory, and current treatments aim solely to relief physical or mental symptoms, since no cures have been discovered yet (46). SIRT-1 and -2 (with some research done also on SIRT-3 and -6) represent the most investigated SIRTs in NDs under a pharmacological perspective (45). Regarding T2D, less studies involving SIRTs modulators have been performed; studies in *in vitro* and *in vivo* settings demonstrated the effectiveness of treatments with SIRT-1 and SIRT-3 activators, or SIRT-2 and SIRT-6 inhibitors, in modulating blood glucose levels in high-fat fed mice (SIRT-1 activator) (47, 48), in improving blood glucose tolerance and insulin resistance in diabetic mice or adipocytes (SIRT-1 and SIRT-3 activator) (49), in improving insulin sensitivity in skeletal muscle cells (SIRT-2 inhibitor) (50, 51), in increasing glucose uptake in cellular studies (SIRT-6 inhibitor) (52) and in improving glucose tolerance and reducing plasma levels of insulin, triglycerides, and cholesterol in T2D murine models (SIRT-6 inhibitor) (53).

In the past decades, extensive research has been done on SIRT-1 modulators, while compounds targeting the other sirtuins have been less studied or faced issues like reduced isoform selectivity, poor water solubility or limited cell membrane permeability.

Of the different enzymatic activities displayed by sirtuins, deacetylation has regularly been the preferred one in the discovery of novel modulators. Therefore, in this thesis, unless specified otherwise, the inhibition or activation of sirtuins will be considered regarding this activity.

2.1 Sirtuin 2 modulators and their application in cancer

SIRT-2 activators have never been discovered, while many inhibitors have been identified in the past years. In many types of cancer, SIRT-2 acts as a tumour promotor and therefore its inhibition may be beneficial. Often SIRT-2 inhibitors act as anti-proliferative agents or display a cytotoxic effect, being this sirtuin involved in cell cycle regulation, and in particular in the G(2)/M transition (20). Nevertheless, in some other cancers, it was shown that SIRT-2 possesses tumour suppressor functions, which however were not further investigated pharmacologically, since no SIRT-2 activators are currently available. In Table 4 a selection of SIRT-2 inhibitors that have been reported with therapeutic effects in *in vitro* and *in vivo* cancer studies is summarized. Isoform selectivity is often a critical feature in SIRT-2 inhibitor discovery, since the crystal structure of this sirtuin resembles particularly the one of SIRT-1 (54). The most selective SIRT-2 inhibitors of Table 4 are AGK2, AK7, NH4-13, NPD11033, AF8, AC-93253, SirReal2, TM and RK-9123016.

Table 4. Overview of selection of SIRT-2 inhibitors: their inhibitory potency towards SIRT-2 and other SIRTs, and their biological effects in cancer studies.

Compound	SIRT-2 IC ₅₀	SIRT-1 IC ₅₀	SIRT-3 IC ₅₀	SIRT-5 IC ₅₀	SIRT-6 IC ₅₀	Biological effects in cancer
AGK2	3.5 μM (58)	30 μM (59)	91 μM (59)	-	-	Anti-proliferative effect on glioma cancer cells (61) and stem cells (62); and blockage of tumour growth in <i>in vivo</i> colorectal cancer mouse models (63)
AK7	15.5 μM (64)	>20 μM	>50 μM	-	-	Reduction of tumour growth on a glioma <i>in vivo</i> mouse model (61)
SirReal2	0.23 μM (56)	>50 μM	>50 μM	-	-	Anti-proliferative effect in lymphoma, colorectal, lung, breast and cervical cancer cells; and blockage of tumour growth in <i>in vivo</i> gastric cancer mouse models (56)
AC-93253	6 μM (65)	7.5-fold less inhibition than SIRT-2	4-fold less inhibition than SIRT-2	-	-	Anti-proliferative effect and downregulation of the c-Myc and N-Myc oncoproteins in neuroblastoma and in pancreatic cancer (66); cytotoxic effect on prostate and lung cancer cells and on pancreatic cancer cells, by triggering apoptosis (65)
NH4-13	87 nM (50)	>50 μM	>50 μM	>50 μM	>50 μM	Anti-proliferative effect on pancreatic, lung, breast and cervical cancer cells; and blockage of tumour growth in <i>in vivo</i> colorectal cancer mouse models (50)
NPD11033	0.46 μM (67)	>100 μM	>100 μM	-	-	Anti-proliferative effect on pancreatic cancer cells (67)
AF8	0.06 μM (68)	11 μM	>50 μM	-	-	Anti-proliferative effect on pancreatic and breast cancer cells; and blockage of tumour growth in <i>in vivo</i> colorectal cancer mouse models (68)
TM	0.4 μM (69)	650-fold less inhibition than SIRT-2	650-fold less inhibition than SIRT-2	-	-	Anti-proliferative effect on colorectal and leukemic cancer cells and promotion of ubiquitination and degradation of c-Myc oncoprotein in different cancer cell lines; and blockage of tumour growth in <i>in vivo</i> breast cancer mouse models (69)
Compounds 6f	3.7 μM (70)	>200 μM	>200 μM	-	-	Anti-proliferative effect on lung and breast cancer cells (70)
Compound 12a	12.2 μM (70)	>200 μM	>200 μM	-	-	Anti-proliferative effect on lung and breast cancer cells (70)
Compound 35	10.4 μM (71)	>100 μM	>100 μM	-	-	Anti-proliferative effect on lymphoma, NSCL, leukemic and breast cancer cells and induced apoptosis in leukemic and breast cancer cells (71)
Compound 39	1.5 μM (71)	>100 μM	>100 μM	-	-	Anti-proliferative effect on lymphoma, NSCL, leukemic and breast cancer cells and induction of apoptosis in leukemic and breast cancer cells (71)

RK-9123016	0.18 μM (55)	> 100 μM	> 100 μM	-	-	Anti-proliferative effect on breast cancer cells, accompanied by a decrease in c-Myc expression (72)
Compound 24a	0.815 μM (73)	-	-	-	-	Anti-proliferative effect on lung cancer cells (73)
γ-mangostin	3.8 μM (74)	22 μM	26 μM	-	-	Anti-proliferative effect on breast cancer cells (74)
Tenovin-D3	21.8 μM (75)	> 90 μM	-	-	-	Anti-proliferative effect on breast cancer cells and promotion of expression of the cell-cycle regulator and p53 target p21WAF1/CIP1 (CDKN1A) in a p53-independent manner (75)
NCO-90	1 μM (76)	> 300 μM	-	-	-	Anti-proliferative effect and induction of apoptosis and autophagy in leukemic cell lines (76)
NCO-141	0.5 μM (76)	> 300 μM	-	-	-	Anti-proliferative effect and induction of apoptosis and autophagy in leukemic cell lines (76)
Salermide	25 μM (77)	43 μM	-	-	-	Anti-proliferative effect and downregulation of the c-Myc and N-Myc oncoproteins in neuroblastoma and in pancreatic cancer (66)

Two inhibitors to be mentioned, since they have been extensively used in the past years by different research groups in cancer as well as in neurodegenerative disease's studies, are AGK2 and SirReal2 (Figure 3) (55-57). AGK2 which was identified from a screening of 200 compounds (58), inhibits SIRT-2 with an IC_{50} of 3.5 μM , SIRT-1 and -3 with IC_{50} of 30 and 91 μM , respectively (59), whereas SirReal2, which was identified through an *in vitro* compound screening of an in-house developed library (60), displays an IC_{50} 0.23 μM for SIRT-2, and above 50 μM for SIRT-1 and -3 (56). Although these compounds are potent inhibitors and are also the most selective ones for SIRT-2, their poor water solubility prevents them from being considered promising drug candidates. Indeed, they are insoluble both in water and in ethanol, and their DMSO solubility upon heating is 10 mg/mL (23 mM) and 84 mg/mL (200 mM), respectively for AGK2 and SirReal2.

For this reason, it is still crucial to seek novel SIRT-2 inhibitors, that are potent, selective and water soluble. In this thesis, the discovery of novel structures as SIRT-2 inhibitors is described in Results and Discussion, paragraph 2.

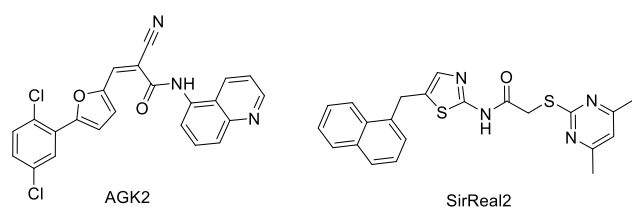


Figure 3. Chemical structures of SIRT-2 inhibitors AGK2 and SirReal2.

2.2 Sirtuin 6 modulators and their application in cancer

Depending on the cancer type, and even on the cancer stage, SIRT-6 has been reported to act as an oncopromoter or an oncosuppressor (78). These studies have been performed by

overexpressing or silencing SIRT-6 expression and, depending on the obtained results, inhibitors or activators have been evoked as promising strategies. In the past decades several SIRT-6 inhibitors have been discovered, but far less activators have been identified. An overview of SIRT-6 modulators that display biological effects in cancer is reported in Table 5 and Table 6. The most common anti-cancer mechanisms of SIRT-6 activators and inhibitors include the blockage of cell proliferation in cellular studies and of tumour growth in animal studies, and the sensitization of cancer cells to existing chemotherapeutics.

SIRT-6 activators

Of the SIRT-6 activators discovered to date, several studies indicate that fatty acids (FAs) containing 14 to 18 carbons, which are endogenous molecules in mice and humans, stimulate SIRT-6 activity. Specifically, FAs, including myristic, oleic, and linoleic acids, increase SIRT-6 catalytic efficiency at physiological concentrations (EC_{50} ranging from 90 μ M to 246 μ M) (7). The most characterised SIRT-6 activators, instead, belong to the MDL family of compounds, that feature a N-phenyl-4-(phenylsulfonamido) benzenesulfonamide structure. MDL-800 (Figure 4), identified through means of Virtual Screening (VS), potently activates SIRT-6 with an EC_{50} of 10 μ M, showing no activity towards all the other sirtuins and HDAC1-11 at concentrations up to 50 or 100 μ M, and targeting SIRT-6 via an allosteric mechanism beyond known substrate sites (Figure 4) (79). Successively, the same research group discovered MDL-811, which displays improved activity (EC_{50} of 5.7 μ M) and bioavailability in mice, without affecting the activity of all the other sirtuins and of HDAC1-11 at concentrations up to 100 μ M (80). MDL-800, being the first cellular active SIRT-6 activator discovered, has been widely exploited by several research groups in different pathological and physiological processes, such as cancer (79, 81), wound healing (82), hepatic injuries (83), heart failure associated to diabetes (84), ageing (85) and renal inflammation and fibrosis (86). From a physicochemical point of view, however, this compound is highly hydrophobic, it is not water soluble, and its DMSO solubility upon heating is 62.6 mg/mL (100 mM), hence researchers face several issues in animal administration or in cellular treatments.

SIRT-6 inhibitors

Two classes of SIRT-6 inhibitors have been quite studied over the years by different research groups: the quinazolinones, such as Compound 5 (Figure 4) (52), and some salicylate-like structures, such as Compound 9 (52) (Table 6). These were first identified along with other SIRT-6 inhibitors in a structure-based screening performed on the CoCoCo database (90) using SIRT-6 crystallographic structure (PDB code = 3K35) (91) (52). They were further optimised by performing different sub-structure searches in the CoCoCo database (90), with the aim of retaining a core structure of the hit compound, but improving isoform selectivity and inhibition potency. More potent analogues were indeed discovered (e.g., Compound 3 (92), and Compound 11 (93)) and two libraries, one of quinazolinones and one of salicylate-like compounds, were created. In particular, the salicylate-like molecules display inhibitory potency in the low μ M range, and a 10-to-30-fold selectivity for SIRT-6 against SIRT-1 and -2 (93). As to the quinazolinone inhibitors, several potent and selective inhibitors were identified with this structure (e.g., Compound 3, (92)). However, the best inhibitor remains the reference structure, Compound 5 (2,4-Dioxo-N-(4-(pyridin-3-yloxy)phenyl)-1,2,3,4-tetrahydroquinazoline-6-sulfonamide) (52), which has an IC_{50} of 106 μ M, and shows poor selectivity for SIRT-6 over SIRT-1 and -2 (92). Since it does not to exert cytotoxic effects

in cellular and animal studies, and since it always elicited a biological response, proving itself better than the other quinazolinones as a consequence (92), it has been tested for the treatment of cancer (92), MS (94), skeletal muscle atrophy (95) and T2D (96). Its mechanism of action is competitive inhibition, since it binds to SIRT-6 in the NAM pocket (Figure 4) (92). This compound is not water soluble and its DMSO solubility is 20.5 mg/mL (50mM). Since Compound 5 will be further discussed in this thesis, with the aim of easing the reading, it will be renamed here “S6”.

Table 5. Overview of a selection of SIRT-6 activators: their potency in enhancing SIRT-6 and other SIRTs deacetylase activity, and their biological effects in cancer studies. To be noted that myristic, oleic and linoleic acids have been included in the list, since they are endogenous activators in mammals, though no biological studies have been performed with them yet.

Compound	SIRT-6 EC ₅₀	SIRT-1 EC ₅₀	SIRT-2 EC ₅₀	SIRT-3 EC ₅₀	SIRT-4 EC ₅₀	SIRT-5 EC ₅₀	SIRT-7 EC ₅₀	Biological effects in cancer
UBCS 039	38 μM	>100 μM	>100 μM	>100 μM	-	100 μM	-	Induction of a time-dependent activation of autophagy in NSCL, cell lung, colon, epithelial cervix carcinoma, and fibrosarcoma tumour cells (87, 88)
MDL-800	10.3 μM (79)	>100 μM	10-fold less activated than SIRT-6	>100 μM	>100 μM	10-fold less activated than SIRT-6	10-fold less activated than SIRT-6	Anti-proliferative effect in hepatic cancer cells and suppression of tumour growth in a mouse model (79) Anti-proliferative effect in NSCL cancer cells (81)
MDL-811	5.7 μM (80)	>100 μM	>100 μM	>100 μM	>100 μM	>100 μM	>100 μM	Anti-proliferative effect on colorectal cancer cells and blockage of tumour growth in patient-derived xenografts and in a spontaneous CRC mouse model (80)
Compound 12q	5.35 μM (89)	171 μM	>200 μM	>200 μM	-	>200 μM	-	Anti-proliferative effect and inhibition of migration of PDAC cells and suppression of tumour growth in a tumour xenograft model (89)
Myristic acid	246 μM (7)	>100 μM	-	-	-	-	-	-
Oleic acid	90 μM (7)	>100 μM	-	-	-	-	-	-
Linoleic acid	100 μM (7)	>100 μM	-	-	-	-	-	-

Table 6. Overview of selection of SIRT-6 inhibitors: their potency of inhibition of SIRT-6 and of other SIRTs, and their biological effects in cancer studies.

Compound	SIRT-6 IC ₅₀	SIRT-1 IC ₅₀	SIRT-2 IC ₅₀	Biological effects in cancer
Compound 5 (renamed "S6")	106 μM (52)	314 μM	114 μM	Sensitization of pancreatic cancer cells to PARP inhibitor Olaparib (92)
Compound 9	89 μM (52)	1.6 mM	751 μM	Reduction of TNF-α production in PDAC cells (93); sensitization of MM cells to chemotherapeutics (97); Anti-proliferative effect in DLBCL cancer cells; and blockage of tumour growth in mouse xenograft (98)
Compound 3	37 μM (92)	424 μM	85 μM	Sensitization of pancreatic cancer cells to anti-proliferating agent gemcitabine and PARP inhibitor Olaparib ((92)); anti-proliferative effect and sensitization to chemotherapeutics in prostate cancer cells (99)
Compound 11	22 μM (93)	599 μM	482 μM	Reduction of TNF-α production in PDAC cells; sensitization of PDAC cells to gemcitabine; anti-proliferative effect in T lymphocyte (93)

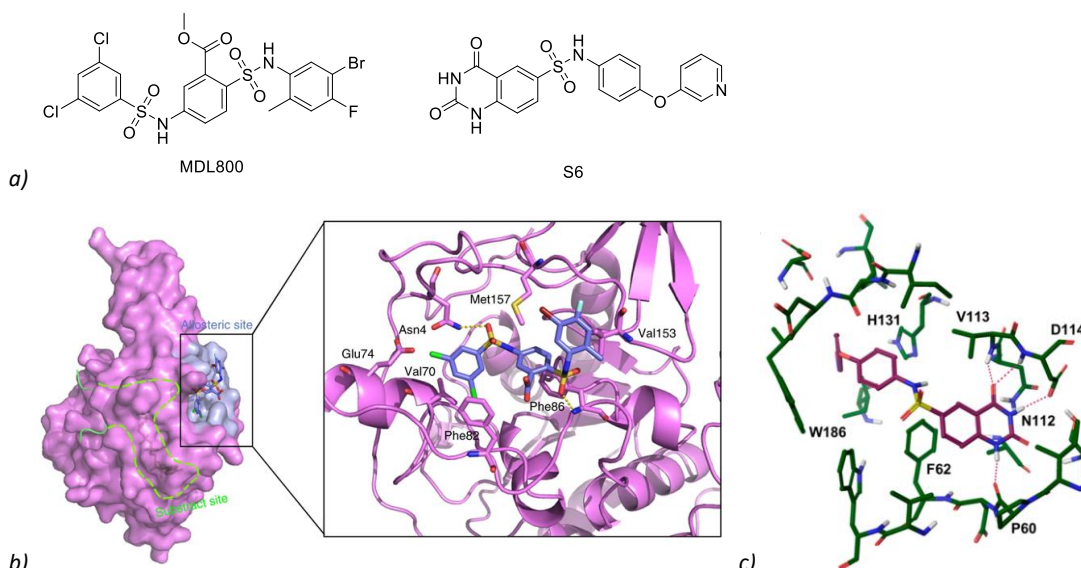


Figure 4. a) Chemical structure of activator MDL-800 and of inhibitor Compound 1, renamed "S6". b) MDL-800 in the allosteric binding pocket of SIRT-6. Figure adapted from (79). c) Pose suggested by the authors: S6 in the NAM pocket of SIRT-6. Figure adapted from (52).

SIRT-6 activators and inhibitors face several issues, from water solubility, to cytotoxicity, to selectivity for SIRT-6 over the other sirtuins. In this thesis, the investigation of S6-like structures as potential novel SIRT-6 inhibitors is described (Results and Discussion, paragraph 2).

2.3 Methods to identify novel sirtuin modulators

2.3.1 Computer-aided drug design

The discovery of inhibitors of an enzyme is often achieved performing first *in silico* analyses, following computational approaches known as computer aided drug design (CADD), then enzymatic activity analyses on recombinant protein, and finally cellular studies.

Through CADD, and in particular by performing virtual screening (VS), it is possible to select among libraries of compounds novel structures that are bioactive with respect to the target

protein, and that are forecasted to possess drug-like physicochemical and pharmacological proprieties (100). This strategy relies on a huge amount of data that needs to be elaborated by qualified personnel using powerful software and expensive computer systems, but it definitely represents the most advantageous way to identify novel bioactive chemical entities.

CADD techniques can be classified in Structure-Based Drug Design (SBDD) and Ligand-Based Drug Design (LBDD). SBDD relies on crystallographic data of the active site of the target protein or of related homologous proteins, that eventually allow the construction of an atomic-resolution model of the target protein. LBDD, instead, is the strategy chosen whenever the protein's 3D structure is not known and it is not possible to obtain it through homology modelling; this technique therefore exploits the knowledge of the chemical structure and of the bioactivity (evaluated via a comparable assay) of all the modulators of the target protein. In a SBDD procedure (Figure 5), in detail, after selecting a library of compounds and choosing the 3D structure (target validation) of the target protein, each compound, called "ligand", is docked within the virtual protein binding site, which means that it is virtually bound to the target protein to form a stable complex, and the preferred poses, which are determined by location, orientation and conformation, are delineated and collected. Furthermore, for each pose, the strength of association or binding affinity between ligand and protein, that is defined by the energy of the bonds, of the interactions (H-bonds, electrostatic, hydrophobic, π/π stacking, and van der Waals interactions), and of the angles, is quantified in a docking score. A stronger binding ligand-protein, which means often a more potent modulator, is associated to a lower docking score. The compounds described by fewer poses and with lower scores are the most promising modulators of the target protein and should be selected at this stage as putative hit compounds for further testing. In the drug discovery process, after assessing the bioactivity of the compounds identified through CADD in *in vitro* studies, their chemical structure is optimized in order to improve inhibitory activity and biological effects. Optimised structures, defined lead compounds, are finally tested *in vivo* (Figure 5).

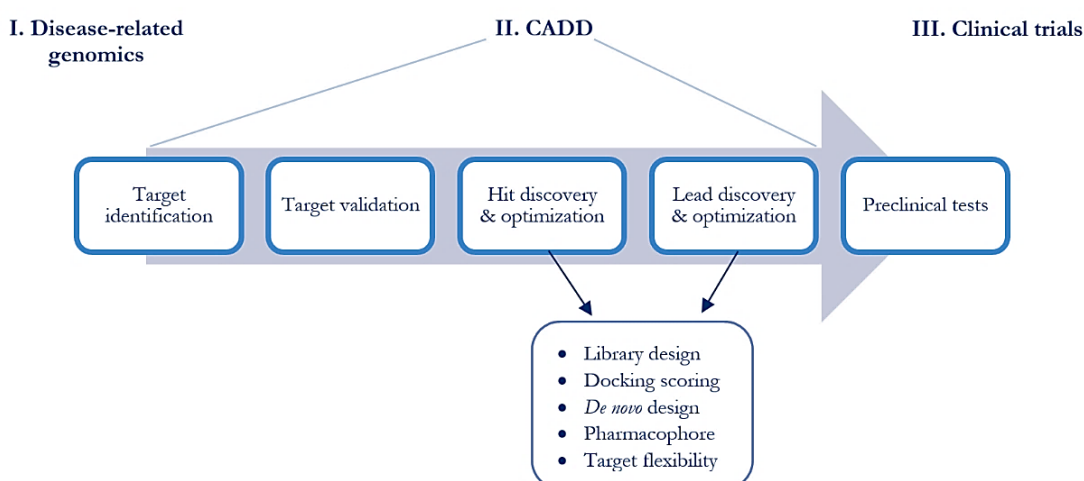


Figure 5. Schematic pipeline of the drug discovery process, with CADD technique described more extensively. Figure adapted from (101).

A review summarising the sirtuin modulators that have been discovered over the years through means of VS and that elicited biological responses in several diseases, sheds light also on the challenges encountered in discovering sirtuin modulators which are selective for one isoform over the others (45). This difficulty arises from the similarity of the crystal structure, and more specifically of the catalytic site, of the 7 sirtuins (11). Many SIRT inhibitors identified in the past decades inhibit with similar potency three or more sirtuin isoforms, being defined therefore as sirtuin pan-inhibitors (45).

In this thesis, a hit-discovery process for the identification of putative SIRT-2 inhibitors and a hit-optimisation one for SIRT-6 inhibitors, is described (Results and Discussion, paragraph 2).

2.3.2 The HPLC-based enzymatic assay

Enzymatic activity of a target protein can be assayed with different techniques. The ones that have been developed in the past decades targeting sirtuins include High performance liquid chromatography (HPLC), Fluorescence Resonance Energy Transfer (FRET) assay and fluorogenic, magnetic beads, *in silico*, and bioaffinity chromatography assays (102). Among these the most used by research groups targeting sirtuins is represented by HPLC. This technique is characterised by unsurpassed precision, specificity, sensitivity, and reproducibility, and it is able to quantify any chemical entity of the enzymatic reaction mixture (e.g., reagents or products), thus giving information of the reaction state (103).

The main steps of an enzymatic activity HPLC assay analysis are the following: after blocking the reaction by removing or denaturing the enzyme, the reaction mixture containing the substrates, the cofactors and the products, called “mobile phase”, is injected into a column, called “solid phase”, which is able to retain different chemical entities at different strengths, according to the physicochemical affinity between them. By quantifying the absorbance of a tracker-molecule (e.g., a reagent or a product) it is possible to fully characterise the enzymatic activity of a target protein and to follow it in real time (Figure 6).

Sirtuins' deacetylase and deacylase reactions (Figure 2) have been often studied over the years with HPLC analyses (104-107). In detail, in the analysis, the recombinant sirtuin is incubated with NAD⁺ and with a peptide resembling the physiological substrate of interest bearing an acetyl or acyl group. Reaction progress can be evaluated by measuring either the amount of product that is formed (e.g., deacetylated/deacylated-peptide), or the one of the substrate (e.g., acetyl/acyl-peptide) that is consumed (Figure 6). Detection and quantification of the tracker-molecule is accomplished by measuring UV absorption at 220, 254 and/or 280 nm (often the peptides are loaded with additional tryptophane to facilitate detection) (107). An HPLC-based enzymatic assay, moreover, allows to characterise the modulation of the enzymatic activity of a target protein by small molecules, such as their activation or inhibition capacity, their selectivity for the intended protein isoform, and their IC₅₀, by comparing the profile of the enzymatic activity in presence and in absence of the molecule. Eventually, these results will allow identifying the best candidates for further biological screening.

In this thesis, the development of an HPLC method to assay the enzymatic activity of several sirtuins and the evaluation of the modulation of their activity by compounds previously identified by VS, are described (Results and Discussion, paragraph 1 and 2).

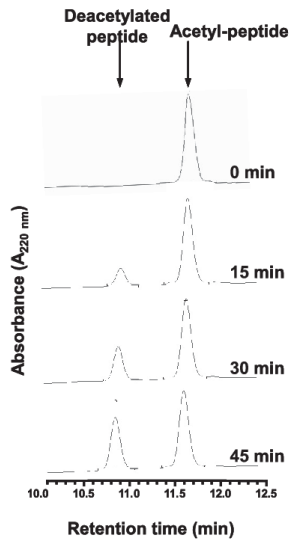


Figure 6. Four HPLC chromatograms in which a SIRT-1 deacetylation reaction mixture is analysed. In an HPLC analysis different chemical entities (e.g., deacetylated and acetylated substrate) are eluted at different retention time (x axis), and can thus be distinguished. The area below each absorbance (y axis) peak represents the amount of that specific entity in the reaction mixture at the time of injection. Over time (0, 15, 30, 45 min), the amount of the deacetylated peptide increases, while the one of the acetylated one decreases. Figure adapted from (107).

3. Skin, cutaneous squamous cell carcinoma and sirtuins

3.1 Skin anatomy and keratinocyte differentiation in healthy human skin

The skin is a large, complex organ with three main functions: protection against microbial, mechanical and thermal injury and hazardous substances, tactile sensation, and regulation body temperature. Normal skin consists of the epidermis, the dermis, the hypodermis, the panniculus carnosus and the adventitia (Figure 7). In the epidermis, keratinocytes, that are the most abundant cell type in the skin, are present in distinct differentiation stages, defining thus functionally distinct keratinocyte populations, which outline four main sublayers. In detail, in the deepest stratum basale (basal layer), keratinocytes are generated from epidermal stem cells and then migrate to the layers above; they continue their differentiation and migration processes first in the subsequent stratum spinosum, then in the stratum granulosum and lucidum, and finally in the stratum corneum, where they undergo cell death in a terminal differentiation stage, called cornification, becoming corneocytes. Eventually, corneocytes of the stratum corneum undergo replacement from new cells that migrate to the upper layer, resulting in desquamation of the upper layer of the epidermis (Figure 7b and c) (108). During the differentiation process, cells face extensive morphological, organellar and molecular alterations as they gradually migrate into the upper layers. Early differentiation, which occurs in the stratum basale, is characterised by high expression of keratin 5 (KRT5) and keratin 14 (KRT14) (109). In the intermediate stage, as keratinocytes reside in the stratum spinosum and granulosum, nucleophagy is initiated, the cells lipid profile faces significant variation, cell membrane is remodelled, keratin filaments and the cornified envelope are formed, and an overall increase in cell stiffness can be observed (110). From a molecular point of view, in the intermediate differentiation processes, a shift in the expression of different proteins occurs: KRT5 and KRT14 levels decrease, while other proteins become more abundant, such as keratin 1 (KRT1) and keratin 10 (KRT10) in the stratum

spinosum, and transglutaminase and late envelope proteins, namely involucrin (INV), filaggrin (FLG), loricrin (LOR), in the stratum granulosum. The switch in expression results largely completed in the stratum lucidum. At last, cornification presents high expression of filaggrin, and completes loss of the nuclei and of cytoplasmic organelles, leading to cell death (109-113).

Within the epidermis, together with keratinocytes other cell types can be found, such as Langerhans cells, which are tissue-resident macrophage of the skin and are located in the stratum spinosum, and melanocytes, that reside in the basal layer and are responsible for the production of melanin, which is a pigment that protects the skin from ultraviolet (UV) radiation.

Below the epidermis is located the dermis, which is composed of fibres, and in which hair follicles, sebaceous glands (oil glands), apocrine glands (scent glands), and eccrine glands (sweat glands), blood vessels and nerves reside. Underlying the dermis, the hypodermis, consists of fat, connective tissue, larger blood vessels, and nerves. Below this, there is first the panniculus carnosus, which is a thin layer of skeletal muscle, and then the adventitia, which is a loose connective tissue layer that connects the skin to the underlying skeletal muscle.

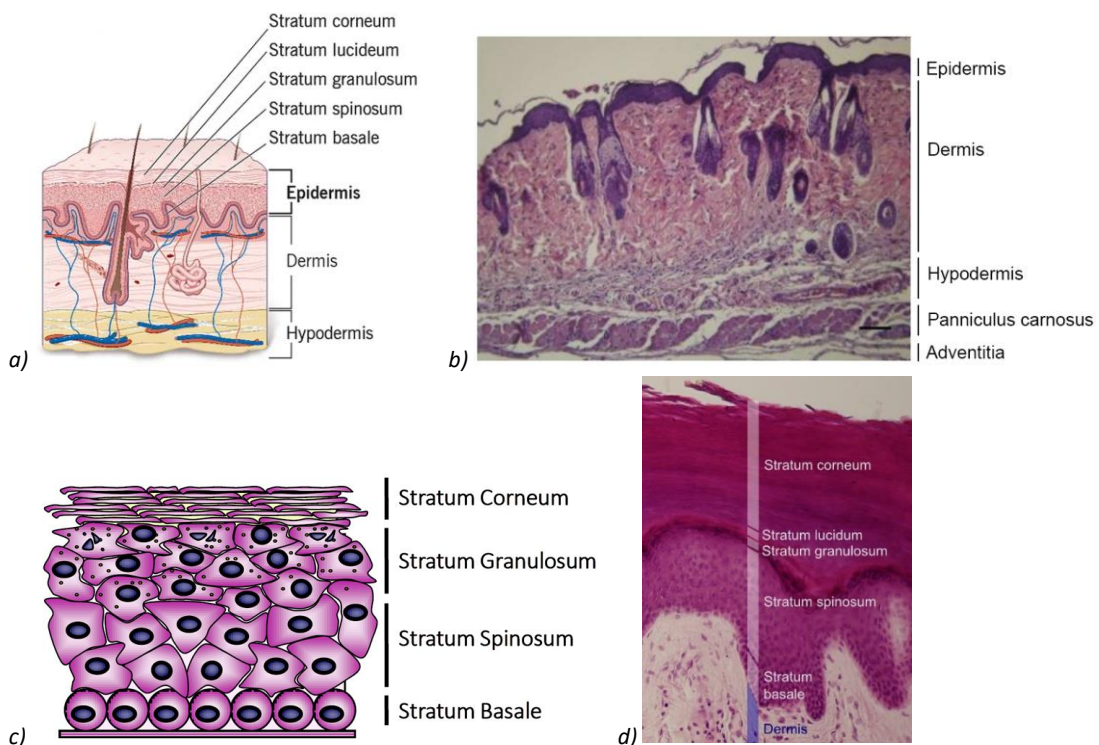


Figure 7. Overview of skin layers. a) Schematic representation of the skin layers hypodermis, dermis and epidermis. In particular, also different sublayers of the epidermis are highlighted. b) Cross-section of murine dorsal skin stained with H&E, depicting all the skin layers: from bottom to top, adventitia, panniculus carnosus, dermis containing hair follicles and glands, hypodermis, and epidermis. Scale bar is 200 μ m. Figure adapted from (114). c) Schematic representation of the epidermis with the morphological alterations that keratinocytes face during migration from the lower to the higher skin layers: from bottom to top, stratum basale, spinosum, granulosum and corneum. d) Cross-section of human skin stained with H&E, depicting all epidermis layers. Figure adapted from wikimedia File:WVSOM_Meissner%27s_corpuslce.JPG.

3.2 Skin cancers and cSCC

3.2.1 Overview of skin cancers and cSCC

Skin cancer represents the most common worldwide cancer, with The World Health Organization estimating more than 1.5 million new cases every year, and 64 000 premature deaths from nonmelanoma and 57 000 melanomas of the skin in the year 2020. The main risk factors promoting skin carcinogenesis include environmental stress, genetic factors and immunosuppression (115). In particular, the main environmental factor causing skin cancers is UV skin damage, which strongly correlates with sun exposure, and is attributed to UVB and UVA radiation. UVB radiation (280–315 nm) is absorbed in the epidermis, where it causes sunburn and DNA damage and where it accelerates the keratinocyte differentiation process (116), while UVA radiation (315–400 nm), being characterised by higher wavelength, penetrates more deeply in the skin and reaches the dermis, where it damages DNA, proteins, lipids and collagen, by inducing ROS generation (Figure 8) (117).

Skin cancer is generally categorised into melanoma and nonmelanoma skin cancer (NMSC), with basal cell carcinoma (BCC) and cutaneous squamous cell carcinoma (cSCC) as the most common NMSC subtypes (118). The classification is based on the cell types from which the tumours originate (Figure 8). Melanomas stem from melanocytes, BCCs from basal cells, namely keratinocytes that reside in the stratum basale, and cSCCs from squamous cells, which are the keratinocytes residing in the stratum spinosum, and that present a scaly cell shape (Figure 7c and d, Figure 8).

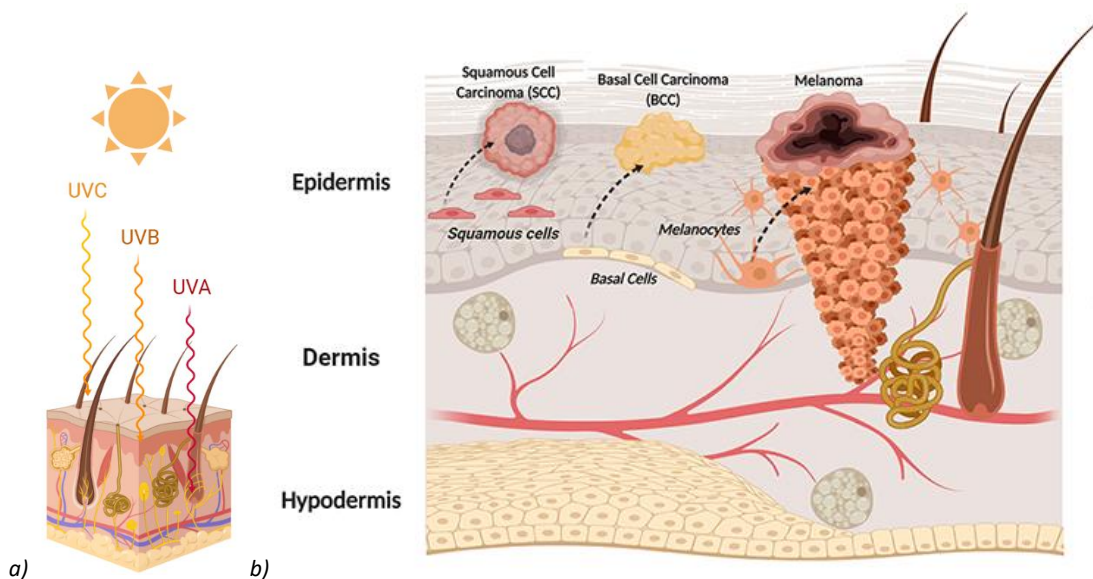


Figure 8. a) Different types of UV radiation penetrating in the skin. Most of the high-energy UVC is absorbed by stratospheric ozone, while UVB is absorbed by the epidermis, and UVA reaches the dermis. b) Schematic representation of cSCC, BCC and melanoma, with squamous cells, basal cells and melanocytes highlighted. Figure adapted from (44).

Cutaneous squamous cell carcinoma is the second most common NMSC. It generally appears as a firm, red nodule, as an open soar or as a flat lesion with a scaly, crusted surface (Figure 9). It arises usually on sun-exposed areas of the body such as the face, ears, neck, lips, and backs of the hands, but it can also develop in scars or chronic skin sores elsewhere, or start in other cancerous skin tissues known as Actinic Keratosis (AK) (119). If untreated, cSCCs can metastasise in liver, lungs and lymph nodes (120). Treatment options for cSCC and AK are surgery, cryotherapy, Photo-Dynamic Therapy (PDT), with surgery being the most common

and effective therapy used (120, 121). For patients with multifocal cSCC, or with weakened immune system, or with the cancer located in specific parts of the body, these cures, however, do not prove always effective, and tumour relapses often occur after the treatments (122). Moreover, a part from creams containing either 5-Fluorouracil (5-FU), the anti-inflammatory drug Celecoxib, or the BCC and AK medication Imiquimod, no other drugs are used to treat topically cSCC or AK (123). Novel and effective medications are therefore needed to treat patients, especially those with skin cancer relapses. cSCC is identified as a squamous cell carcinoma, since it originates in squamous cells. These types of cells are found in several other tissues a part from the skin, such as the passages of the respiratory and digestive tracts, and the lining of the hollow organs of the body. Cancers that arise from them are epidermoid carcinomas and are defined “SCCs”. Examples include bladder, kidney, cervical and anal SCC, head and neck SCC and SCC of the lung, which is a type of non-small cell lung cancer.

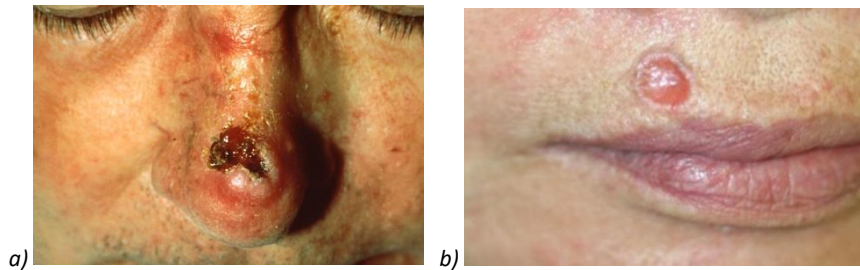


Figure 9. Lesions of cSCC. a) A lesion whose surface appears scaly and ulcerate. Photo taken from the National Cancer Institute, AV-8500-3609. b) A lesion that appears as a red lump. Figure adapted from (124).

3.2.2 Molecular markers of cSCC

In cSCC, from a molecular point of view, an alteration of the expression of several proteins of different layers of the skin can be observed. Keratins, in particular, together with being differentiation markers of normal skin, represent optimal markers for tumour pathology. cSCCs are characterised by abundant expression of keratins that are either involved in keratinocyte hyperproliferation, which is the fundamental pathological condition responsible for cancers, or that are induced upon injury stress or inflammation, or that are simple epithelial keratins; these include keratins 5, 6, 8, 14, 16, 17 and 18 (109). In detail, KRT5 and KRT14 normally reside in the stratum basale, which is the keratinocyte generation layer of the epidermis. KRT6 and KRT16, instead, are often expressed as a keratin pair and characterise epidermal hyperproliferation, which is a process occurring not only in cancer, but also in hyperproliferative epidermal disorder and in skin wound healing. Another keratin overexpressed in cancer and that is induced following skin wounding is KRT17; this resides in the stratum basale along with the aforementioned KRT5 and KRT14, and it is involved in the regeneration and subsequent migration of keratinocytes upon wounds. KRT8 and KRT18, instead, are distributed in normal epithelial tissues, as well as in various mesenchymal tumours, where they are co-expressed with the type III intermediate filaments vimentin and desmin, that are well documented cancer markers (125, 126). Keratins KRT1 and KRT10, being massively involved in keratinocytes' differentiation, can be considered more “keratinisation”- and less tumour- markers, although alteration in their expression can be still observed in cSCCs (109). KRT10, in particular, as it is more abundant in the stratum spinosum where keratinocytes are in a more advanced differentiation stage, specifically induces cell

cycle arrest in keratinocytes and inhibits their proliferation. In cSCC, a decrease in KRT10 expression often accompanies keratinocyte hyperproliferating tumour progression (127). Keratinocyte differentiation and tumour development can be seen therefore as inversely related events (128).

Epithelial tumour progression often involves epithelial-mesenchymal transition (EMT), which is a process normally associated with various non-pathological conditions, such as embryonic development and wound healing, that require a migration and a transient dedifferentiation of epithelial cells, followed by differentiation into specialised cell types. EMT plays a crucial role also in cancer, in particular in cancer cell migration, invasion and metastatic dissemination. EMT can be initiated by various intrinsic signals (e.g., gene mutations) as well extrinsic signals (e.g., growth factor signalling) (129). From a cellular perspective, in EMT, by altering the expression of the adhesive and migratory and thus of the cytoskeletal proteins, epithelial cells lose their epithelial characteristics to be converted into non-polarized, motile and invasive mesenchymal cells. Moreover, extracellular matrix (ECM) components are scattered, forced to migrate or degraded, in order to clear the tumour microenvironment, thus facilitating cell detachment from the primary tumour and invasion in the underlying mesenchyme, such as fibroblasts or vascular endothelial cells, and thereafter also in other tissues. Briefly, epithelial cell-cell adhesion proteins (e.g., E-cadherin), tight junction proteins, desmosomal proteins, and cell polarity proteins are downregulated, whereas cell-cell adhesion mesenchymal proteins (e.g., N-cadherin), other mesenchymal structural proteins, as vimentin and fibronectin, and the enzymes responsible for the degradation of the extracellular matrix, namely the MMPs (matrix metalloproteinases), result overexpressed (130-132). To date, the widest used markers of the EMT, and therefore of invasive and metastasised epithelial cancers, remain vimentin, N-cadherin and E-cadherin. It should be noted that not all tumours disseminate and metastasise following EMT: some undergo a partial or incomplete EMT, while others are involved in alternative mechanisms (133).

3.2.3 cSCC in animal studies: the two-stage skin carcinogenesis mouse model

Research on the mechanisms of epithelial carcinogenesis and on the alteration of physiological factors in cancer initiation, progression and metastasis, can be best accomplished by using a chemically induced skin cancer mouse model. The development of cancer is viewed generally as a multistep process (134, 135), in which a DNA-mutating event affecting stem cells, such as carcinogen exposure (136), is followed first by a long latency, then by cell multiplication and finally by cancer progression (137, 138). The multi-stage cSCC pathology in humans can be well reproduced with a two-stage skin carcinogenesis mouse model, in which tumour initiation occurs after the administration of a single high dose of a carcinogen on the dorsal skin (DS) of the mouse, followed by continuous treatments with inflammation- or tumour- promoting agents. Alternatively, repeated applications of a lower dose of the carcinogen or continuous exposure to ultraviolet (UV) light yields the same tumour development. Moreover, this protocol simulates the exposition to multiple low doses of carcinogens and of promoting agents, that is the main cause of human skin cancers.

In detail, in the two-stage skin carcinogenesis model, three cancer phases can be distinguished: initiation, promotion and progression (Figure 10).

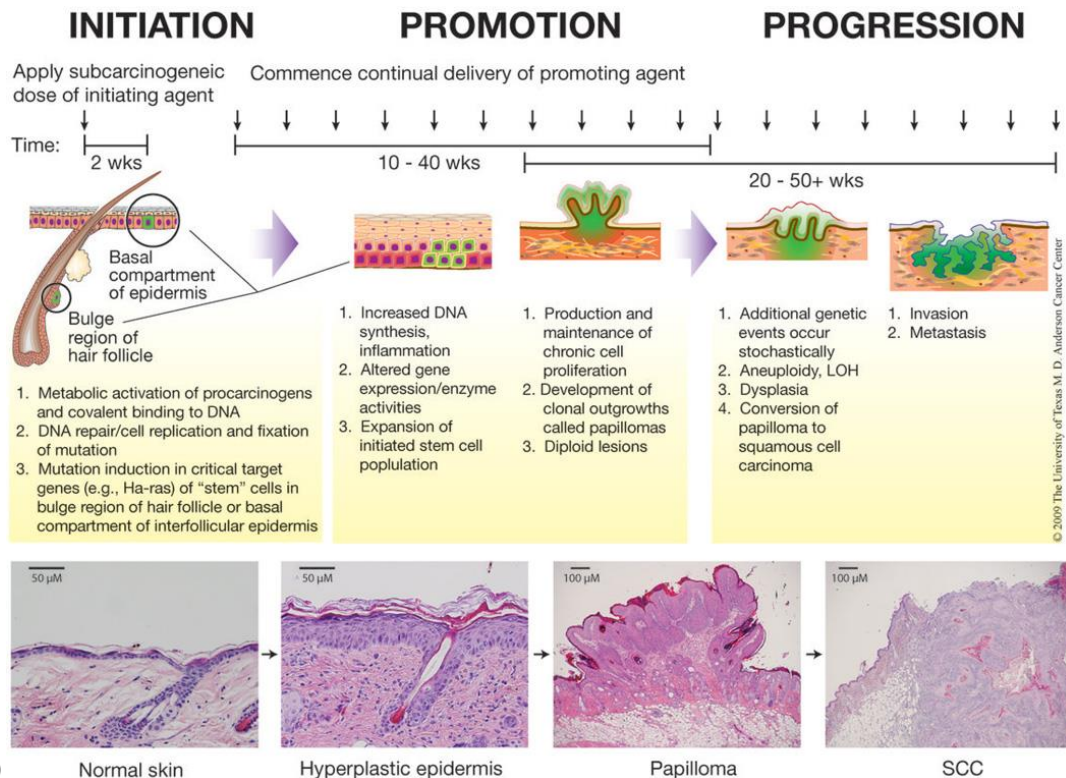
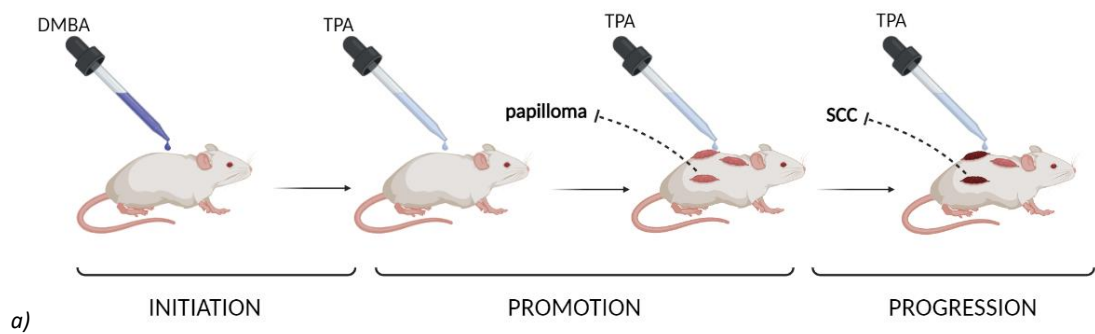


Figure 10. a) DMBA-TPA two-stage skin carcinogenesis protocol in mice: during initiation, a sub-carcinogenic dose of a mutating agent (e.g., DMBA) induces mutations in target genes in keratinocytes; in the promotion step repeated application of a tumour-promoting agent (e.g., TPA) stimulates epidermis hyperplasia, and papillomas begin to arise on the DS of the mouse; in the last stage of the protocol, the progression, papillomas begin to convert to SCCs. b) For each step of the tumorigenesis (normal skin, hyperplastic skin, papilloma, SCC) a representative H&E analysis is depicted. Figure adapted from (157).

Initiation occurs with the topical application of a single sub-carcinogenic dose of a carcinogen such as 7,12-dimethylbenz[*a*]anthracene (DMBA), which mutates key genes in epidermal keratinocytes and in primary keratinocyte stem cells (139-142). These mutations occur often in proto-oncogenes, as for example in Hras1, Kras or Nras, that are then converted to oncogenes, driving thus the tumour formation. In the subsequent promotion stage, mouse DS undergoes prolonged exposure to a tumour growth-promoting agent. One of these agents commonly used is 12-*O*-tetradecanoylphorbol-13-acetate (TPA), whose molecular targets include protein kinase C (PKC) and Wnt/ β -catenin signalling (142). At this stage, enhanced cell signalling, increased DNA synthesis and production of growth factors, induction of a local inflammatory reaction, and proliferation of basal keratinocytes are reported. Mutated cells clonally expand to outgrow neighbouring cells, in a hyperplastic (tissue enlarging) process.

This is evidenced by an overall increase in epidermis thickness (that can be determined in histochemical analyses), and by the development of clonal outgrowths of the skin called papillomas (Figure 10) (143, 144). In the last stage of the DMBA-TPA protocol, called “progression”, papillomas are converted into SCCs, which appear as flattened and growing downward lesions (Figure 10). SCC lesions are invasive and highly vascularised; thus, they tend to metastasise to other organs, especially lungs, liver and lymph nodes. The frequency of progression papilloma-to-SCC depends on the genetic background of the mouse, with some phenotypes being more prone than others to carcinogenesis and cancer progression. The most used mice in this skin cancer protocol are CD-1, SENCAR, and FVB mice (145, 146). The great potential of the two-step carcinogenesis model is evidenced also in the high correspondence of the genetic pattern of the mouse SCC with the one from human SCCs (described in Introduction, paragraph 3.2.2). Briefly, during the papilloma-to-SCC progression, E-cadherin and keratins KRT1 and KRT10 are downregulated, while KRT13 is overexpressed (147-150); KRT8 is then observed in late stages of papilloma progression and in SCCs (151). Conversely, loricrin is present in hyperplastic epidermis and papillomas, while its expression is abruptly decreased in SCCs. In SCCs, in addition, the alteration of expression of numerous genes associated with EMT has been reported (152).

Tumour development can be conveniently monitored across the different stages of the protocol, by visually evaluating the presence and evolution of papillomas and/or of SCCs on the DS of the mouse; molecular analyses are performed only at the end of the study, by sacrificing the animal and harvesting the tissues of interest. Furthermore, this mouse model is particularly suited to assess the effects of dietary factors/dietary manipulations and of anti-cancer therapies on different stages of tumour development (153, 154).

Although the two-stage skin carcinogenesis mouse model can be considered one of the best to study cSCC, it presents some limitations: the first example is the absence of correspondence of mice papillomas to any human skin cancer condition (even though the late SCCs from this mouse model are a good representation of human ones); in another example, the most important target for gene mutation in human non-melanoma skin cancer is p53, while in the initiation process in the DMBA-TPA mouse model is Hras (155); moreover, the rate of metastasis of skin tumours in the mouse model is quite low, making this protocol of limited utility to study metastasis (156).

In this thesis, the pharmacological effects of two SIRT-6 modulators, specifically the activator MDL-800 and the inhibitor S6 (previously described in Introduction, paragraph 2.2), is assessed in a DMBA-TPA skin cancer induced mouse model (Results and Discussion, paragraph 4).

4. Sirtuins in skin and skin cancer

Sirtuins have been found to be implicated in a variety of skin-specific cellular functions and processes, including keratinocyte differentiation, ageing, UV damage response, oxidative stress, wound healing, skin diseases and skin cancers (158). They have been demonstrated to be expressed in the skin, in several cellular, *in vivo* and *ex vivo* studies (159). In particular, in the skin turnover process, as keratinocytes differentiate, the genetic profile of the 7 sirtuins is modified (Table 7). In detail, SIRT-4 and -5 transcripts are transiently upregulated, while SIRT-1 and -7 are slightly downregulated during differentiation, as was shown in an *in vitro* skin reconstruct model. In the same study, expression of SIRT-2, -3 and -6 was not altered; however, skin reconstructs consist of both differentiated and undifferentiated

keratinocytes, and these latter might mask weak modulations of gene expression caused by differentiation. SIRT-6 correlation with keratinocyte differentiation has been further investigated by Lefort and colleague, that discovered the induction of differentiation of healthy and cancerous keratinocytes following SIRT-6 knockdown (this study is described more extensively in paragraph 4.2). SIRT-2 and -3, however, should be further investigated in order to define their actual involvement in keratinocyte differentiation. Other skin-related physiological process in which sirtuins likely play a role are wound healing and photodamage pathways. In independent studies, it was shown that wound healing was accelerated following pharmacological activation of SIRT-1, SIRT-2 and -3 in *in vivo* settings (160), while it was impaired in SIRT-1, -6, -7 knockdown (KO) mouse models (160-162). As for sirtuins' role in UV radiation (UVR) responses, SIRT-1 displays a protective role in UVR treated skin in a mouse model (163), while normal human epidermal keratinocytes (NHEKs) exposition to UVB or both UVA and UVB radiation results in SIRT-3 degradation, SIRT-4 fluctuating levels and SIRT-6 upregulation (159, 164, 165) (Table 7).

Table 7. Sirtuin expression profile during keratinocyte differentiation in a skin reconstruct model *in vitro*, and in photodamage response (159). Abbreviations: UP, upregulated. DOWN, downregulated. unv, unvaried response.

Skin condition\Sirtuin	SIRT-1	SIRT-2	SIRT-3	SIRT-4	SIRT-5	SIRT-6	SIRT-7
Keratinocyte differentiation	DOWN	unv	DOWN	UP	UP	unv	DOWN
UV radiation response	UP	-	DOWN	DOWN/UP	-	UP	-

Sirtuins' dysregulation has been observed also in many skin-related diseases, including psoriasis, melanoma, cSCC and BCC.

Psoriasis is a chronic inflammatory skin disease characterised by keratinocyte hyperproliferation, by dysfunctional differentiation of keratinocytes and thus, by aberrant growth of the epidermal layer of the skin (166). In psoriatic skin, all sirtuins are downregulated, with the exception of SIRT-6 and -7, that are instead highly expressed (Table 8) (167, 168). SIRT-1, and to less extent SIRT-2, -3, -5 and -6, have been further investigated in this disease, suggesting that they regulate inflammation and proliferative mechanisms in keratinocytes. Briefly, SIRT-1 inhibition plays a role in oxidative stress and inflammatory skin reactions, while its activation suppresses keratinocyte proliferation and improves UV treatment effectiveness (169-176); likewise, SIRT-2 inhibition aggravates skin inflammation (177); upregulation of SIRT-3 and also of SIRT-5, conversely, attenuate oxidative stress, inflammation and excessive cell proliferation (178, 179); finally, SIRT-6 exerts pro-proliferative and pro-inflammatory effects in keratinocytes and psoriatic tissues (38).

The 7 isoforms generally are expressed differently in one same skin cancer type (Table 8), and each isoform moreover, may not possess always an unambiguous role in one same cancer type, with some sirtuins that have been reported to act as both tumour suppressors and promoters. Briefly, in melanoma SIRT-2, -3, -6 and -7 are overexpressed in both human melanoma cell lines and clinical tissue samples, and are involved in drug resistance and cancer cell growth; conversely, the roles of SIRT-1, -4 and -5 in this cancer requires further investigation, as they have been poorly studied (SIRT-4) or display carcinogenic as well as oncosuppressor functions (SIRT-1 and -5) (53, 158, 180, 181). In BCC, with the exception of SIRT-2 and -3, all sirtuins are upregulated, suggesting that they may play a role in BCC pathogenesis (experiments were performed on cancerous tissues obtained from BCC

patients) (182). In cSCC, all sirtuins are upregulated; their tumour suppressor or promotor function is described more extensively in the next paragraph.

Table 8. Sirtuin expression in psoriasis and in the three main types of skin cancer: melanoma, cSCC and BCC. Analyses were performed in different studies on healthy and cancer cells, in animal settings or in human cancer biopsies. Expression of sirtuins in cSCC is further detailed in Table 9. Abbreviations: UP, upregulated. DOWN, downregulated. unv, unvaried response.

Skin disease\Sirtuin	SIRT-1	SIRT-2	SIRT-3	SIRT-4	SIRT-5	SIRT-6	SIRT-7
Psoriasis (167)	DOWN	DOWN	DOWN	DOWN	DOWN	UP	UP
Melanoma (158, 180, 181, 183, 184)	UP	UP	UP	-	UP/DOWN	UP	UP
cSCC (159)	UP	UP	UP	UP	UP	UP	UP
BCC (182)	unv	DOWN	DOWN	unv	unv	unv	unv

4.1 Sirtuins in cSCC

In cSCC, all sirtuins are upregulated both at the mRNA and at the protein levels (Table 9) (116, 159, 164). In detail, sirtuins' expressions display a 3- to 16-fold increase in cSCC tissues compared to healthy tissues of the same patient. In addition, all sirtuins are overexpressed in cancer cells A431 and in immortalised keratinocytes HaCaT, compared to normal keratinocytes NHEK. In AK samples obtained from human biopsies, SIRT-2, -3, -5, -6 and -7 expression is significantly higher compared to adjacent healthy skin, whereas SIRT-1 and -4 variations do not reach significance.

Further research to clarify the roles of sirtuins in tumorigenic processes in cSCC has been accomplished so far solely for SIRT-1, -2 and -6.

SIRT-1 can be identified as a tumour promotor in cSCC, with studies showing its involvement in two pathways that are implicated in cSCC development, such as the miR-199a-5p/SIRT-1/CD44ICD signalling pathway (185), and the miR-30c/SIRT-1 one (186). In the first study (185), SIRT-1 is a direct target of the anti-cancer miRNA miR-199-5p, which specifically suppresses cancer cell proliferation and migration (187); the expression of the two genes is inversely correlated. Following SIRT-1 inhibition by miR-199a-5p, the intracellular proteolysis product of the cell-matrix and cell-cell interactions transmembrane CD44, namely CD44ICD, is downregulated and this activates the transcriptional machinery involved in several tumorigenic processes (188, 189). The modulation of the miR-199a-5p/SIRT-1/CD44ICD axis results in the repression of cSCC stem cells (CSCs), and therefore also of tumour formation and migration. CSCs are the cells with self-renewal ability that give rise to the transient amplifying cells, believed to be the cells that are then responsible for the bulk tumour. CSCs are characterised by low proliferation rate, high tumorigenic capacity, and thus stronger chemotherapy resistance compared to cells from the bulk tumour mass. Although CSCs' features are not fully defined for cSCC, they possess a great potential for the development of novel cancer therapeutics that aim to target the cells of origin of the cancer. Chemotherapeutics could be therefore designed to halt cancer progression by eliminating the bulk tumour mass, and simultaneously by dismantling the tumour-promoting microenvironment (190).

The oncogenic role of SIRT-1 is reported in addition in a work by Liu and colleagues (186). Briefly, SIRT-1 is targeted directly by miRNA MiR-30c and the two genes are inversely correlated. miRNA MiR-30c overexpression in SCC cells downregulates SIRT-1, and cell proliferation and chemotherapeutic resistance are repressed. When SIRT-1 is upregulated

unrelated from MiR-30c expression, it restores chemoresistance and hyperproliferation of the SCC cells, thus proving further evidence of the oncogenic function of this sirtuin in cSCC. SIRT-2, similarly to the other sirtuins, is overexpressed in cSCC both at the mRNA and at the protein levels (159). A separate study, though, has shown that SIRT-2 protein is downregulated in cSCC and that SIRT-2 KO increases tumour growth in a DMBA-TPA skin cancer mouse model. SIRT-2 deletion, in addition, causes an increase of the levels of the basal keratinocyte keratin and hair follicle stem cell marker KRT15 and of the simple epithelial keratin KRT19, often used as a cSCC tumour marker, as well as a downregulation of loricrin in both normal skin and tumours; moreover, it upregulates the CSC marker CD34 in the skin tumours. This suggests that SIRT-2 has pro-differentiation and oncosuppressive roles in cSCC (191). Given the discrepancy of the mRNA and protein levels of SIRT-2 in independent studies further elucidation of the function of this sirtuin in cSCC is still necessary. Conversely to SIRT-1, the role of SIRT-6 in cSCC is not unambiguously defined, as some research supports its oncogenic function, and some other demonstrates its association to tumour suppression mechanisms; the following paragraph delves further into this topic.

Table 9. Fold difference of SIRTs expression in AK and cSCC human tissues: mRNA expression of the cancerous tissue is compared to the one of the normal adjacent tissue (samples used in the experiments were taken from 3 AK and 5 cSCC patients). Table adapted from (159).

Skin cancer type\Sirtuin	SIRT-1	SIRT-2	SIRT-3	SIRT-4	SIRT-5	SIRT-6	SIRT-7
AK	1.4 ±0.1	3.5±1.6	5.7±2.8	2.9±2.3	2.1±0.4	17.8±8.3	7.9±3.8
cSCC	4.8±1.5	4.3±2.2	3.4±0.7	4.5±1.0	8.4±2.6	8.7±2.8	15.7±7.4

4.2 Sirtuin 6 overview and its role in cSCC

SIRT-6, as described in paragraph 2, possesses three enzymatic activities, such as the deacetylase, the deacylase and the ADP-ribosyl transferase (Figure 2), and each of them is specific to certain substrates at defined physiological conditions (Table 2). In detail, SIRT-6 deacetylates lysins K9, K18, K27 and K56 on histone 3 (H3) (32, 192), lysin K549 on the acetyltransferase general control nonrepressed protein 5 (GCN5) (193). In addition, its deacylation activity consists of defatty-acylation of lysins K19 or K20 of tumour necrosis factor- α (TNF- α), then of lysine K9 of H3 with the removal of 6- to 16-carbon chain fatty-acyl groups (7, 194), and finally of lysins H3K18 and H3K27, by removing long-chain octenoyl groups (32). Finally, SIRT-6 ADP-ribosylates itself (195), as well as Poly ADP-ribose polymerase 1 (PARP1) (9) and Kruppel-associated box-associated protein-1 (KAP1) (10).

SIRT-6 regulates multiple cellular and molecular pathways, including those responsible for telomere integrity, gene transcription, DNA repair, metabolism and glucose homeostasis (196-198).

This sirtuin contributes to double-strand break (DSB) repair in several ways: first, by mono-ADP ribosylating PARP1, thereby activating it (9); then by recruiting Sucrose nonfermenting 2 homolog (SNF2H) to DNA strand breaks, while it deacetylates H3K56 (199); and by stabilising DNA-dependent protein kinase (DNA-PK) as it deacetylates H3K9 (200). Moreover, it plays a critical role in telomere maintenance, by interacting again with SNF2H (201), by deacetylating H3K9 and H3K56 (202-204), and by deacetylating H3K18, preventing therefore mitotic errors and cellular senescence (31). Moreover, through H3K9 deacetylation, SIRT-6 can silence nuclear factor-kappa B (NF- κ B) genes, causing a repression of NF- κ B and a decrease of NF- κ B-dependent apoptosis and senescence, thus counteracting ageing (205). SIRT-6 regulates also glucose homeostasis: this sirtuin inhibits multiple glycolytic genes,

including HIF-1 α target gene promoters, and represses HIF-1 α transcriptional activity, by deacetylating H3K9; as consequence glycolysis is downregulated, while mitochondrial respiration is enhanced (43). Again, by deacetylating H3K9, it blocks IGF-AKT signalling, thus modulating insulin-like growth factor 1 (IGF-1) levels (206); and also, by deacetylating GCN5, it modulates the acetylation levels of PGC-1 α , which is regulator of gluconeogenesis (193). In addition, SIRT-6 represses the transcription of the sterol regulatory element binding proteins 1 and 2 (SREBP1 and SREBP2) genes by binding and deacetylating their promoters on H3K56 and H3K9, thus reducing cholesterol levels and protecting against the physiological damage of obesity (207). Furthermore, SIRT-6 plays a role in cancer metabolism, as it modulates cellular myelocytomatosis (c-Myc)-target genes by deacetylating H3K56 on their promoters; as a consequence, SIRT-6 co-represses c-Myc activity in the context of ribosomal gene expression, which is associated with tumorigenesis (208).

Given these functions, SIRT-6 can be predicted to be an oncosuppressor, as it is a positive regulator of genomic integrity and of cancer metabolism, as well as an oncopromoter, since it plays a critical role in glucose homeostasis and metabolism.

The function of SIRT-6 in cancer is likely tissue specific, since it acts equally as tumour suppressor or promotor depending on the cancer type (Table 3). As for cSCC, the increase of the levels (protein and mRNA) of SIRT-6 in human SCC tissues (Table 9) suggests that SIRT-6 is oncogenic in this tumour. Some research groups confirmed this prediction first by discovering SIRT-6 involvement in keratinocyte differentiation, being inversely related to miR-34a and to several differentiation markers, and thus potentially acting as a pro-proliferative agent in keratinocyte-derived cancers (116), and then by determining its role in cyclooxygenase-2 (COX-2) promotion, inducing therefore inflammation, which in turn often leads to tumorigenesis (164) (Figure 11). Notwithstanding these results, SIRT-6 was reported by another research group to exert a tumour suppression function in the skin, specifically by halting cancer stem cells' proliferation, which is driven by enhanced glycolysis, and thus counteracting tumour aggressiveness (209) (Figure 11).

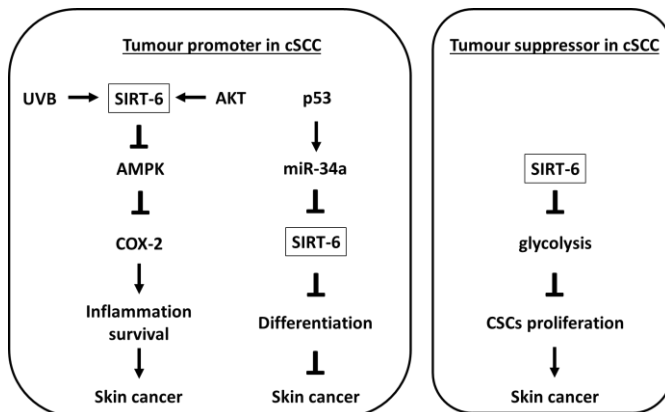


Figure 11. Diagram showing the proposed functions of SIRT-6 in cSCC, acting as tumour promoter (116, 164) or suppressor (209).

In the first study (116), it was shown that miRNA miR-34a contributes to keratinocyte tumour suppression via a p53/miR-34a/SIRT-6 axis, by inducing keratinocyte differentiation (Figure 11). In particular, tumour suppressor p53, which represents a crucial gene in the mediation of cellular responses to UV radiation and to other DNA-damaging agents (210), activates miR-

34a, which in turn inhibits SIRT-6, and as a consequence keratinocyte differentiation is enhanced. In SCCs, losses of p53 or of miR-34a result in SIRT-6 overexpression and also in poorly differentiated cells and tissues (Figure 12). SIRT-6 silencing in cancerous and healthy keratinocytes (SCC13 and HKC cells respectively), reduces cellular proliferation and is sufficient to trigger a differentiation response similar to the one obtained by miR-34a activation, by upregulating KRT1, KRT10, INV and LOR (Figure 13). This hints the critical role of this sirtuin in keratinocyte differentiation and proliferation, and especially in keratinocyte-derived cancers.

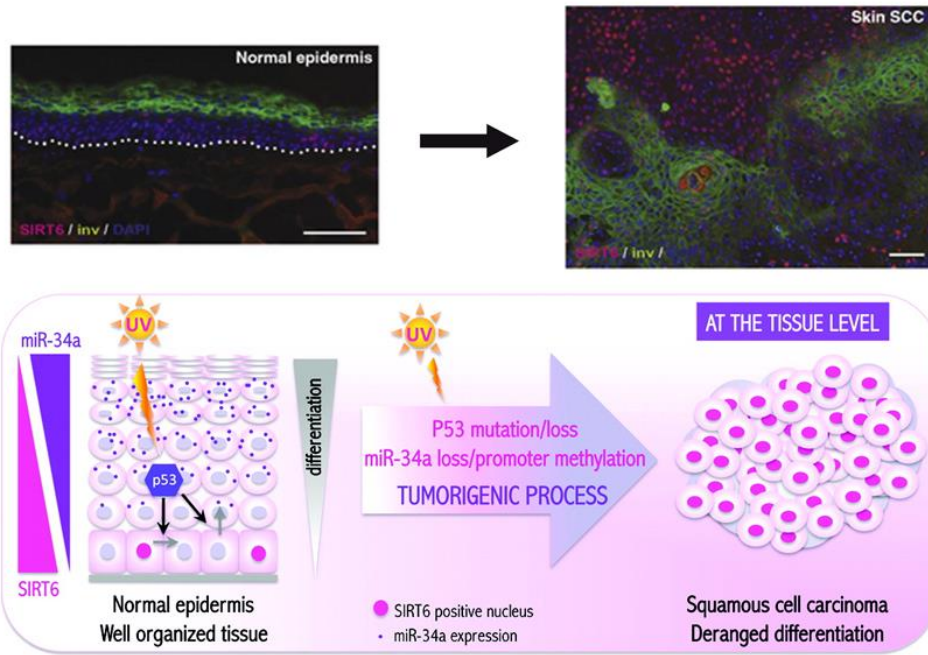


Figure 12. On the top: Immunofluorescence analysis of SIRT-6 (red) and involucrin (green) expression in normal skin and SCC tissues taken from a cSCC patient, with DAPI for counterstaining. In the SCC tissue, SIRT-6 is upregulated while the differentiation marker involucrin is deranged. Scale bar: 200 μ m. Figure adapted from (116). On the bottom: schematic overview of miR-34a and SIRT-6 expression in normal epidermis and in cSCC, with keratinocyte differentiation features described for each tissue. In normal epidermis (skin representation on the left), following exposure to DNA-damage agent, such as UV radiation, p53 activation increases expression of miR-34a, which in turn inhibits SIRT-6 expression. However, in a tumorigenic process (arrow), p53 faces mutations and it is inactivated, causing further loss also of miR-34a. In SCCs (skin representation on the right), p53 and miR-34a are downregulated, while SIRT-6 is overexpressed and cells display aberrant differentiation. Figure adapted from (211).

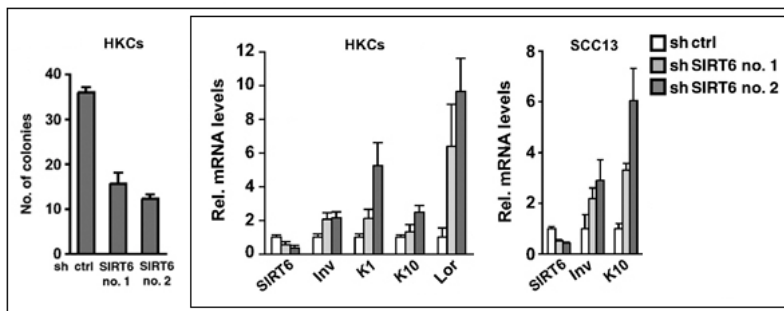


Figure 13. SIRT-6 silencing, performed with two different plasmids (sh SIRT-6 no.1 and no.2), decreases the number of colonies in human keratinocytes (HKCs) cell culture, as well as increasing the differentiation markers involucrin (INV), keratin 1 (K1), keratin 10 (K10) and Loricrin (LOR) in HKCs and in SCC13, which are SCC cells. Figure adapted from (116).

In a second study regarding SIRT-6 in cSCC (164), it was discovered that SIRT-6 regulates COX-2 expression via the adenosine monophosphate-activated protein kinase (AMPK) pathway, affecting inflammation and therefore contributing to skin tumorigenesis (Figure 11). Specifically, following UVB radiation exposure, SIRT-6 is activated by protein kinase B (AKT), and in turn represses AMPK signalling, which upregulates then COX-2, known to promote cell proliferation and survival in a cancer niche (212, 213). Moreover, skin-specific SIRT-6 deletion (cKO) in a skin carcinogenesis mouse model (obtained with the DMBA-TPA protocol) suppresses cell proliferation and epidermal hyperplasia, and consequently reduces tumorigenesis and tumour multiplicity, compared to wild type (WT) animals (Figure 14a). The key role of SIRT-6 in cell proliferation is confirmed by the decreased epidermal hyperplasia following UVR exposure in SIRT-6 cKO mice compared to the WT ones. In addition, in SIRT-6 silenced human keratinocytes a lower level of COX-2 (mRNA and protein) leads to upregulation of the apoptotic marker cleaved caspase-3, and thus to a significant increase of apoptosis (Figure 14b). These results strengthen the suggestion that SIRT-6 is a tumour promoter in cSCC.

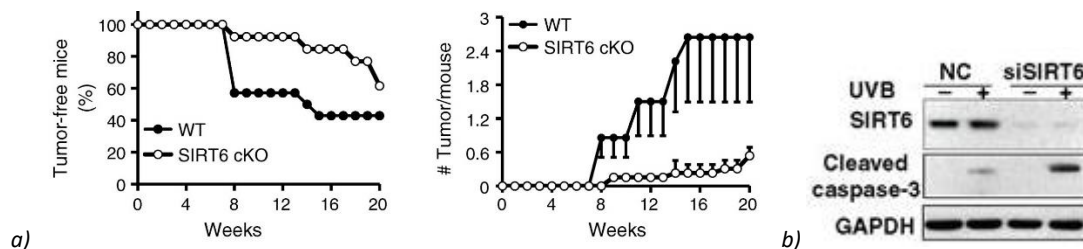


Figure 14. a) Percentage of tumour-free mice (left) and average tumour number per mouse (right) from SIRT-6 WT and cKO mice treated with DMBA and TPA in a skin carcinogenesis protocol. SIRT-6 cKO mice display decreased tumorigenesis and tumour multiplicity. b) Immunoblot analysis of SIRT-6, cleaved caspase-3, and GAPDH in human keratinocytes NHEK transfected with siRNA targeting SIRT-6 (siSIRT6) or negative control siRNA (NC) at 14 hours post-UVB. Apoptotic marker cleaved caspase-3 level is increased in siSIRT-6 transfected cells compared with NC cells. Figure adapted from (164).

In another study (209) however, it was demonstrated that SIRT-6 exhibits oncosuppressive functions in cSCC, in contrast with the oncopromoter role discovered previously by the research groups of Drs Dotto (116) and He (164). In cSCC, SIRT-6 acts as a modulator of aerobic glycolysis, also known as the Warburg effect, which is found to be enhanced specifically in cSCC CSCs (Figure 11). CSCs are known to be the tumour-driving cells (described more extensively in the previous paragraph), and actually consist of several subsets of cells. Among these, the CD34⁺ CSCs can be distinguished from the others, because of their higher glycolysis and enhanced pentose phosphate pathway and glutathione (GSH) metabolism, that provide them with a stronger defence against oxidative stress; these CSCs represent in particular the actual cells-of-origin of the tumour. It can thus be concluded that enhanced glycolysis and reduced GSH are among the main drivers in SCC. In a SIRT-6 skin cKO mouse model treated in a DMBA-TPA skin carcinogenesis protocol, SIRT-6 deletion enhances glycolysis (and specifically aerobic glycolysis), which exacerbates CSCs population. This causes an increase in cell cancer proliferation, an earlier onset of tumours (Figure 15a), significantly larger tumours (Figure 15a) and complete progression of papillomas into SCCs, in SIRT-6 cKO mouse compared to the WT one. Consistently, the authors found that SIRT-6 silenced cSCC cells (SCC13) overexpress glycolytic genes, and also that cancerous tissues taken from cSCC patients both in early and in advanced stages of tumorigenesis are

characterised by an inverse correlation of expression of SIRT-6 and of the glycolytic genes. Moreover, SIRT6-deficient CD34⁺ CSCs exhibit higher expression of genes involved in glycolysis, in the pentose phosphate pathway (PPP), in the GSH metabolism and in redox balance (Figure 15b); as a consequence, these cells present increased level of GSH, decreased ratio GSSG/GSH (oxidized vs reduced forms of glutathione), and lower levels of ROS. SIRT-6 deleted CD34⁺ CSCs feature thus better protection from oxidative stress compared to normal CSCs, become more proliferative and increase thereafter cancer aggressiveness. In conclusion, SIRT-6 acts also as a tumour suppressor in cSCC via modulation of glycolysis and by targeting specifically CSCs' proliferation.

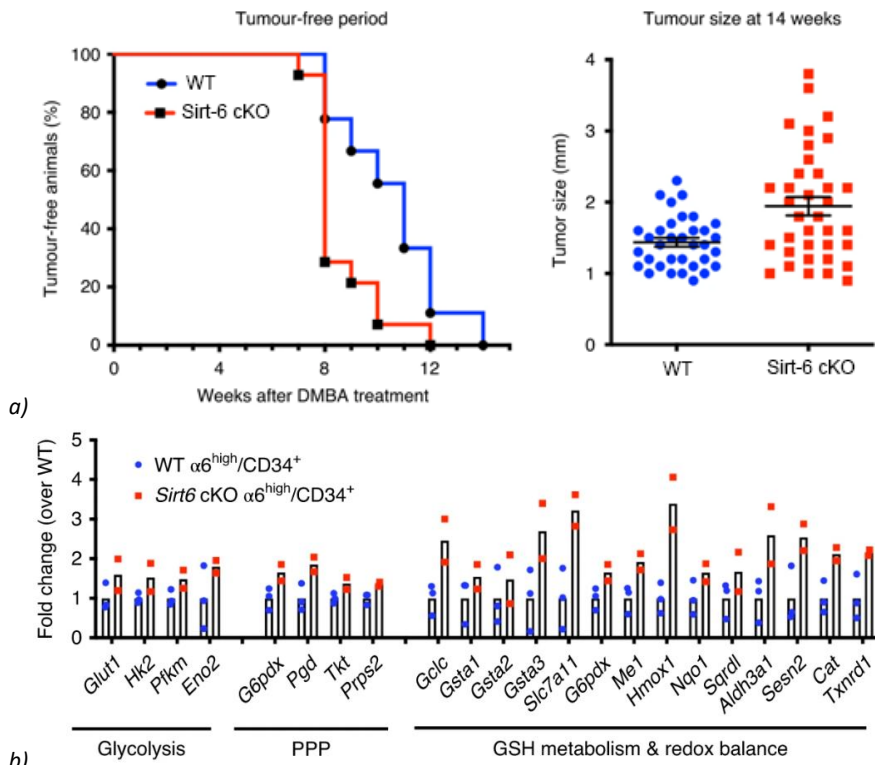


Figure 15. a) Tumour-free period before tumour onset, and tumour size at 14 weeks after DMBA treatment, in SIRT-6 WT or SIRT-6 cKO animals. b) Fold changes in expression of genes associated with glycolysis, PPP and GSH metabolism and redox balance, in SIRT-6 WT or cKO CD34⁺ CSCs compared to CD34⁺ CSCs in the same tissues. Figure adapted from (209).

Given the discrepancy of the three different studies described above, further work is still needed to clarify if SIRT-6 behaves as an oncopromoter or suppressor in cSCC. Moreover, no studies have been performed yet on the pharmacological modulation of SIRT-6 in this type of cancer.

In this thesis, the effects of the pharmacological activation and inhibition of SIRT-6 are compared, using a DMBA-TPA mouse model which is treated topically with the SIRT-6 activator MDL-800 or with the inhibitor S6 (Results and Discussion, paragraph 4).

5. Microemulsions for topical application

5.1 Topical drug administration

In pharmacology, drug administration is performed in three main ways, namely the enteral/gastrointestinal, the parenteral and the topical routes. Specifically, the enteral administration includes the oral and rectal ones, while the parenteral comprises among others the epidural, the intraarterial, the intramuscular, the intraperitoneal and the intravenous administrations. Each route presents advantages and disadvantages, and specific strategies should be implemented in order to provide the highest therapeutic effects, as well as the lowest side-effects. For the treatment of skin-related conditions, topical drug delivery should be the preferential route, as it directs the drugs to the site of action, avoiding systemic effects and circumventing gastrointestinal metabolism and enzymatic drug degradation. Moreover, since the delivery of the drug is localised, its bioavailability is increased, and it can be administered in a lower concentration compared to other routes, thus further reducing its side-effects (214).

When a topical formulation is applied on the skin, it aids the permeation of the drug across the stratum corneum (Figure 7), after which the drug itself reaches the epidermis and/or dermis, interacting thus with its pharmacological target (215). Drugs with transdermal activity, on the contrary, will be able to diffuse further, crossing also the hypodermis (Figure 7) and reaching the blood vessels below the skin, exerting therefore systemic therapeutic effects (216). The stratum corneum is the outermost layer of the skin, and is composed mainly of insoluble keratins (70%) and lipid (20%) (217), thus being characterised by very high density (1.4 g/cm^3 in the dry state) and low hydration of 15%–20% (217). This skin component represents therefore a crucial physical barrier for the skin layers below, preventing skin water loss and inhibiting the penetration of xenobiotics into the dermal layers. In light of these characteristics, the permeation of drugs represents a challenge in topical drug delivery (218, 219). Topical formulation effectiveness depends on several parameters that are related both to the skin and to the medication features, such as the drug's physicochemical properties, the skin pH, and the dosage form. The first factor affecting drug absorption through the skin is the hydrophilicity of the drug. The three pathways for absorption are quite lipophilic, therefore hydrophilic drugs will face more challenges in skin absorption compared to the lipophilic ones (220). The second factor is the pH level of the skin: the skin pH is acidic across all layers (221-224); therefore, topical drugs presenting some polar moieties are forecast with better absorption. The third factor affecting the drug absorption is the dosage form. This consists of a mixture of the active pharmaceutical ingredient (API) and of the excipients, which are inactive components that facilitate drug absorption, define viscosity of the dosage form, enhance the API's solubility, or aid the dosage form's thermodynamic stability, therefore extending the drug's shelf-life. The choice of the excipients and of their amount in the formulation should be defined by the route of administration, by the intended dosage form and by the API's properties. It should be noted, moreover, that lists of approved excipients, including their maximum dose to be administered to humans, are available from the Food and Drug Administration (FDA) and from the European Medicines Agency (EMA). In Italy, in addition, it is available for pharmacists also the document "Farmacopea Ufficiale" (FU), which clears the characteristics needed from drugs used in the Italian territory.

5.2 Colloidal systems, emulsions and microemulsions for topical use

5.2.1 Colloidal systems for topical use

Liquid, solid and semisolid dosage forms are among the most common. In particular, for topical use the formulations are found in the semisolid form, and they include creams, foams, gels and ointments among others. Liquid and solid topical medications also exist, and they are represented mainly by emulsions and lotions, the first, and powders, the second.

Creams, emulsions, foams and gels are classified as colloidal systems. A colloid is a mixture of two substances that normally would be immiscible; specifically, it consists of the microscopic dispersion of one substance throughout a medium of dispersion (diameter of the particles dispersed is in the range 0.001 – 1 μm). A colloid presents two phases, namely the dispersed phase and the continuous phase. In particular, in foams, a gas is dispersed into a liquid, and in gels a liquid is dispersed into a solid, whereas in creams and emulsions, both the continuous and the dispersed phase are liquids. Different colloidal systems are obtained through different preparation procedures, and contain different excipients that specifically characterise them. In general, colloidal systems are prepared by distributing the particles of the dispersed phase into the continuous phase, through milling, spraying, or shear stress (e.g., shaking, mixing, or high shear mixing).

As for the physicochemical properties, the interaction between the particles of the two phases is described by the Gibbs free energy of the system ΔG , which is given by the combination of the electrostatic interactions and the van der Waals forces (of note, physicochemical events reach an equilibrium when ΔG is minimised). If ΔG is minor than the thermal energy of the particles kT , where k is the Boltzmann constant and T is the absolute temperature, which provides kinetic energy to the particles, the colloidal particles present weak attraction or repulsion towards each other, and therefore the particles of the dispersed phase will remain in suspension in the continuous phase. The colloidal system is therefore stable and its properties are isotropic, meaning they are uniform in all directions. Conversely, if ΔG is greater than kT , the colloidal particles attract to one another, and the system is instable; in this case flocculation, coagulation or precipitation are observed (Table 10).

Table 10. Overview of the thermodynamics of a colloidal system.

Colloid	Free energy of the system	Colloidal particles' interactions	Physical appearance
Stable	$\Delta G < kT$	Weak attraction and repulsions	Isotropic mixture
Instable	$\Delta G > kT$	Attraction	Phase separation

Here, a few colloidal systems that are often used as topical formulation are described more in detail.

The first example is given by gels, that are classified into hydrogels and lipogels. A liquid phase, such as water or oil, for hydrogels or lipogels respectively, is dispersed into a porous and permeable solid, creating a particularly flexible 3D network (225). Into this biocompatible and biodegradable structure, drugs can be dispersed for drug delivery, and can then be released to the target site (226).

The second example is given by emulsions, which are liquid colloids. These can be classified into oil-in-water (O/W) and water-in-oil (W/O) emulsions, with the first type consisting of small droplets of oil dispersed in a continuous water phase, and with the second one presenting instead water droplets dispersed in an oil phase (Figure 16a). In emulsions, droplets of the two different phases are bound together by specific molecules called

surfactants. The amphiphilic characteristic of these compounds, meaning they possess both polar and hydrophobic sections (Figure 16b), confers them the ability to locate at the interface of the two immiscible liquids, decreasing the interfacial tension of the two phases. These can therefore mix and the emulsion is stabilised (227). The stabilisation of the dispersion can be tuned in addition by modifying the viscosity of the mixture; in this case, some thickening agents are added. For a topical medication purpose, the drug can be dissolved either in the water or in the oil phase of the emulsion, depending on its hydrophilicity, and the droplet thus obtained will be dispersed in the other phase of the emulsion. Specifically, hydrophilic drugs should be dissolved in the water phase of W/O emulsions, whereas lipophilic drugs in the oil phase of O/W ones (Figure 16b). Emulsion and microemulsions are described more extensively in the next paragraph.

As for creams, these are semi-solid emulsions, and therefore can be classified as O/W and W/O creams (Figure 16a). Their composition is similar to the one of emulsions, as they are made of a water and of an oil phase, as well as of surfactants, presenting however in addition thickening agents, which increase the mixture's viscosity without modifying the other properties, such as waxes. Drug encapsulation in creams should be accomplished following the same principles applied for emulsions.

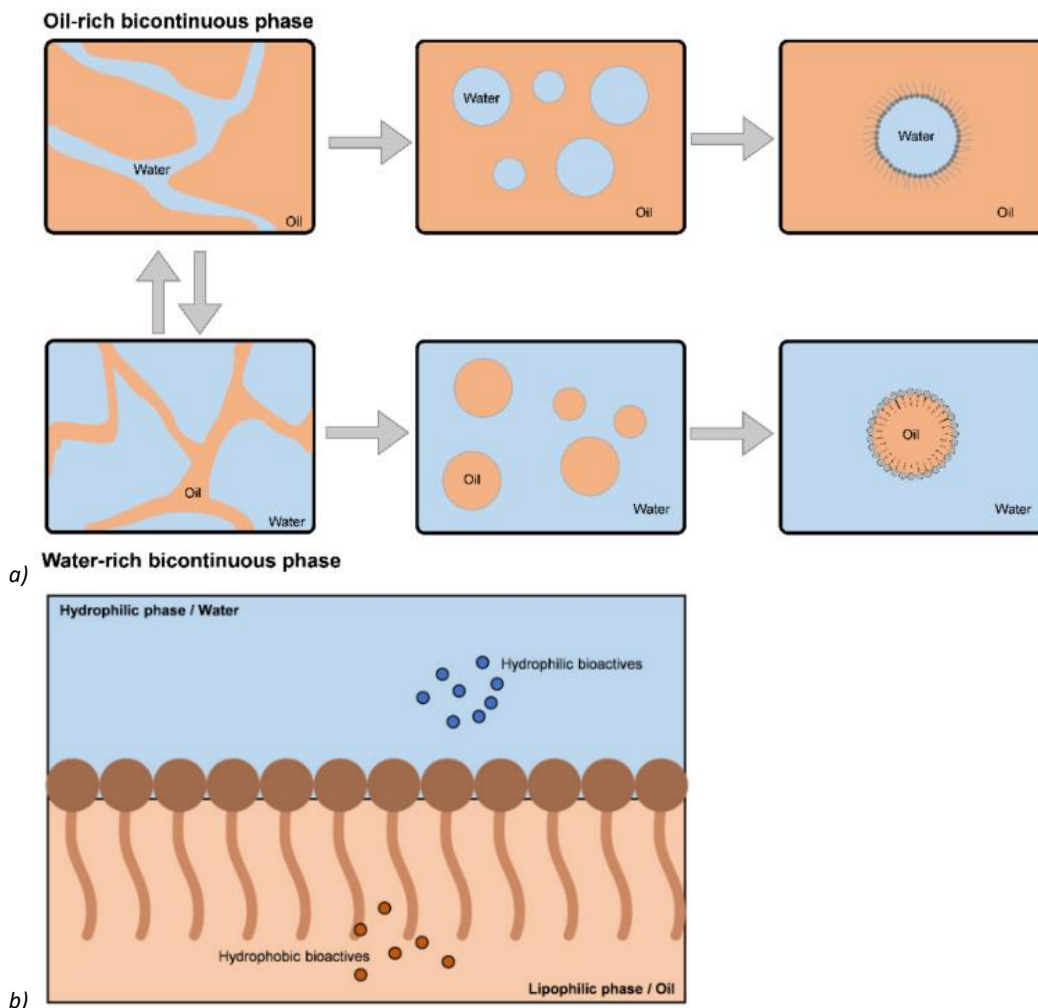


Figure 16. a) Representation of colloidal dispersions of O/W and W/O types. b) Schematic representation of surfactant and drug placement in the O/W interface. Figure adapted from (228).

5.2.2 Emulsions, microemulsions and nanoemulsions for topical use

Among the colloidal systems, emulsions possess a high potential of increasing skin permeation of drugs, in virtue of their isotropic characteristics and of their double water and oil phase profile, which allows them to disrupt the lipophilic stratum corneum, to be absorbed by the skin and to deliver both polar and lipophilic drugs (229).

In particular, two emulsions subtypes are increasingly being explored in the last decades as carriers for the delivery of drugs and of cosmeceuticals to the skin: microemulsions (MEs) and nanoemulsions (NEs). MEs and NEs differ from emulsions mainly for their droplet size, and therefore for their viscosity and thermodynamical stability. The differences from the other types of emulsions are a result of various conditions during the emulsion preparation procedure, and also of the presence of different components in the mixture. Specifically, MEs and NEs contain a cosurfactant in addition to the emulsion components, and this enhances emulsification as well as increases the fluidity of the surfactant interface (230).

Emulsions are prepared by stirring the water and the oil phases together with the surfactant and, if MEs or NEs, eventually also with the cosurfactant (Figure 17). Emulsification will occur upon mixing when an energetic stability will be reached in the system, such as low interfacial tension as well as weak repulsive force between two phases. To be noted that increased viscosity of the medium might help creating and maintaining the suspension of the dispersed phase into the continuous phase. Emulsions and MEs are prepared by simple stirring of the mixture, while NEs by ultrasound or high-shear homogenisation (217).

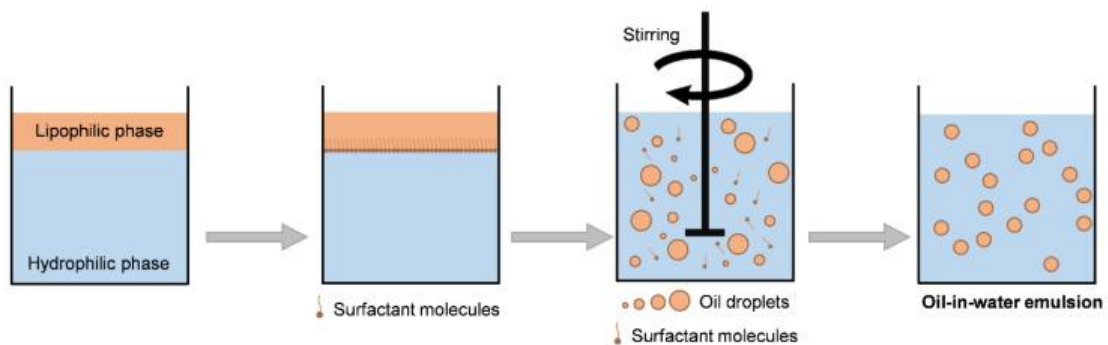


Figure 17. Schematic representation of Water in Oil (W/O) and Oil in Water (O/W) emulsions. Figure adapted from (228).

MEs and NEs are characterised by smaller droplet sizes, with MEs' droplet size of approximately 100-400 nm and NEs' droplet size in the range 1-100 nm (228).

As a consequence of smaller particle size and thus of lower viscosity, MEs and NEs have a milky or translucent aspect, in contrast with emulsions, that usually appear as cloudy dispersions. As for stability, MEs are characterised by a high thermodynamic stability, and thus by a longer shelf life, compared to classic emulsions, that have smaller surface area per unit volume and are unstable (228). NEs are less stable than MEs, and as such, being more kinetically and less thermodynamically stable, they require lower surfactant concentration for their emulsification.

Emulsion properties, such as O/W or W/O type, drop size, stability, and viscosity, are affected by several parameters, such as the components of the emulsion (the water phase, the oil phase, the surfactant), the oil-water ratio, the amount of surfactant and cosurfactant and the mechanical mixing conditions, including the stirring speed (231). Emulsion properties, however, do not depend on these parameters in a linear way, but according to different

patterns given by each variable as a single agent and also in relation with the other variables (232, 233).

The most common excipients used to prepare emulsions, MEs and NEs for topical delivery are now briefly described.

Water phase: Purified water is the most common liquid used for the water phase (234-236), even though there have been reports of preparations using also phosphate buffer pH 7.4 (237, 238).

Oil phase: Over the years, several substances have been chosen as single components or as combination to represent the oil phase. Examples include fatty acids, alcohols, esters of fatty acids and alcohols, medium-chain triglycerides, the glycerol triesters, and terpenes. Briefly, oleic acid is a fatty acid that has been used in many studies, followed by palmitic, palmitoleic, stearic and linoleic acids (239-242); alcohols, on the contrary, are less common, with some researches reporting specifically the use of octanol (243) and decanol (235, 244). Esters, instead, are commonly used as the oil phase in emulsions, MEs and NEs, and these include isopropyl myristate (IPM) (245, 246), isopropyl palmitate (247), ethyl oleate (237, 248), isostearyl isostearate (234, 249) and cetearyl octanoate (247). Examples of medium-chain triglycerides are the ones obtained from caprylic acid and capric acid (250-252), while terpenes used include squalene, limonene, cineole, camphor and menthol (240, 249, 253, 254).

Surfactant: Surfactants can be classified based on their charge, as non-ionic or ionic, which in turn can be further categorised into anionic or cationic ones. Non-ionic surfactants are generally considered safer than the ionic ones, since they are less irritant; cationic, and especially anionic surfactants, are cytotoxic to human and animal skin, being thus potent skin irritants (255). Non-ionic surfactants display a polar head that allows the bind to water particles of the aqueous phase, and one or more alkyl chains, intended instead for the non-polar interactions with the oil phase. They can be represented by lecithin and polysorbates, which are ethoxylated sorbitan (a derivative of sorbitol) esters with fatty acids, such as Tween 80 and Tween 20, Span 20 (256), among others. The advantage of non-ionic surfactant over the ionic ones is represented not only by their low skin toxicity, but also by their ability to enhance drug permeation through the skin, by interacting with the lipids of the stratum corneum. Anionic and cationic surfactants bear in their hydrophilic part a negative or positive charge, respectively. Anionic surfactants include soaps, sodium lauryl sulphate, dioctyl sodium sulphosuccinate, and phosphate esters (257), while cationic ones that are usually used are quaternary ammonium compounds (258, 259).

Cosurfactant: Cosurfactants are components solely of MEs and NEs, and not of emulsions, and can be short-chain alkanols, e.g., ethanol, long-chain alkanols, e.g., 1-butanol and decanol, or propylene glycol. Cosurfactants play a critical role in certain MEs and NEs, stabilising the dispersion and aiding drug permeation through skin (256).

Other components: Depending on the solubility of the drug to be delivered to the skin, an additional component can be present in the dispersion, namely the dissolution solvent of the drug. If the API is highly polar, it can be easily dissolved in water, which will then be dispersed as droplets in the continuous oil phase. In most of the cases, however, drugs are partially or completely insoluble in water and other solvents are added to dissolve them completely before adding them to the aqueous or oil phase. Lipophilic drugs, in particular, are dissolved

in petrolatum, dimethyl sulfoxide (DMSO) and mineral oil (220), and this solution is dissolved in the oil phase, which is then dispersed into the continuous water phase.

Another component that can be added to the emulsion/ME/NE is a thickening agent, which increases viscosity of the water or oil phase, thus aiding the creation of the droplets and their stability in the dispersion. Such agents can be hydrocolloids, e.g., acacia and tragacanth, polyethylene glycols (PEGs), that exist with different carbon-length chains, glycerine, and other polymers, like cellulose derivatives (260).

To be noted, that the preferred measurement unit of different agents varies based on the physicochemical properties of the entity. For example, while liquids and solids are quantified in volume and weight respectively, and measured in molarity or g/L, polymers, such as PEG and cellulose derivatives, are quantified in drops (gtt) and their preferred measurement unit is % p/V or % p/p.

5.3 Microemulsions as carriers for lipophilic drugs

MEs and NEs are optimal drug carriers since their reduced droplet size favours drug delivery in several ways. First, smaller particles encapsulate a higher amount of the API, improves thus drug solubility (261-263) and consequently its bioavailability. Second, it increases the retention time of APIs on the skin, since smaller droplets have better chance to adhere to cell membranes, and therefore enhances drug effectiveness (264, 265). MEs and NEs are therefore, more specifically, micro- and nano-carriers. Both have been used for topical administration of hydrophilic and lipophilic drugs in several studies, and it was demonstrated by the improved bioavailability of the APIs when formulated in these systems compared to other topical dosage forms (266-269).

Lipophilic APIs are characterised by a poor water solubility, which can be explained by the poor presence of polar groups in the chemical structure, or by a higher molecular weight (MW). The lipophilicity/hydrophilicity of a compound is usually described by the partition coefficient $\log P$, which is the ratio of concentrations of the compound in a mixture of two immiscible solvents at equilibrium; lipophilic compounds possess high values of $\log P$. Although skin permeability is less challenging for lipophilic drugs compared to hydrophilic ones, the skin remains a very effective barrier from external agents, and optimal drug delivery strategies should be implemented. Given by the lipophilic profile of the stratum corneum, promising lipophilic drug carriers are represented by MEs, and specifically by O/W MEs. This type of ME is characterised by a higher oil-water ratio, which allows a better dissolution of the drug and a higher encapsulation rate, as well as by a greater thermodynamic stability compared to emulsions and to NEs (270).

In this thesis, the development of O/W microemulsions containing two lipophilic compounds, namely the SIRT-6 inhibitor S6, and the SIRT-6 activator MDL-800, and their topical application on mice DS is described (Results and Discussion, paragraph 3, 4).

SUMMARY of the undertaken TASKS to reach our AIMS

1. Development of HPLC-based methods to identify SIRT6 modulators

With the goal of discovering novel sirtuins' modulators, and specifically SIRT-6 and SIRT-2 modulators, a first set of experiments aimed at the identification of suitable enzymatic activity assays, that are tailored for the detection of the deacetylation catalysed by SIRT-1, -2, -3 and -6 and of the deacylation catalysed by SIRT-6. An HPLC-based assay method was the one chosen for this purpose. The deacetylase activity was planned to be specifically investigated with an acetylated peptide (H3K9Ac), while the deacylase one with a palmitoylated peptide (H3K9Palm). Considering that SIRT-6 deacetylase activity is quite weak and results may have been below the HPLC detection limits, a known SIRT-6 activator was incubated along with recombinant SIRT-6. Several compounds were therefore screened with this prospect.

2. Discovery of novel sirtuin inhibitors

After the definition of suitable methods to investigate the enzymatic activity of different sirtuins, the aim was to screen several compounds for the discovery of novel sirtuin inhibitors. Specifically, one first objective was the identification of SIRT-6 inhibitors. Compounds that are derivatives of the SIRT-6 inhibitor S6, and that were forecast to improve its water solubility, were selected through a CADD analysis in a hit-to-lead process. They were tested in the SIRT-6 deacetylation assay with the purpose of identifying inhibitors that improved also the inhibition potency of S6. Eventually, SIRT-6 modulators were further characterised in *in vitro* studies, evaluating their pro-differentiating effects in keratinocytes and their synergism with cSCC drugs 5-FU and Celecoxib in a SCC cells co-treatment. One other objective was the screening of different families of compounds with a backbone structure resembling the one of SIRT-2 inhibitor SirReal2, or of other families of SIRT-2 inhibitors, such as thienopyrimidinones and indoles with a 3-cyclic structure, in order to discover novel SIRT-2 inhibitors. This was planned to be accomplished in a two-step process: putative SIRT-2 inhibitors were first identified by CADD in a hit identification process, and then were tested on recombinant sirtuins.

3. Development of a stable O/W ME containing SIRT-6 modulators for topical application

With the aim of treating with the SIRT-6 inhibitor S6 or with the SIRT-6 activator MDL800 the DS of mice undergoing a skin cancer carcinogenesis protocol, a first goal is the development of an appropriate dosage form for topical application containing S6 or MDL-800. Different options, such as lipogels, O/W emulsions and O/W microemulsions were investigated. Moreover, at this stage, bulk quantities of MDL-800 had to be synthesised.

4. *In vivo* evaluation of SIRT-6 pharmacological modulation in a skin cancer mouse model

Once the formulations containing the SIRT-6 inhibitor S6 or the SIRT-6 activator MDL-800 were prepared, the *in vivo* studies were performed. Briefly, mice undergoing a DMBA-TPA two-stage carcinogenesis protocol were treated with the S6- or MDL-800-containing

formulations. Three protocols were used: two aiming at defining a preventive effect of SIRT-6 modulation, with the formulations applied prior to either DMBA or TPA, and one with a therapeutic approach, in which DS was treated with the formulations after the papillomas arose on the mice skin.

5. Is SIRT-2 involved in cSCC?

Along with defining the role of SIRT-6 in cSCC, one smaller investigation aimed at clarifying the involvement of SIRT-2 in this type of cancer, by analysing the expression of this sirtuin at different stages of skin carcinogenesis in DMBA-TPA treated mice. Preliminary studies on the pharmacological effect of SIRT-2 inhibitors on cultured cancerous keratinocytes were also performed.

RESULTS AND DISCUSSION

1. Development of HPLC-based methods to identify SIRT6 modulators

With the goal of discovering novel sirtuins' modulators, and specifically SIRT6 and SIRT2 inhibitors, a first set of experiments aimed at the identification of suitable enzymatic activity assays, that are tailored for determination of the deacetylation catalysed by SIRT1, -2, -3 and -6 and of the deacylation catalysed by SIRT6. At first, fluorescence- or chemiluminescence-based commercial kits, commonly used for the discovery of HDAC and sirtuin modulators, were chosen for this purpose. Unfortunately, these drug discovery systems did not prove reliable for the screening of the compounds, because of the innate fluorescence and chemiluminescence of the putative modulators that interfered with the results. Consequently, other assays had to be exploited for the purpose, and the choice fell on the HPLC-based deacetylation/deacylation assay; this technique is described in Introduction, paragraph 2.3.2.

The final goal was the discovery of novel SIRT2 and SIRT6 inhibitors, that are potent and isoform selective over the other sirtuins. Therefore, the HPLC techniques were developed in order to assay the deacetylase activity of SIRT1, -2, -3, and -6 and the deacylase activity of SIRT6, and in particular its depalmitoylase one (Figure 2). The sirtuin substrates chosen for the screening are two peptides of 11 residues resembling acetyl H3K9 and palmitoyl H3K9, and these were produced by solid-phase peptide synthesis (Table 23 in Materials & Methods). These substrates are particularly suitable for assaying the activity of SIRT6, since they both represent two of the preferred targets of this sirtuin. Although SIRT1, -2, -3 deacetylate preferentially other substrates (Table 2), H3K9 is found also among their targets. Besides, several research groups assayed the enzymatic activities of SIRT1, -2, and -3 using H3K9Ac peptides as well (102, 271).

During the assay development process, it was observed that the SIRT6 deacetylation products were undetectable by HPLC analysis. This is in accordance with the known weak deacetylase activity of this sirtuin, in contrast to SIRT1, -2 and -3, that are instead strong deacetylases. Thus, in order to examine this enzymatic activity as well, known SIRT6 deacetylation activators were added to the reaction mixture. After comparing the activation potency of three different compounds (described in Materials & Methods), the activators chosen were compound MDL-800 (described in Introduction, paragraph 2.2), and palmitic acid (PA), which, along with the other fatty acids, is an endogenous SIRT6 activator (7).

For each sirtuin and reaction type, after testing several reaction conditions, such as protein, NAD⁺ and peptide concentration, as well as reaction buffer and reaction time, the optimal ones were defined (Table 11); furthermore, different trials were carried out to assess the best procedure to block the enzymatic reaction. Briefly, the optimised procedure consists of the following steps. First, the recombinant sirtuin is incubated with NAD⁺, with the peptide, with DMSO, which is the vehicle of the compounds used in the subsequent screening of modulators, and eventually with the SIRT6 activator and with MgCl₂, which might contribute to the stabilisation of the recombinant protein; reactions are carried at 37°C and are then quenched by adding 3 volumes of an acidic methanol (MeOH) solution. After removal of the protein by centrifugation, aliquots of the supernatants containing the remaining reaction components are subjected to HPLC analysis.

Table 11. Reaction conditions defined for SIRT-1, -2, -3, -6 deacetylation or deacylation. Reactions are carried out at 37°C, in a total volume of 30 μ L. Abbreviation: Pep, peptide. conc, concentration. PA, palmitic acid.

Enzymatic reaction	Deacetylation				Deacylation	
	SIRT-1	SIRT-2	SIRT-3	SIRT-6		SIRT-6
Sirtuin conc	17.3 nM	0.27 μ M	0.2 μ M	4.59 μ M	4.59 μ M	4.59 μ M
NAD ⁺ conc	500 μ M	100 μ M	100 μ M	500 μ M	500 μ M	100 μ M
Pep-H3K9Ac conc	240 μ M	240 μ M	200 μ M	240 μ M	240 μ M	
Pep-H3K9Palm conc	-	-	-	-	-	120 μ M
Activator conc	-	-	-	MDL800: 100 μ M	PA: 150 μ M	-
DMSO	1 μ L	1 μ L	1 μ L	1 μ L	1 μ L	1 μ L
MgCl ₂ conc	-	-	-	4 mM	-	4 mM
Reaction buffer	20mM NaH ₂ PO ₄	20mM NaH ₂ PO ₄	20mM NaH ₂ PO ₄	20mM Tris pH 7.4	20mM Tris pH 7.4	20mM Tris pH 7.4
Reaction time	10 min	10 min	10 min	1 h	1 h	30 min

Along with exploring the reaction conditions, with the aim of setting a method able to give clear and reproducible results, also different HPLC settings were compared. The chosen ones are described in detail in Materials & Methods. Moreover, a few tests on the stability of the peptides in the quenching buffer were carried out, reproducing the waiting time of the samples in the vial before being analysed. It was assessed that the best wavelength for detecting all the entities in the reaction mixtures is 220 nm. Moreover, since the H3K9Ac peptide is unstable in the HPLC glass vial and within 30 min is partially absorbed to it, whereas the H3K9 and H3K9Palm peptides are stable up to a few hours at RT and at 4°C in the same vials, it was determined that the tracker-molecule for studying the deacetylation should be the deacetylated peptide H3K9, while for the depalmitoylation either the H3K9 or H3K9Palm peptides can be quantified.

At last, it was evaluated the accuracy of the technique, in order to define the minimum number of needed replicates, since one single analysis can be cost- and time-consuming. It was observed an inter-day and inter-user accuracy of minimum 90%; therefore, further experiments were chosen to be carried out by performing analysis solely once or twice. In conclusion, at this stage, assays to study the deacetylation/deacylation of several sirtuins, with the aim of identifying their modulators, were assessed.

2. Discovery of novel sirtuin inhibitors

After the definition of suitable methods to investigate the enzymatic activity of different sirtuins, the aim was to screen several compounds for the discovery of novel sirtuin inhibitors.

Investigation of novel SIRT-6 inhibitors

The first objective was the identification of novel SIRT-6 inhibitors, in a hit-to-lead drug discovery process. The chosen hit compound was the SIRT-6 inhibitor S6 (described in Introduction, paragraph 2.2). From a structural point of view, S6 is quite hydrophobic and its poor water solubility hampers often its administration in cellular and animal studies; as for its SIRT-6 modulation, it presents an IC₅₀ of 106 μ M. With the aim of discovering SIRT-6 inhibitors that improve water solubility and IC₅₀ of S6, the following steps were performed.

Identification of putative SIRT-6 inhibitors through CADD.

The parameters to consider in order to improve the solubility of a compound are mainly the chemical structure and the functional groups; the potency of inhibition depends instead on the interactions that the molecule is able to create with the active site of the enzyme. For this reason, prior to the CADD process aiming at identifying potential lead compounds, knowledge regarding the physicochemical properties and docking characteristics of the hit compound S6 was collected (S6 docking in SIRT-6 binding site is depicted in Figure 4c). Desired lead compounds were identified as those bearing the functional groups suggested to interact with SIRT-6, namely the quinazoline-2,4(1H,3H)-dione scaffold (blue in Figure 18a), and presenting also hydrophilic groups, such as the sulphonamide (red in Figure 18a). Different functional groups were therefore planned to be investigated on the remaining part of the molecule, in connection to the sulphonamide.

In one first screening, 25 compounds were selected from within a 1-million compound database of the mcule platform, for their *in silico* improved water solubility, with respect to compound S6. These compounds were S6-derivatives, and presented a common substructure (Figure 18a).

In a second CADD stage, the identified 25 compounds were subjected to VS, and in particular to SBDD, by using Autodock Vina: they were docked into SIRT-6 crystal structure and their binding affinity to SIRT-6 active site was evaluated. Ten compounds were finally selected (Figure 18b; their chemical denomination is described in Materials & Methods). These compounds were forecast with an improved binding affinity to the SIRT-6 active site compared to the inhibitor S6, because of their fewer poses available and of their stronger hypothesised bonds with SIRT-6. A subsequent drug profile evaluation of the 10 compounds, specifically of their *in silico* absorption-distribution-metabolism-excretion (ADME) properties, confirmed that they were expected not to be chemically or biologically instable, nor dangerous or toxic.

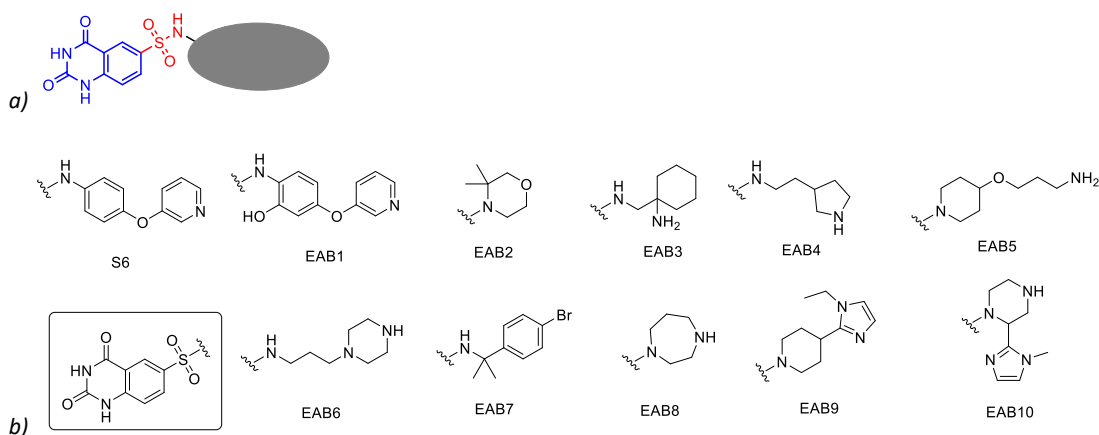
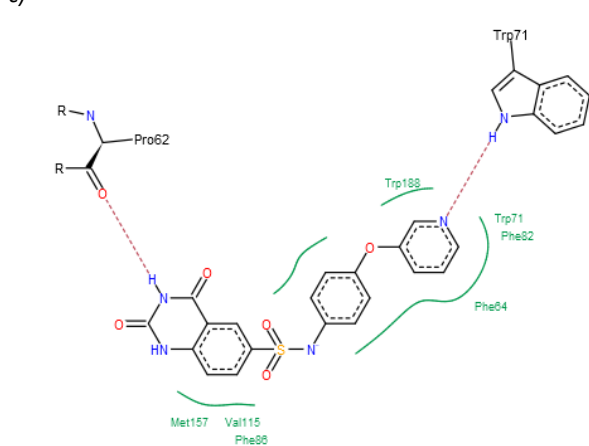
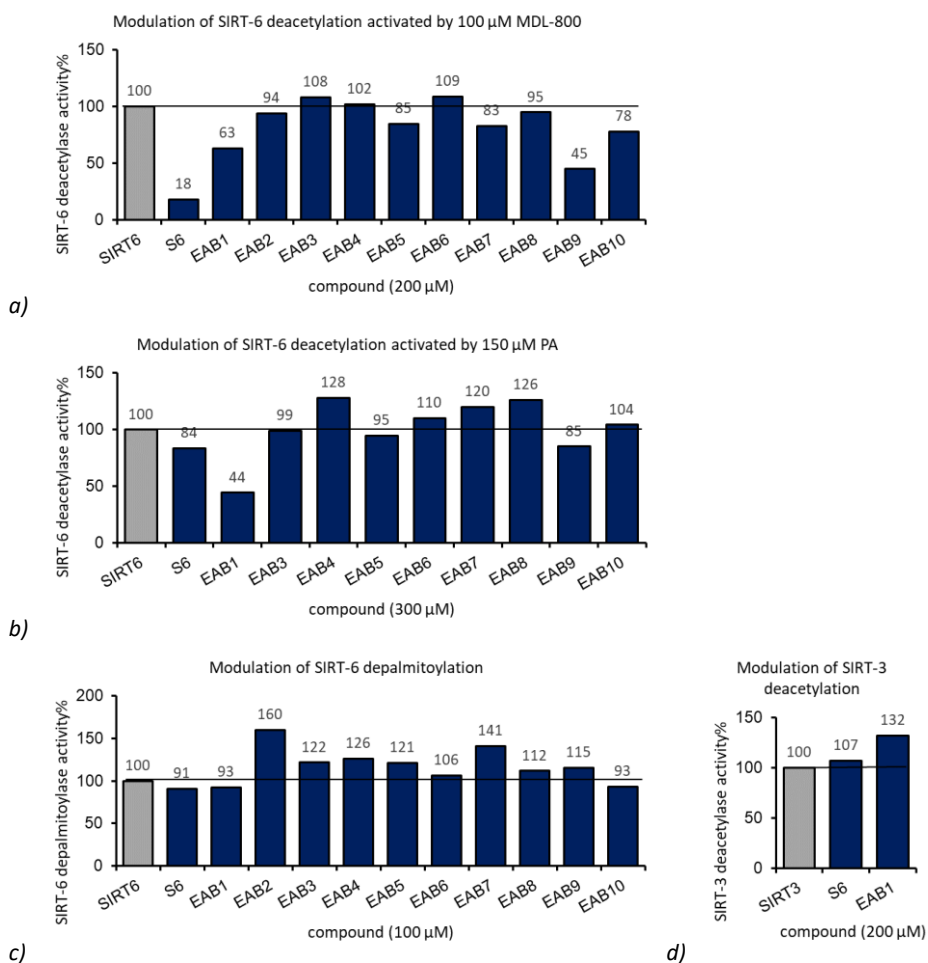


Figure 18. a) General structure of S6-derivatives: the quinazoline-2,4(1H,3H)-dione building block is depicted in blue, while the sulphonamide is in red; the right building block (in grey) was modified in order to improve water solubility and inhibition potency. b) Chemical structures of compound S6 and of 10 S6-derivatives selected through CADD as potential SIRT-6 inhibitors.

Evaluation of SIRT-6 modulation in an enzymatic activity assay.

The 10 compounds selected from the CADD process were examined with sirtuins enzymatic activity assays, and specifically for both the deacetylation and the depalmitoylation activities of SIRT-6. When deemed promising SIRT-6 inhibitors, they were further characterised in the

modulation of the activity of other sirtuins. The final concentration of the compounds was 100 μM in the depalmitoylation assay, 200 and 300 μM in the SIRT-6 deacetylation activated by MDL-800 or PA respectively, and 200 μM in the SIRT-3 deacetylation one. It was observed that SIRT-6 deacetylation is inhibited by S6, EAB1 and EAB9, while its depalmitoylation is activated by EAB2 and EAB7 (Figure 19a, b, c).



e) Figure 19. Residual enzymatic activities of SIRT-6 in presence of the compounds identified through CADD and of hit compound S6: SIRT-6 deacetylation activated by MDL-800 (a) or by PA (b), SIRT-6 depalmitoylation (c), SIRT-3 deacetylation (d), $SD < 10\%$. e) Predicted binding mode for S6 in SIRT-6 active site, in alternative to the one depicted in Figure 4c.

Of the 10 compounds, only EAB1 modulates SIRT-6 deacetylase activity in a comparable way to the hit compound S6. Moreover, both compounds EAB1 and S6 do not modulate significantly SIRT-6 deacetylase activity at 100 μ M nor SIRT-3 deacetylase one at 200 μ M (Figure 19c and d). The other compounds did not prove to modulate significantly SIRT-6. Given the present results, one explanation of the poor inhibition of the selected structures could be that probably the hydrophobic rings of compound S6 are crucial for the interaction of the inhibitor with SIRT-6 active site, and by removing these groups in the newly identified compounds, the inhibition potency is lost. Indeed, the 10 compounds were selected through a CADD process that relied on *in silico*-based knowledge, such as the interactions between S6 and SIRT-6 active site (Figure 4c), and not on experimental data obtained by the crystallisation of the hit compound within SIRT-6. In light of the results obtained through the enzymatic activity assays, a new docking pose of S6 in SIRT-6 active site can be suggested (Figure 19e); in this, S6 interacts with SIRT-6 active site through its quinazolinone scaffold and through the pyridine moiety.

Evaluation of the *in vitro* effects of a selection of compounds.

Although the 10 compounds identified through CADD did not prove better inhibitors than the hit compound S6, a selection of them was still tested on cells to evaluate if they are cell membrane permeable, and if they exerted some other effects *in vitro*. Considering the crucial role of SIRT-6 in cSCC (as described in Introduction, paragraph 4.2), cellular studies were chosen to be performed on cancerous keratinocytes (SCC13 cells).

SCC13 cells were treated for 21 h with a selection of compounds, namely EAB2, EAB3, EAB5, along with the SIRT-6 inhibitor S6 and the SIRT-6 activator MDL-800 (added at 50 μ M final concentration), and their effects on the enzymatic activity of intracellular SIRT-6 and on keratinocyte differentiation were evaluated. As internal control, results were compared to the ones obtained from SIRT-6 silenced SCC13 cells. In detail, SIRT-6 modulation was investigated by Western Blot (WB) analyses of the acetylation level of the SIRT-6 substrate H3K56, namely H3K56Ac, while the keratinocyte differentiation was investigated by evaluating the level of the differentiation marker keratin 1 (Figure 20b and c). The results confirmed that S6 and MDL-800 are indeed a SIRT-6 inhibitor and activator respectively, and that they are effective *in vitro*. When SIRT-6 is inhibited or silenced the acetylation level of its substrates increases, while when activated, it decreases (Figure 20a). Moreover, SIRT-6 inhibition is accompanied by an increase of the level of Keratin 1, thus confirming pharmacologically the hypothesis that SIRT-6 KO induces keratinocyte differentiation, as it was previously described in the work by Lefort and colleagues (116).

As for the compounds EAB2, EAB3 and EAB5, these proved to be cell-membrane permeable, as they modulated the levels of H3K56Ac and keratin 1. The increased acetylation level of H3K56 means that the enzymatic activity of SIRT-6 was modulated, and that these compounds inhibited this sirtuin even more potently than the known SIRT-6 inhibitor S6. Furthermore, these compounds increased keratin 1 protein level as it was observed for S6, suggesting that they might inhibit SIRT-6 and induce keratinocyte differentiation in a similar way to the known SIRT-6 inhibitor. The *in vitro* modulation of SIRT-6 by EAB2, EAB3 and EAB5, however, is not in accordance with the results obtained from the enzymatic activity assays. One explanation could be that in the SIRT-6 deacetylation assay, the activators MDL-800 and PA added to the SIRT-6 reaction mixture may interfere in the binding of the compounds to the active site of SIRT-6. Indeed, although MDL-800 and PA represent a valid alternative for

SIRT-6 deacetylation screening, as they aid the weak SIRT-6 reaction progression, their activation mechanisms imply a modification of the protein structure, thus reshaping the actual active site of SIRT-6, and possibly altering the outcome of the enzymatic activity assay (Figure 4b).

Cell viability after treatment with the compounds was also assessed. In particular, SCC13 cells were treated with the SIRT-6 inhibitor S6, with the activator MDL-800 and with all the compounds identified through CADD (EAB1 to 10), at different concentrations, and tested with the SRB assay. After 48 h treatment, all the S6-derivatives were not toxic up to 100 μM concentration, in agreement with the ADME profile prediction performed during the CADD analyses; S6 reduced cell viability by 30% at 25 μM concentration, while MDL-800 dramatically reduced it already in the low μM range (cell viability of 70% at 0.3 μM concentration).

Further experiments were performed to evaluate if a selection of these modulators in combination with known cSCC drugs improved their chemotherapeutic effect. The drugs chosen were 5-FU and Celecoxib, that represent after surgery the most common therapeutic options for cSCC patients. After 72 h treatment of SCC13 with 5-FU (1.6 μM) or Celecoxib (12.5 μM) in combination with compounds S6, MDL-800, EAB2, EAB3 and EAB5 at different concentration ranges, it was observed that all the compounds had an additive effect with 5-FU and with Celecoxib. One slight synergic effect was observed solely for EAB3, which at low μM concentrations amplified cell death by 5-FU; this effect was however reversed at higher concentrations of EAB3 (Figure 21).

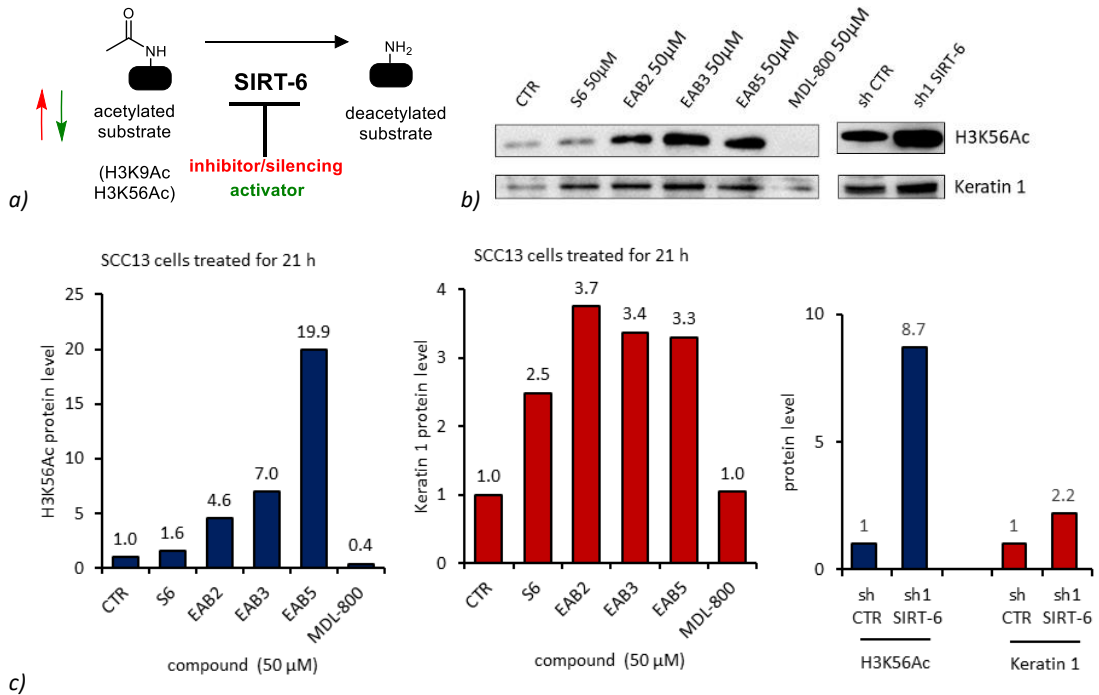


Figure 20. a) Substrate acetylation levels when SIRT-6 is inhibited/silenced or activated. b) Effects on acetylation level of H3K56 and on keratin 1 level, of the treatment of SCC13 cells with SIRT-6 inhibitor S6, SIRT-6 activator MDL-800 and compounds identified through CADD, EAB2, EAB3 and EAB4. Results were compared to the ones obtained from SIRT-6 silenced SCC13 cells.

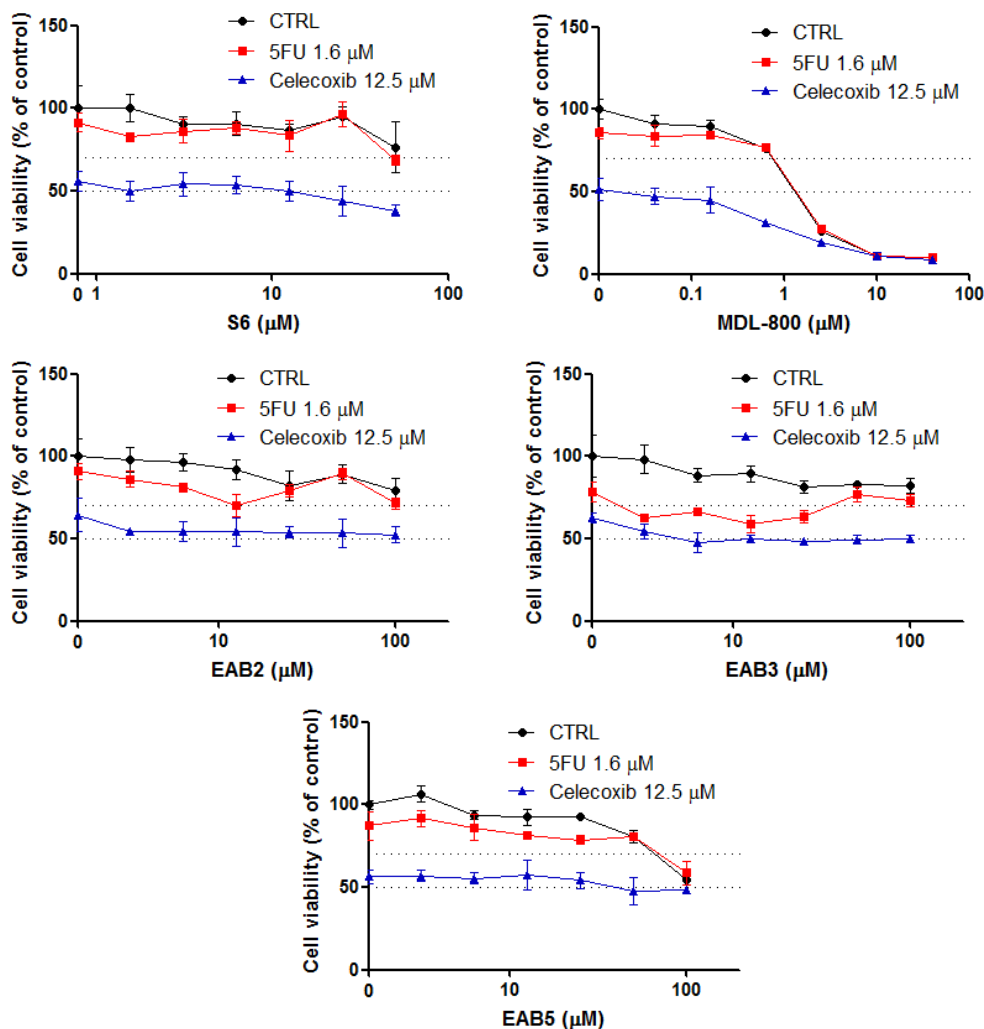


Figure 21. Cell viability of SCC13 cells treated with S6, MDL-800, EAB2, EAB3 and EAB5 (at different ranges of concentrations), in combination with 5-FU (1.6 μM) and Celecoxib (12.5 μM), for 72 h.

In conclusion, several potential SIRT-6 inhibitors were identified through CADD, and three compounds, namely EAB2, EAB3 and EAB5, seemed to be potent SIRT-6 inhibitors and not toxic in SCC cells. EAB1 was also identified as a SIRT-6 inhibitor; for this compound, however, chemical synthesis is more challenging than for inhibitor S6, and the alternative option of purchasing this compound is also considered not feasible. Given also the great resemblance of this compound to the known SIRT-6 inhibitor S6, it was chosen to not fully characterise this compound further.

The SIRT-6 inhibitors, in addition, were able to recreate pharmacologically the pro-differentiating effects of the silencing of SIRT-6 in keratinocytes, showing the potential of SIRT-6 inhibition in cSCC (116).

In this thesis project, *in vivo* studies with a SIRT-6 inhibitor were performed (Results & Discussion, paragraph 4). The novel inhibitors were not chosen for this purpose, since they require further physicochemical and biological characterisation. S6 was selected for the study for two main reasons: although it is not a potent inhibitor, it has been widely characterised in previous *in vivo* studies (as described in Introduction, paragraph 2.2), and in addition, its lipophilicity, which is often a drawback for its administration to cells and animals, might actually benefit the preparation of the formulations for the intended topical treatment.

Discovery of novel SIRT-2 inhibitors

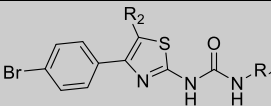
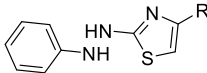
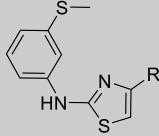
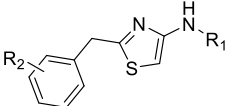
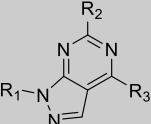
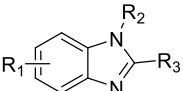
The second objective regarding sirtuin modulators, was the identification of novel SIRT-2 inhibitors in a hit compound discovery process. The following steps were performed.

Identification of putative SIRT-2 inhibitors through CADD.

At first, CADD, and specifically SBDD, was performed with the aim of identifying potential SIRT-2 inhibitors. These experiments were executed in collaboration with Prof. Elena Cichero, DIFAR, University of Genoa.

By exploiting the knowledge of well characterised SIRT-2 inhibitors, three scaffolds were identified as promising backbones for the discovery of novel SIRT-2 inhibitors. Specifically, inhibitor SirReal2 (described in Introduction, paragraph 2.1), which is characterised by a thiazole core, led to the identification of several compounds containing a thiazole group. These included thiazoles decorated with an ureide, or with a hydrazine, or with flexible substituents, such as benzyl-amino thiazoles, or with a rigid thiazole structure, such as amino-aryl thiazoles. Moreover, the availability of X-ray crystallography data of SIRT-2 inhibitors bound in the active site of SIRT-2 motivated the selection of two more scaffolds as potential core structure of novel SIRT-2 inhibitors. In detail, SIRT-2 inhibitors thienopyrimidinones (272) and indoles with a 3-cyclic structure (273), led to the identification of few pyrazolopyrimidines and benzimidazoles, respectively. At this stage, 24 compounds were selected (Table 12) and were ready for *in vitro* testing.

Table 12. Potential SIRT-2 inhibitors: thiazoles decorated with an ureide, with a hydrazine, with an amino-aryl group or with a benzyl-amino group; pyrazolopyrimidines; benzimidazoles. Abbreviation: CMP, compound.

Family of compounds	Scaffold	Compounds
THIAZOLES DECORATED WITH AN UREIDE		CMP 1 to 6
THIAZOLES DECORATED WITH A HYDRAZINE		CMP 7 to 14
AMINO-ARYL THIAZOLES		CMP 15 to 17
BENZYL-AMINO THIAZOLES		CMP 18 to 20
PYRAZOLO PYRIMIDINES		CMP21, CMP22
BENZOIMIDAZOLES		CMP23, CMP24

Evaluation of SIRT-2 modulation in an enzymatic activity assay.

The 24 compounds selected from the CADD process were examined with the HPLC-based SIRT-2 deacetylation activity assay. When deemed promising SIRT-2 inhibitors, they were further characterised by determining their IC₅₀ and by evaluating their selectivity for SIRT-2

over the other sirtuins. The modulation of SIRT-2 by the selected compounds at 150 μM was compared with the one of the known SIRT-2 inhibitor, AGK2 (described in Introduction, paragraph 2.1). Most of the tested molecules displayed an inhibitory effect against SIRT-2 deacetylase activity (Figure 22). In particular, all ureides (CMP 1 to 6) and some hydrazines (CMP8, CMP11 and CMP13) and pyrazolopyrimidines (CMP22) almost abrogated its enzymatic activity (>90% inhibition), while the amino-aryl thiazoles (CMP 15 to 17) and the benzyl-amino thiazoles (CMP 18 to 20) exhibited less inhibitory ability (36-88% inhibition). The benzimidazoles (CMP23, CMP24), instead, exerted minimal inhibitory action (<20% inhibition) at the studied concentration.

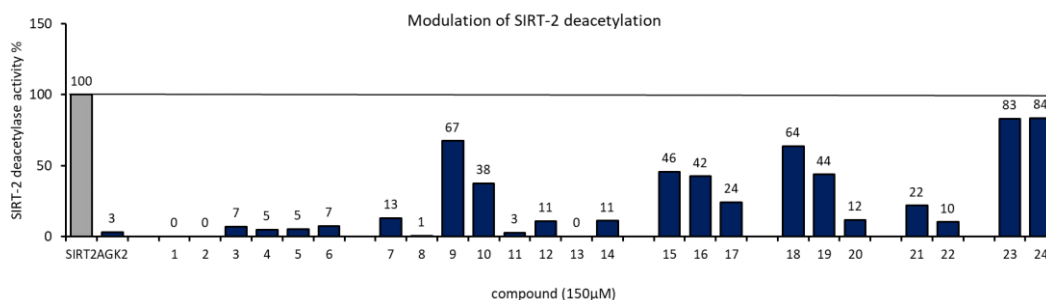


Figure 22. Residual enzymatic activity of SIRT-2 in presence of the compounds identified through CADD and of AGK2 (150 μM). SD <10%.

The compounds inhibiting SIRT-2 more potently (>75% inhibition) were collected for further testing. These were 14 in total and included all the ureides (CMP 1 to 6), several hydrazines (CMP 11 to 14), the amino-aryl thiazole CMP17, the benzyl-amino thiazole CMP20 and the pyrazolopyrimidines CMP 21 and CMP22.

The IC_{50} for SIRT-2 was further evaluated for a selection of these compounds (CMP1, CMP2, CMP4, CMP17) (Figure 23). As shown in Table 13, the IC_{50} values ranged from 26 to 149 μM .

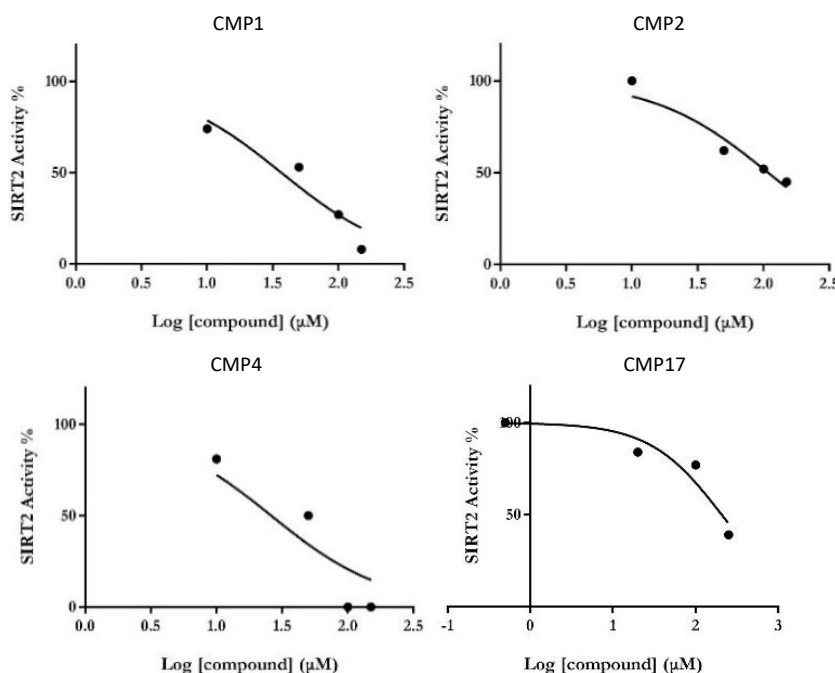


Figure 23. Dose-response curves and IC_{50} values, determined for SIRT-2 inhibitors CMP1, CMP2, CMP4 and CMP17.

Table 13. IC_{50} of a selection of SIRT-2 inhibitors.

SIRT-2 inhibitor	SIRT-2 IC_{50}
CMP1	36.7 ± 2.5 μ M
CMP2	108.4 ± 3.5 μ M
CMP4	26.1 ± 3.9 μ M
CMP17	149 ± 13 μ M

Evaluation of the modulation of the activities of other sirtuins.

In order to evaluate the selectivity of the compounds for SIRT-2 over the other sirtuins, the 14 compounds exhibiting >75% inhibition for SIRT-2 were selected for further HPLC-based enzymatic activity analyses with other sirtuins. In particular, the compounds were tested at the final concentration of 150 μ M in the deacetylation reaction of SIRT-1, SIRT-3 and SIRT-6, with this last one being promoted by the addition of the SIRT-6 activator MDL-800, and also in the depalmitoylation of SIRT-6. The residual enzymatic activities for each sirtuin are reported in Table 14 and in Figure 24.

Table 14. Overview of residual enzymatic activities of SIRT-2, SIRT-1, SIRT-3 and SIRT-6 of a selection of SIRT-2 inhibitors. Abbreviation: CMP, compound. deAc, deacetylase. dePalm, depalmitoylase.

Compound family	CMP	SIRT-2 deAc activity%	SIRT-1 deAc activity%	SIRT-3 deAc activity%	SIRT-6 deAc +MDL-800 activity%	SIRT-6 dePalm activity%
Reference inhibitor	AGK2	3	-	35	46	108
Thiazoles decorated with an ureide	CMP1	0	14	94	58	107
	CMP2	0	1	77	85	100
	CMP3	7	2	86	103	106
	CMP4	5	0	80	93	97
	CMP5	5	0	64	109	93
	CMP6	7	8	76	133	104
	CMP7	13	27	52	58	135
Thiazoles decorated with a hydrazine	CMP8	1	20	73	94	145
	CMP11	3	15	76	21	110
	CMP12	11	41	86	52	105
	CMP13	0	40	70	96	116
	CMP14	11	35	79	59	104
Amino-aryl thiazole	CMP17	24	5	113	25	99
Benzyl-amino thiazole	CMP20	12	18	59	47	125
Pyrazolopyrimidines	CMP21	22	24	67	102	111
	CMP22	10	25	80	62	114

Inhibitors that are selective for SIRT-2 over the other sirtuins present a low SIRT-2 residual activity, while a high one for the other sirtuins. As general trend, most of the SIRT-2 inhibitors tested modulate also SIRT-1, while the other sirtuins are less affected. The compounds that inhibited SIRT-1 in a similar extent to SIRT-2 (>80% inhibition) included all the ureides, few hydrazines (CMP8, CMP11), the amino-aryl thiazole CMP17 and the benzyl-amino thiazole CMP20. Pyrazolopyrimidines showed approximately 75% inhibition for SIRT-1.

Conversely, SIRT-3 enzymatic activity was reduced just by few compounds, such as the hydrazine CMP7 (48%) and the benzyl-amino thiazole CMP20 (41% inhibition). Notably, the depalmitoylase activity of SIRT-6 was not affected by the presence of the different compounds, whereas the deacetylase activity of this sirtuin was modulated by some of the compounds, apparently without following a class-specific rule.

Of the 14 SIRT-2 inhibitors tested, many inhibit SIRT-1 and -2 to a similar extent, with other sirtuins being less affected, concluding that they can be considered dual SIRT-1/SIRT-2

inhibitors rather than just SIRT-2 modulators. Identifying SIRT-2, as well as SIRT-1, selective inhibitors proves often quite challenging, since these two sirtuins present a high homology of their catalytic domain, as confirmed by the large group of substrates recognised and modified by both protein isoforms. Nevertheless, these molecules can be considered promising hit compounds as dual SIRT-1/SIRT-2 inhibitors, that can counteract several pathological conditions that require the inhibition of both sirtuins, and be characterised and developed as such.

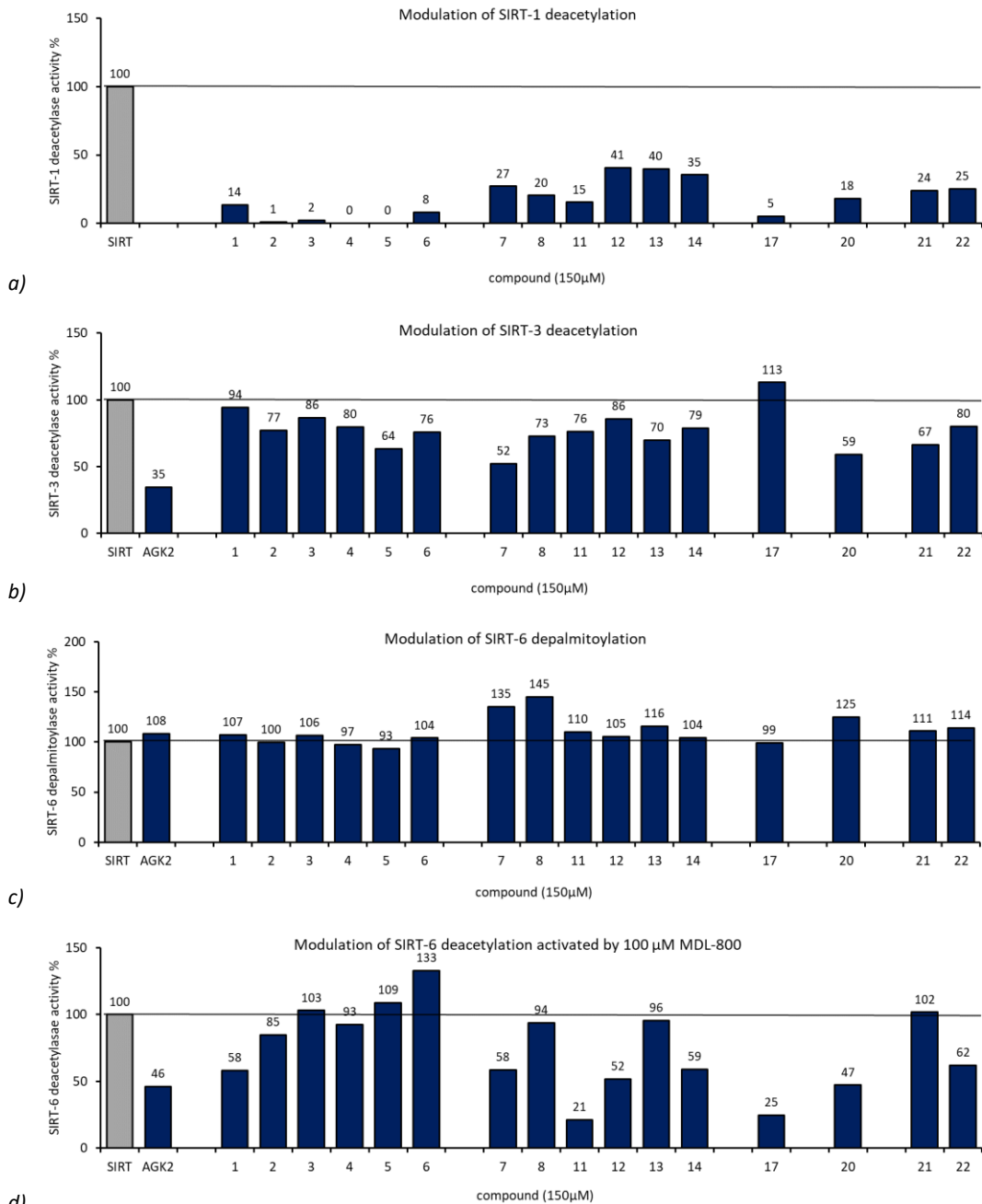


Figure 24. Overview of residual enzymatic activities of different sirtuins in presence of the SIRT-2 inhibitors (150 μM): SIRT-1 deacetylation (a), SIRT-3 deacetylation (b), SIRT-6 depalmitoylation (c), and SIRT-6 deacetylation activated by MDL-800 (d). SD <10%.

3. Development of a stable O/W ME containing SIRT-6 modulators for topical application

With the goal of treating with the SIRT-6 activator MDL800 and with the SIRT-6 inhibitor S6 the dorsal skin of mice undergoing a skin cancer carcinogenesis protocol, a first set of experiments aims at the development of an appropriate dosage form for topical application containing S6 and MDL-800.

The purpose of this part of work is therefore the identification of a formulation with the following characteristics:

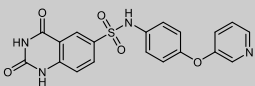
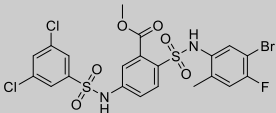
- suitable for topical administration and consisting of FU approved excipients;
- effective for drug delivery to the skin; tailored for lipophilic drug delivery, being S6 and MDL-800 quite hydrophobic compounds;
- in a balanced form between liquid and semi-solid, in order to ease the mouse administration by pipetting the dosage form on the mouse DS, and by ensuring that is not too fluid to slide away from the skin after the application;
- thermodynamically stable for at least a 3 months period (the duration of the *in vivo* study).

Several steps were carried to achieve this goal, as they are described below.

Characterisation of the physicochemical properties of compounds S6 and MDL-800 and identification of the best solvent to dissolve them.

First, the known physicochemical properties of S6 and MDL-800 were collected: both compounds are stable as powders for long periods and, while S6 follows the drug-likeness Lipinski's rule of Five, MDL-800 violates it (Table 15). Moreover, given the rigid chemical structure and the few polar groups, they are forecast to be quite lipophilic. Their poor water solubility in several water-based solvents or mixture of solvents was confirmed experimentally, as they did not dissolve in water, ethanol, acetone or DMSO/PBS in 1:2 ratio already at 3 mM concentration. The only solvent that dissolves both compounds is DMSO, in which S6 solubilises at a concentration of 24 mg/mL (58.5 mM), and MDL-800 at 64 mg/mL (102 mM).

Table 15. Known physicochemical properties of compounds S6 and MDL-800. (*) Data taken from ChEMBL. (**) Data taken from already published works (52, 274).

Proprieties	S6	MDL-800
Chemical structure		
MW (g/mol)	410.4	626.3
Physical aspect	Brown powder	White powder
Powder stability	Stable at -20°C, long term	Stable at -20°C, long term
logP	2.2*	5.6*
Solubility in DMSO	50 mM (20.5 mg/mL)**	100 mM (62.6 mg/mL)**
pKa	7.91*	6.91*
Molecular species	neutral	neutral
Hydrogen bond acceptors	6	6
Hydrogen bond donors	3	2
Rotatable bonds	5	7
Lipinski's rule of 5 violations	NONE	YES (MW>500, logP>5)

Investigation of several formulations: lipogels, O/W emulsions, O/W microemulsions.

Several formulations forecasted with the desired characteristics for the topical application of S6 and MDL-800 were then explored. These include lipogels, O/W emulsions and O/W microemulsions. To each formulation DMSO was added to simulate the vehicle of S6 and MDL-800. All formulations were set on stability studies and the best formulation was finally selected.

Lipogels

Lipogels were prepared by mixing syntesqual, DMSO and different amounts of Lipogelag, varying thus the gel viscosity (Table 25). Syntesqual was chosen as the oil of the lipogel, since it is a synthetic molecule possessing properties of both squalene and squalane, which are components of the skin, and represents a stable oil widely used in the cosmetic industry. Lipogelag is instead a mixture of C10-C18 triglycerides, polyisoprene and silica, possessing gelling properties for oleolytes. The lipogels prepared appeared as clear, transparent and light-yellow mixtures. Nevertheless, all the 8 formulations thus prepared did not prove to be suitable for the intended application, for two reasons mainly: first, their viscosity was too low, and second, already at 3 days from their preparation, phase separation occurred and reconstitution of the original lipogels was not possible to be obtained by shaking the mixture. Other solutions were then to seek.

O/W emulsions, O/W microemulsions

In addition to lipogels, also other drug delivery systems were reviewed. At first, emulsions, and specifically O/W emulsions, were prepared by mixing purified water (as water phase), IPM (as oil phase), the surfactant Tween-20 and DMSO (Table 26 in Materials & Methods). These formulations appeared as milky translucent dispersions. Phase separation however occurred already after 3 days and system's stability was not able to be restored completely upon novel mixing for all 5 emulsions.

The ME technology was then considered. Several O/W MEs were prepared using purified water as the main water phase component, and either syntesqual or IPM as the mail oil phase substance. IPM was chosen in particular for its known broad use in cosmetics and in topical medical preparations when aiming at ameliorating the skin absorption. The O:W ratio was another critical parameter considered during the planning of the experiments, as a higher O:W ratio is preferred, in order to dissolve better the lipophilic compounds S6 and MDL-800. The surfactants chosen were Tween-20 or Tween-80, which are often used in O/W ME preparation; they are non-ionic surfactants, therefore not toxic. The main differences between the two substances rely in their chemical structures: Tween-20 is a laurate, while Tween-80 is an oleate. Tween-80, as is bears a longer aliphatic tail, is more lipophilic and more soluble in organic solvents and in oils compared to Tween-20. Furthermore, it has a higher MW compared to Tween-20; therefore, along with its surfactant activity, when used as excipient, it also increases the viscosity of the ME. In the water phase, eventually also thickeners like PEG 7 GC, PEG 200 or PEG 400 were added; they are known to contribute to the stability of the ME as well, by modifying the viscosity of the dispersion in different fashions. Finally, in the oil phase, DMSO was added to simulate the vehicle of the SIRT-6 modulators. A summary of the 25 MEs prepared is reported in Table 27. Similar to the emulsions prepared previously, all MEs appeared as milky translucent dispersions upon preparation.

Following stability studies simulating the 3-months 4°C shelf-life conditions of the subsequent *in vivo* studies allowed the identification of 6 formulations suitable for the topical application purposes (Table 17). Briefly, ME-3, -4, 16, -18, -21, -25 are the MEs with a higher O:W ratio, that are characterised by a viscous form (not too fluid and not semi-solid), that are easy to pipette and that are able to reconstitute completely upon simple hand agitation whether phase separation occurs. Formulation ME-25 (Table 16) was then specifically recognised as the best to continue within the formulation studies, as it presents higher O:W ratio (4:1) and higher amount of DMSO, thus facilitating the APIs' solubility in the ME; moreover, it displays little phase-separation, and is able to return to a stable ME condition upon simple hand agitation.

Table 16. Composition of the formulation ME-25, which is the one selected for the further *in vivo* studies.

Formulation	O:W ratio	Water phase		Oil phase		Volume prepared
		Water	Surfactant	Oil	DMSO	
ME-25	4 : 1	0.4 mL	Tween 20 6 gtt	Syntesqual 1.6 mL	DMSO 0.4 mL	2.4 mL

Table 17. Overview of the O:W ratio and of the viscosity and stability observations of the O/W ME formulations following a 4°C long-term storage simulation. The MEs considered most suitable for topical application of compounds S6 and MDL-800 are highlighted.

Formulation	O:W ratio	Texture (F: fluid, V: viscous; SS: semi-solid)	Ease of pipetting	Phase separation	Ability to disperse again upon agitation	Suitable for further studies
ME-1	1 : 1	F	YES	PARTIAL	YES	
ME-2	4 : 1	F	YES	COMPLETE	-	
ME-3	4 : 1	F	YES	PARTIAL	YES	YES
ME-4	2.3 : 1	V	YES	-	-	YES
ME-5	4 : 1	F	YES	COMPLETE	-	
ME-6	4 : 1	V	-	-	-	
ME-7	2.3 : 1	V	-	-	-	
ME-8	3:1	F excessively	YES	COMPLETE	YES	
ME-9	1.5 : 1	F excessively	-	PARTIAL	YES	
ME-10	8 : 1	F excessively	YES	COMPLETE	-	
ME-11	4 : 1	F excessively	YES	-	-	
ME-12	4.7 : 1	V	-	-	-	
ME-13	2.3 : 1	V	-	PARTIAL	YES	
ME-14	3 : 1	SS	-	PARTIAL	YES	
ME-15	2.8 : 1	SS	-	-	-	
ME-16	3.2 : 1	V	YES	PARTIAL	YES	YES
ME-17	2.7 : 1	F	YES	PARTIAL	-	
ME-18	2.7 : 1	V	YES	PARTIAL	YES	YES
ME-19	2.7 : 1	F excessively	YES	COMPLETE	YES	
ME-20	3.2 : 1	F excessively	YES	PARTIAL	YES	
ME-21	2.7 : 1	V	YES	COMPLETE	YES	YES
ME-22	3 : 1	V	-	COMPLETE	YES	
ME-23	3 : 1	V	-	PARTIAL	YES	
ME-24	3 : 1	V	-	PARTIAL	YES	
ME-25	4 : 1	V	YES	PARTIAL	YES	YES

Development of O/W MEs loaded with compounds S6 and MDL-800.

The formulation ME-25 was then loaded with the compounds S6 and MDL-800. The first step was the definition of the dose to apply to each mouse, such as the amount of APIs to be delivered and volume of ME to apply to the DS during each treatment (Table 18). Following

this, the MEs containing S6, MDL-800 or their DMSO vehicle were prepared. The dispersions thus obtained were then stored at 4°C for 6 months, simulating the storage condition that they have to undergo during the *in vivo* studies.

Visual inspections at 1 week, at 1, 3 and 6 months after preparation revealed a homogenous dispersion with a milky and translucent appearance and a texture similar to the one of ME-25; this means that the APIs do not affect the stability profile of the formulation and that they have been effectively encapsulated in the systems (Figure 25). Moreover, similarly to ME-25, at 3 and 6 months the drug-loaded MEs displayed a suitable viscosity for the intended topical application and they were easy to pipette; furthermore, they presented little phase separation and were able to restore the dispersion's stability upon gentle hand agitation. At the 3-month timepoint, the chemical stability of the APIs contained in the MEs tested by HPLC revealed that S6 and MDL-800 were both stable in the MEs and were not degraded.

Once it was certified the stability of the S6- and MDL-800-loaded MEs, bulk amounts of the formulations were prepared for the following *in vivo* study. In particular, about 90 mL were prepared of each type of formulation, namely ME-BLK containing the APIs' vehicle DMSO, ME-S6 loaded with S6 (4 mg/mL), and ME-MDL-800 loaded with MDL-800 (10.67 mg/mL). To be noted that compound MDL-800 was readily synthesised prior to the MEs' preparations, while compound S6 was purchased.

Table 18. Desired dose of S6 and MDL-800 to apply to the mouse DS in the *in vivo* studies.

Compound	Dose per mouse	Amount of the compound in 1 dose (150 µL of ME) considering an average mouse weight of 20 g
S6	30 mg/kg	0.6 mg
MDL-800	80 mg/kg	1.6 mg



Figure 25. O/W ME containing MDL-800 (left) and S6 (right). The formulations appear as milky, clear dispersions.

4. Skin cancer progression delayed by a SIRT-6 inhibitor in an *in vivo* cSCC mouse model

SIRT-6 is involved in a variety of cancer-related mechanisms (44), including several in skin cancers and in cSCC (details in Introduction, paragraph 4.1). Given the discrepancy of the different studies on the role of SIRT-6 in cSCC, with some reporting the oncosuppressive role of this sirtuin and with some others its pro-tumorigenic one, and acknowledging that no studies have ever been performed on the pharmacological modulation of SIRT-6 in this type of cancer, the goal of this part of project was the topical treatment of a skin cancer mouse model with a SIRT-6 inhibitor, identified in S6, and with a SIRT-6 activator, namely MDL-800. The skin cancer mouse model used was the one obtained from the two-step carcinogenesis protocol DMBA-TPA, that results in the formation of benign tumours, namely the papillomas, progressing to aggressive cSCC and finally to invasive tumours. The topical treatment of the mice skin with the sirtuins modulators was achieved by applying the MEs containing the APIs vehicle (BLK), or S6 or MDL-800 to the DS of mice. The application of the MEs was performed

following three different approaches: in the first the aim was the investigation of a therapeutic effect of both modulators on the skin cancer progression, while in the other two the goal was to define the involvement of SIRT-6 in the early phases of carcinogenesis, such as the initiation and the promotion. The treatment plan is depicted in Figure 26. To be noted that mice of the first group were treated for a longer period in the carcinogenesis protocol (28 weeks), compared to the ones of group 2 and 3 (17 weeks) in order to evaluate cancer progression to SCCs. Details of the concentrations of the APIs within the MEs and of the composition of the MEs are reported in Results & Discussion, paragraph 3.

For each group, the different treatments (BLK, S6 and MDL-800) were compared first by evaluating the papilloma and tumour incidence on the DS at a 13 weeks timepoint and at sacrifice, then by analysing the DS and the papillomas with molecular and immunohistochemical techniques, such as WB, Haematoxylin & Eosin (H&E) and Immunofluorescence (IF). In particular, after confirming by WB the modulation of SIRT-6 by S6 and MDL-800, skin cancer progression markers were analysed by WB and IF and skin morphology was assessed by H&E.

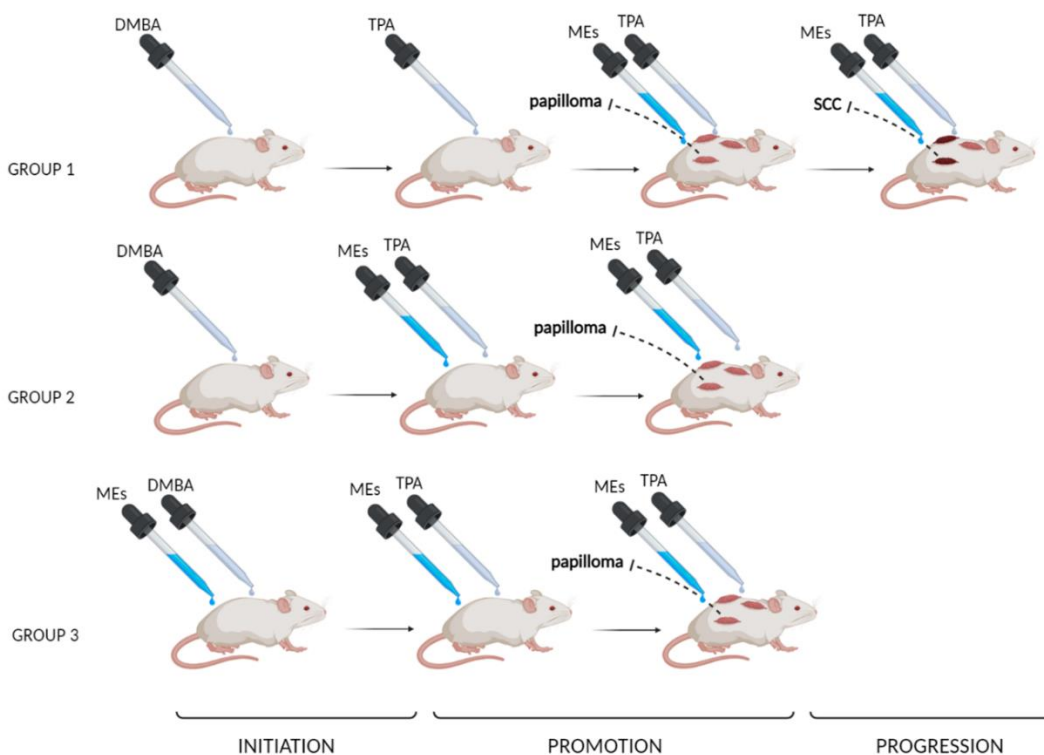


Figure 26. Treatment plan of the 2-stage carcinogenesis mouse model with MEs (containing the SIRT-6 modulators or the compounds' vehicle): in group 1 the treatment has a therapeutic approach, while in group 2 and 3 it is a preventive one.

Evaluation of SIRT-6 expression at different stages of skin carcinogenesis.

Although SIRT-6 expression in cSCC has been analysed by several research groups, that reported its overexpression in cSCC human tissues (Table 9), a full profile of the levels of this sirtuin at different stages of skin carcinogenesis was still to investigate.

At different time points of a previously developed skin carcinogenesis mouse model obtained with a DMBA-TPA treatment (described in Materials & Methods), the abundancy of this sirtuin in DS samples was examined. It was observed that SIRT-6 steadily increased during all

the tumorigenic steps (Figure 27). Drawing conclusions from these results, the best therapeutic plan would be the treatment of mice DS with a SIRT-6 inhibitor. Nevertheless, treatment with the activator MDL-800 and at different stages of carcinogenesis were also performed.

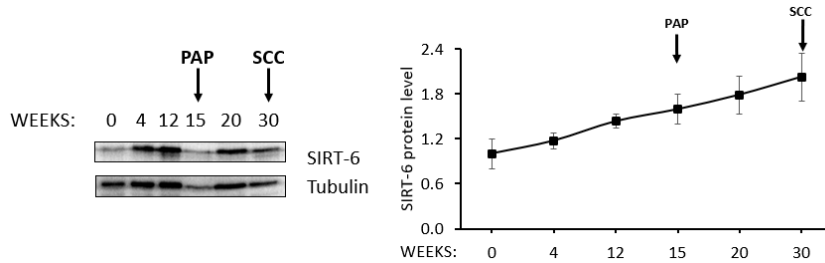


Figure 27. SIRT-6 protein level in DS of mice at different stages of skin carcinogenesis.

Preventive approach: MEs treatment started at the promotion stage with TPA.

The group of mice treated with MEs (BLK, S6, MDL-800) at the promotion stage of carcinogenesis, namely in correspondence with TPA treatment (classified as group 2), aims at the investigation of a preventive effect of SIRT-6 modulation in skin cancer; this represents the best characterised treatment group, as it was evaluated by visual inspection and by several techniques.

At first, visual inspection of mice DS at 13 weeks and at sacrifice (17 weeks), showed that S6 reduced papillomas' frequency at both timepoints compared to control group, whereas MDL-800 at 13 weeks had little effect and at 17 weeks it displayed an opposite effect to S6 (Figure 28).

SIRT-6 modulation by S6 and MDL-800 was assessed by evaluating the acetylation levels of SIRT-6 substrates H3K9 and H3K56 by WB analyses (Figure 29). When SIRT-6 was inhibited by S6 the acetylation levels of the substrates increase, while when activated by MDL-800 they decreased, compared to control group. This result confirmed first that MEs were able to pass the skin barrier, then that they were able to successfully release the APIs to the epidermis, and then that the SIRT-6 modulators were able to reach their target, exerting their effects.

Once it was confirmed SIRT-6 modulation by S6 and MDL-800 *in vivo*, it was investigated if this had an effect on skin cancer progression, and in particular on EMT, and on keratinocyte proliferation.

EMT plays a crucial role in cancer, in particular in cancer cell migration, invasion and metastatic dissemination; its molecular markers can therefore give an indication of the stage of cancer progression. SIRT-6 inhibition by S6 had a positive effect on the progression of papillomas to SCCs, by halting the EMT in S6-treated lesions. In detail, at the protein level, the mesenchymal tumour marker vimentin is absent in S6-treated lesions, while E-cadherin is abundant in a comparable way to the control group. This results in a high E-cadherin/vimentin ratio, which is associated to a more epithelial phenotype and to a less advanced EMT, and therefore to a less advanced carcinogenic stage (Figure 30); this result was confirmed by IF analyses (Figure 31b and Figure 32). In contrast to SIRT-6 inhibition, its activation by MDL-800 accelerated the lesions' transition from an epithelial to a mesenchymal phenotype: MDL-800-treated lesions expressed vimentin to a similar extent to

the control group, and this was observed by WB and by IF (Figure 31b and Figure 32). Although the E-cadherin/vimentin ratio was similar to the one of the control group (Figure 30), E-cadherin IF stained sections showed that in MDL-800-treated lesions, the expression of this epithelial marker is reducing (Figure 31b), hinting a more advanced stage of the EMT, and thus of carcinogenesis, in these lesions. This can be concluded also by observing that the skin tumour marker keratin 8 is expressed solely in MDL-800-treated lesions, and not in the S6 ones or in the control group. The histological examination of papillomas by H&E confirmed the more advanced stage of tumour progression in MDL-800-treated papillomas compared to the control group, as well as the benign nature of the papillomas of the S6-treated mice (Figure 31a).

Epidermal hyperproliferation, which is a process occurring in cancer, along with hyperproliferative epidermal disorders and skin wound healing, is characterised often by an overexpression of keratin 6. IF staining with this protein revealed that both S6- and MDL-treated mice, along with the control group, presented epidermal hyperplasia.

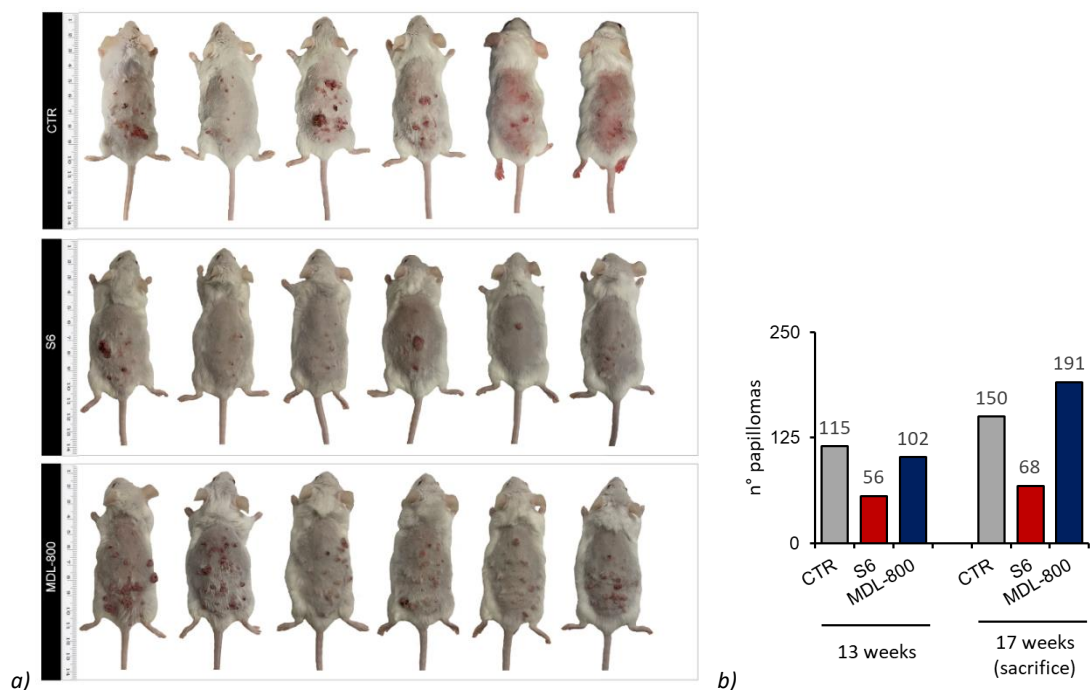


Figure 28. a) Appearance of DS of group 2 mice at sacrifice (17 weeks). b) Frequency of papillomas on DS of group 2 mice at 13 weeks and at sacrifice (17 weeks).

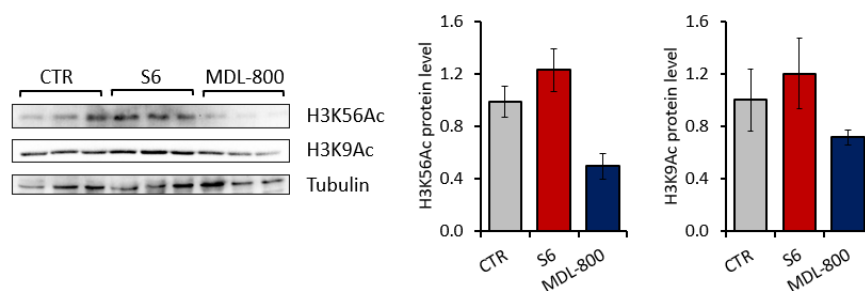


Figure 29. Effects on the acetylation levels of H3K9 and H3K56 of the treatment of mice DS with S6 and MDL-800 in a preventive approach (group 2 treatment).

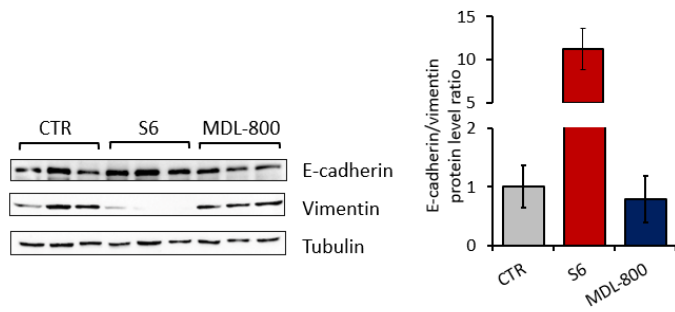
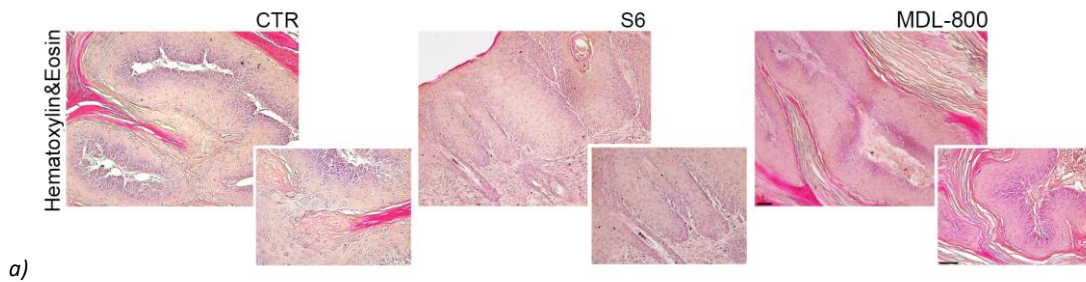
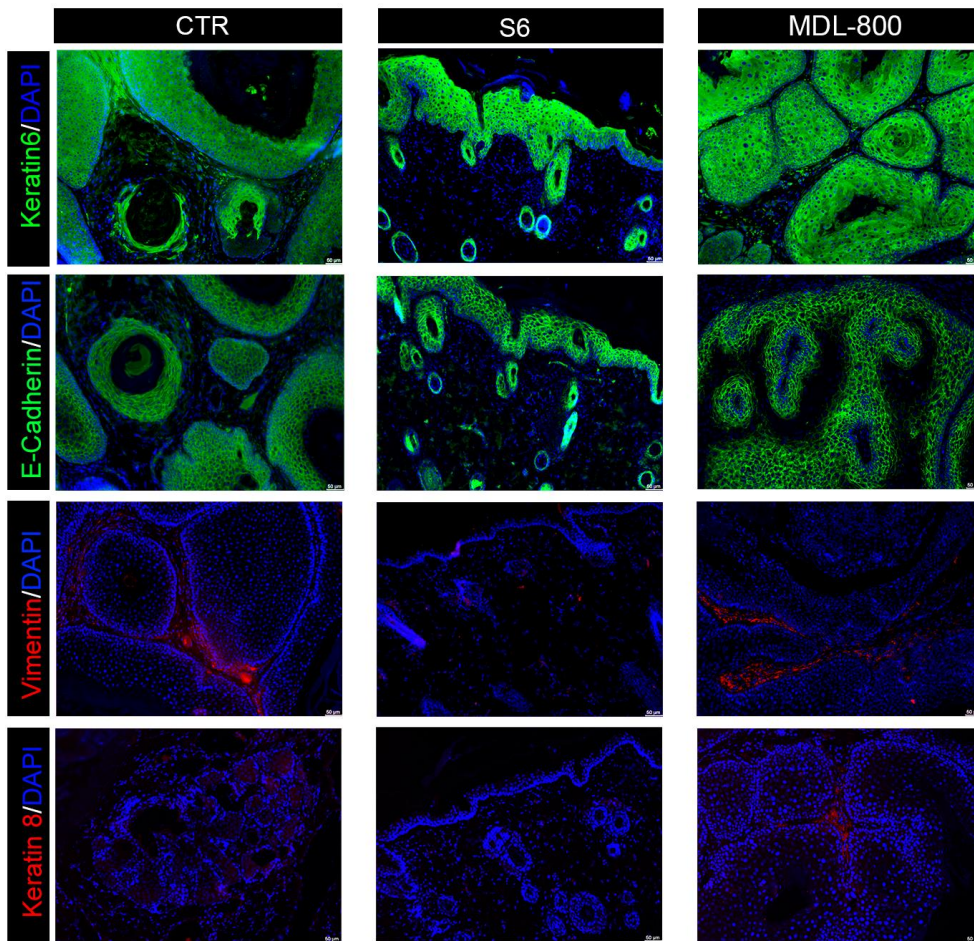


Figure 30. Effects on the levels of EMT markers E-cadherin and vimentin of the treatment of mice DS with S6 and MDL-800 in a preventive approach (group 2 treatment), by WB analysis.



a)



b)

Figure 31. a) H&E staining of histological sections of the same samples. 10x and 20x magnification (black bar: 50 μ m). b) IF staining with EMT markers E-cadherin and vimentin, and epidermal hyperproliferating marker keratin 6, and skin tumour marker keratin 8 of the same samples. 10x magnification (white bar: 50 μ m).

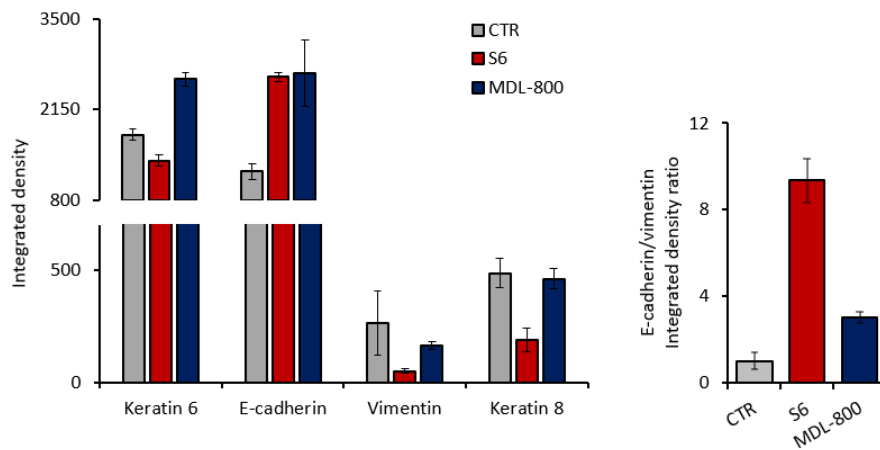


Figure 32. Densitometric analysis of the levels of keratin 6, E-cadherin, vimentin and keratin 8 of the IF staining.

Therapeutic approach: MEs treatment started after the papillomas appearance on the DS of mice.

The group of mice treated with MEs (BLK, S6, MDL-800) at the progression stage of carcinogenesis, namely after the arising of papillomas (classified as group 1), aims at the examination of a therapeutic effect of SIRT-6 modulation in skin cancer. Although this treatment group has been less characterised than group 2 and is currently under investigation, the overview of the DS of the mice of this group of sacrifice are reported here (Figure 33). To be noted that size and number of papillomas are not an indication of tumour progression, with small tumours that can be highly invasive, or with big papillomas that can be only superficial, with an epithelial phenotype.

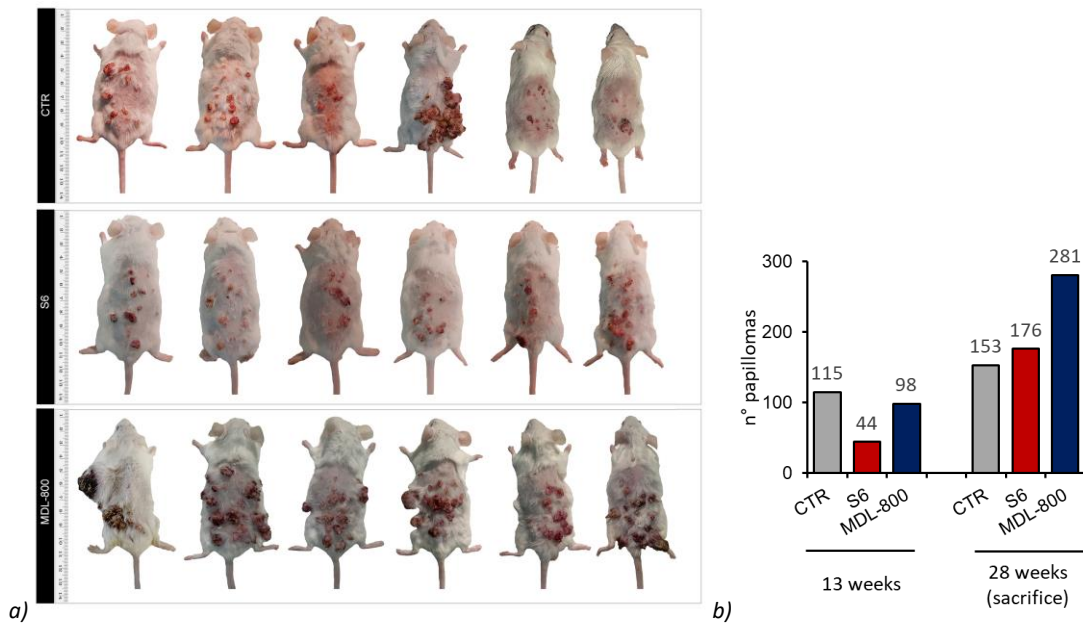


Figure 33. a) Appearance of DS of group 1 mice at sacrifice (28 weeks). b) Frequency of papillomas on DS of group 1 mice at 13 weeks and at sacrifice (28 weeks).

Preventive approach: MEs treatment started before the initiation stage with DMBA.

The group of mice treated with MEs (BLK, S6, MDL-800) prior to the initiation stage of carcinogenesis, namely before DMBA treatment (classified as group 3), aims at the examination of the preventive effect of SIRT-6 modulation in skin cancer. Although this treatment group has been less characterised than group 2 and is currently under investigation, the overview of the DS of the mice of this group of sacrifice are reported here (Figure 34).

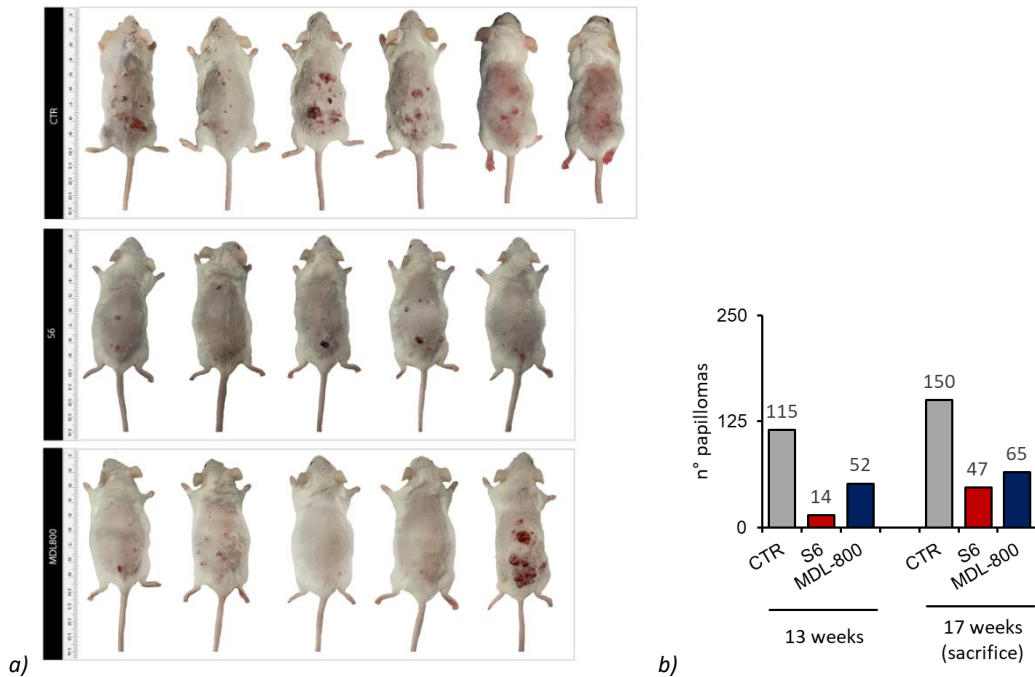


Figure 34. a) Appearance of DS of group 3 mice at sacrifice (17 weeks). b) Frequency of papillomas on DS of group 3 mice at 13 weeks and at sacrifice (17 weeks).

In conclusion, it was observed that SIRT-6 expression increases throughout the different stages of skin carcinogenesis of a DMBA-TPA mouse model. This is in accordance with the results obtained so far from the topical treatment of DS of mice with the SIRT-6 inhibitor and activator.

When SIRT-6 was inhibited in a preventive approach (group 2), skin cancer progression was delayed. Specifically, skin lesions were less invasive, since the skin tumour markers vimentin and keratin 8 were not observed, and since they displayed a higher E-cadherin/vimentin ratio, in contrast to the control group. On the contrary, activation of SIRT-6 in the same set of experiments had a negative or neutral effect on the skin lesions.

5. Is SIRT-2 involved in cSCC?

Along with defining the role of SIRT-6 in cSCC, one smaller investigation aimed at clarifying the involvement of SIRT-2 in this type of cancer.

SIRT-2 has been reported with a controversial role in cSCC, with one group demonstrating its overexpression both at the mRNA and at the protein levels in human cSCC tissues (159), and with one other showing instead its downregulation in human cSCC tissues and its oncosuppressive role in DMBA-TPA mice studies (191). In order to shed a light on the role of this sirtuin, its expression was analysed in DS tissues collected from DMBA-TPA treated mice at different stages of carcinogenesis. mRNA results showed that SIRT-2 is expressed quite homogeneously throughout the initiation, the promotion and the papilloma formation stage, while it presents a sharp 5-fold increase in advanced SCC tissues compared to healthy tissues (Figure 35). This result confirms the observations of the Jacobson's group, suggesting an oncopromoter role of this sirtuin in cSCC.

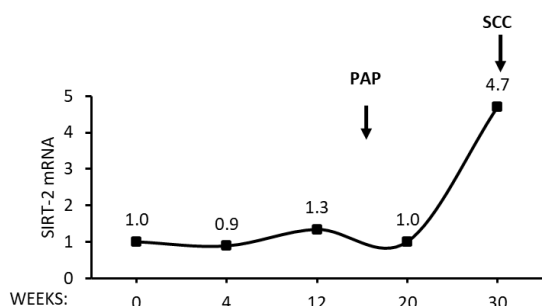


Figure 35. mRNA expression of SIRT-2 in DS of mice at different stages of skin carcinogenesis.

In virtue of these results, few studies on the pharmacological effect of SIRT-2 inhibitors on cultured cancerous keratinocytes were further performed.

Among the SIRT-2 inhibitors discovered through CADD and described in paragraph 2, 10 compounds were chosen for the treatment of cancerous keratinocytes. In particular, the compounds displaying either the highest inhibitory potential against SIRT-2 activity or the lower interference with the other sirtuins (CMP 1, 3, 4, 5, 6, 7, 11, 12, 13 and 22) were selected. Viability analyses by SRB assay were performed on immortalized normal human keratinocytes (HaCaT) and on cancerous keratinocytes (SCC13) treated for 24 with the compounds at concentrations in the 0.1 – 10 μ M range. All inhibitors, except for CMP6, CMP7 and CMP13, displayed cytotoxic effects on both SCC13 and HaCaT cells, reducing their cell viability (Figure 36). Moreover, two compounds, namely CMP1 and CMP5, exerted a stronger effect on SCC13 compared to HaCaT cells, pointing out these two compounds for further characterisation.

These results can be placed in the wider picture of the cytotoxic and anti-proliferative properties of the SIRT-2 inhibitors. SIRT-2 is involved in cell cycle regulation, and in particular in the G(2)/M transition (20), and its disruption halts cell proliferation. Because of these features, SIRT-2 inhibitors are often used in cancer studies as therapeutic agents (as described in Introduction, paragraph 2.1). These experiments suggest that SIRT-2 inhibitors could be used as anti-cancer agents also in cSCC together with other cancer types.

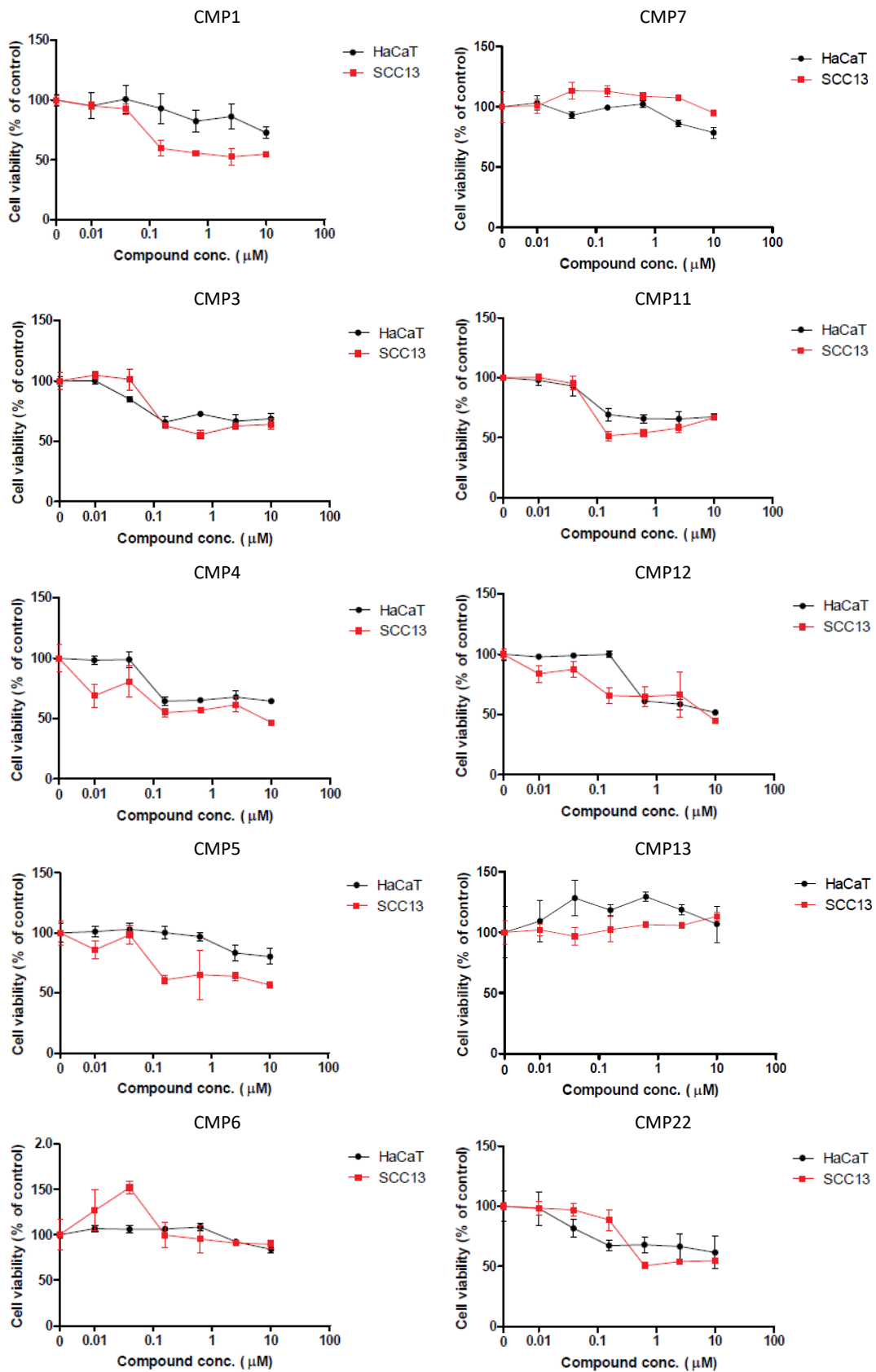


Figure 36. Cell viability of SCC13 and HaCaT cells treated with different SIRT-2 inhibitors for 24 h.

CONCLUSIONS

In this PhD project, the two main goals were the discovery of novel sirtuin inhibitors, and specifically of SIRT-2 and of SIRT-6, and the evaluation of SIRT-6 pharmacological modulation in a skin cancer mouse model.

At first, HPLC-based methods were developed in order to screen the enzymatic activity of SIRT-1, SIRT-2, SIRT-3 and SIRT-6, and specifically their deacetylation (SIRT-1, -2, -3, -6) and their deacylation (depalmitoylation of SIRT-6). Given the weak deacetylase activity of SIRT-6, two activators were added to the reaction mixture, in order to aid reaction progression, and obtain reliable results. The two activators chosen were the commercially available compound MDL-800 and the endogenous SIRT-6 activator palmitic acid.

Once the methods were set up, screenings to identify novel SIRT-6 inhibitors in a hit-to-lead discovery process were performed. The chosen hit compound was the SIRT-6 inhibitor S6, which was aimed to be improved in its water solubility and inhibition potency. Several inhibitors with an S6-derivative structure were discovered (compounds EAB1, EAB2, EAB3, EAB5). EAB2, EAB3, and EAB5 were cell membrane permeable, were not toxic in SCC cells (SCC13) and inhibited SIRT-6 more potently than the hit compound S6. Nevertheless, further characterisation of these compounds is still needed prior to their validation in *in vivo* studies. Screening of libraries of compounds for the discovery of novel SIRT-2 inhibitors was also performed. Compounds with a core structure resembling inhibitors already discovered by other groups were identified in a hit discovery process. These included thiazoles, either decorated with an ureide, or with a hydrazine, or with flexible substituents, such as benzyl-amino thiazoles, or with a rigid thiazole structure, such as amino-aryl thiazoles, then also pyrazolopyrimidines and benzimidazoles. Enzymatic activity assays on SIRT-2, as well as on other sirtuins led to the discovery of 14 compounds that inhibited SIRT-2 more than 75% at 150 μ M concentration, and did not modulate SIRT-3 and SIRT-6. SIRT-1 was inhibited by the majority of the compounds to a similar extent to SIRT-2, indicating that the identified compounds can be considered dual inhibitors of SIRT-1/SIRT-2.

Moreover, the effect of SIRT-2 and SIRT-6 modulators was investigated in cSCC.

Specifically, with the aim of applying topically on mice dorsal skin treated in a skin carcinogenesis protocol a SIRT-6 activator and a SIRT-6 inhibitor, a suitable formulation containing the two modulators was developed. The SIRT-6 activator chosen was compound MDL-800, while the SIRT-6 inhibitor was compound S6. The formulation type chosen for their topical treatment was the microemulsion technology. This allows the dissolution of both compounds that are quite lipophilic and its physicochemical characteristics aid drug absorption after topical application. The formulations prepared were specifically oil-in-water microemulsions. These were tested for stability and both the formulation and the compounds within it were stable after 3 months at 4°C.

The topical application of the formulations containing S6 and MDL-800 was performed on a 2-step carcinogenesis mouse model. In particular, a DMBA-TPA protocol was carried out and treatment with the SIRT-6 modulators was performed at different stages of carcinogenesis. A therapeutic and two preventive approaches were followed. It was observed that SIRT-6 inhibition delays skin cancer progression when the mice skin was treated with compound S6 since the first stages of carcinogenesis. The role of SIRT-6 during more advanced stages of the skin carcinogenesis protocol remains to be investigated. Moreover, an optimized time

window for the treatment would need to be carefully defined for translation of SIRT-6 targeting into the clinical setting.

SIRT-2 inhibitors were also tested on cSCC, as therapeutic options. After assessing SIRT-2 expression in skin tissues of different stages of carcinogenesis of DMBA-TPA treated mice, and concluding that in cSCC SIRT-2 might behave as an oncopromoter, SIRT-2 inhibitors, and in particular a selection of the ones previously identified, were tested on keratinocytes. SIRT-2 inhibitors exerted cytotoxic and anti-proliferative effects in both healthy (HaCaT) and cancerous keratinocytes (SCC13). Two compounds, namely CMP1 and CMP5, were able also to decrease cell viability more selectively in the SCC13 compared to the HaCaT cells.

MATERIALS AND METHODS

MATERIALS

Reagents and solvents were purchased from Sigma-Aldrich S.r.l., Milan, Italy, from Life Technologies Italia, Monza, Italy, and from VWR International S.r.l., Milan, Italy and used as received, unless otherwise indicated. Solvents used for HPLC analyses and for ME preparations were of analytical grade.

Preparation of the compounds.

SIRT-6 activator MDL-800 (CAS# 2275619-53-7) was purchased from Sigma-Aldrich S.r.l., Milan, Italy (CAT# SML2529); SIRT-6 inhibitor S6 (CAS# 1214468-35-5) from BLD Pharmatech GmbH, Kaiserslautern, Germany. (CAT# BD01051158); SIRT-2 inhibitor AGK-2 (CAS# 304896-28-4, CAT# A3193), Celecoxib (CAT# C2816) and 5-FU (CAT# F0151) from Zentek S.r.l., Milan, Italy.

Putative SIRT-6 inhibitors were purchased from SIA Enamine, Riga, Latvia, and from Life Chemicals Europe GmbH, Unterhaching, Germany; in order to ease the denomination, they were renamed EAB1 to EAB10. The compound details are summarised in Table 19. Putative SIRT-2 inhibitors, instead, had been obtained by chemical synthesis and were kindly provided by Prof. Enrico Millo and Dr. Alice Parodi, DIMES, University of Genoa, and by professors Silvia Schenone and Michele Tonelli, DIFAR, University of Genoa. These include: thiazoles decorated with an ureide (CMP 1 to 6), with a hydrazine (CMP 7 to 14), with an amino-aryl group (CMP 15 to 17) or with a benzyl-amino group (CMP 18 to 20); pyrazolopyrimidines (CMP21, CMP22); and benzimidazoles (CMP23, CMP24). The scaffolds of these compounds are depicted in Results and Discussion, paragraph 2.

Upon arrival, all compounds were dissolved in DMSO and stored at -20°C.

Table 19. List of putative SIRT-6 inhibitors.

Novel compound name	Chemical name	supplier	CAT#
EAB1	N-(2-hydroxy-4-(pyridin-3-yloxy)phenyl)-2,4-dioxo-1,2,3,4-tetrahydroquinazoline-6-sulfonamide	Life Chemicals	F9994-0199
EAB2	6-((3,3-dimethylmorpholino)sulfonyl)quinazoline-2,4(1H,3H)-dione	Enamine Ltd	Z815160334
EAB3	N-((1-aminocyclohexyl)methyl)-2,4-dioxo-1,2,3,4-tetrahydroquinazoline-6-sulfonamide	Enamine Ltd	Z1491069431
EAB4	2,4-dioxo-N-(2-(pyrrolidin-3-yl)ethyl)-1,2,3,4-tetrahydroquinazoline-6-sulfonamide	Enamine Ltd	Z2443125360
EAB5	6-((4-(3-aminopropoxy)piperidin-1-yl)sulfonyl)quinazoline-2,4(1H,3H)-dione	Enamine Ltd	Z2443412359
EAB6	2,4-dioxo-N-(3-(piperazin-1-yl)propyl)-1,2,3,4-tetrahydroquinazoline-6-sulfonamide	Enamine Ltd	Z2466219411
EAB7	N-(2-(4-bromophenyl)propan-2-yl)-2,4-dioxo-1,2,3,4-tetrahydroquinazoline-6-sulfonamide	Enamine Ltd	Z408268790
EAB8	6-((1,4-diazepan-1-yl)sulfonyl)quinazoline-2,4(1H,3H)-dione	Enamine Ltd	Z2442913983
EAB9	6-((4-(1-ethyl-1H-imidazol-2-yl)piperidin-1-yl)sulfonyl)quinazoline-2,4(1H,3H)-dione	Enamine Ltd	Z1142819502
EAB10	6-((2-(1-methyl-1H-imidazol-2-yl)piperazin-1-yl)sulfonyl)quinazoline-2,4(1H,3H)-dione	Enamine Ltd	Z2443975859

SIRT-1, -2, -6 fluorescent and chemiluminescent kit.

The SIRT-1 deacetylase activity assay kit was SIRT1 Direct Fluorescent Screening Assay Kit, Cayman Chemicals, CAT# 10010401. The SIRT-2 deacetylase assay kit was SIRT2 Direct Fluorescent Screening Assay Kit, Cayman Chemicals, CAT# 700280. The SIRT-6 deacetylase activity assay kit was CHEMILUM DE LYS® HDAC/SIRT Chemiluminescent drug discovery kit, Enzo Life Science, CAT# BML-AK532-0001.

Reagents for peptide synthesis.

The amino acids used in the peptides' synthesis were purchased from Advanced Biotech Italia, Seveso, Italy. These were specifically Tryptophan (W), Glycine (G), Threonine (T), Serine (S), Lysine (K), Arginine (R), Alanine (A), and Glutamine (Q).

Reagents for enzymatic reactions.

Recombinant human SIRT-1 (CAT# 10011190) and SIRT-2 (CAT# 10011191) were supplied from Cayman Chemical; recombinant human SIRT-3 (CAT# SRP0117) was obtained from Sigma-Aldrich S.r.l, Milan, Italy. Palmitic acid, myristic acid and MDL-800 were purchased from Sigma-Aldrich S.r.l., Milan, Italy, dissolved in DMSO and stored at -20°C.

Reagents for MDL-800 synthesis.

Reagents for MDL-800 synthesis were purchased from BLD Pharmatech GmbH, Kaiserslautern, Germany. Details of each reagent are reported in Table 20.

Table 20. Summary of the reagents used in the synthesis of compound MDL-800. Supplier: BLD Pharmatech GmbH.

Compound	CAS#	CAT#
5-Bromo-4-fluoro-2-methylaniline	627871-16-3	BD102969
Methyl 2-(chlorosulfonyl)-5-nitrobenzoate	1039020-81-9	BD750937
3,5-Dichlorobenzene-1-sulfonyl chloride	705-21-5	BD3150

Reagents for the preparation of the formulations.

Vevy Europe S.p.A., Genoa, Italy, provided Lipogelag (CAT# 04.3535) and Syntesqual (CAT# 03.1133). IPM and PEG 7 GC were purchased from Merck Life Science S.r.l., Milan, Italy, while Tween-20, Tween-80, PEG 200 and PEG 400 from Sigma-Aldrich S.r.l., Milan, Italy. Compound S6 was provided from BLD Pharmatech GmbH, as described above, while compound MDL-800 was synthesised as described in the Methods section.

Cell culture material.

HaCaT, SCC13 and HEK293 cell lines were obtained from ATCC (LGC Standards S.r.l, Milan, Italy). Gibco™ Keratinocyte SFM 1X medium supplied with prequalified human recombinant Epidermal Growth Factor 1-53 (EGF 1-53) and Bovine Pituitary Extract (BPE) (CAT# 17005042) was purchased from Thermo Fisher Scientific, Italy. Dulbecco's Modified Eagle's Medium, high glucose (CAT# D5796) was supplied from Sigma-Aldrich S.r.l., Milan, Italy.

Materials for viral transfection.

Empty plasmid pRETROSUPER (pRS) was kindly provided by Dr. Thijn Brummelkamp (Netherlands Cancer Institute, Amsterdam, The Netherlands), while plasmid pRS SIRT-6 sh1 was a kind gift of Dr. Katrin F. Chua (Department of Medicine, Stanford University School of

Medicine, Stanford, CA). TransIT®-293 Transfection Reagent (CAT# MIR 2704) was obtained from Mirus Bio, Madison, WI.

Animals.

Sixty male CD-1 mice at 56-62 days of age were used; they were purchased from Charles River Laboratories Italia S.r.l., Milan, Italy.

Materials for the skin carcinogenesis protocol and for the topical treatments.

For the carcinogenesis protocol, 7,12-dimethylbenz[a]anthracene (DMBA) (CAT# D3254) was purchased from Sigma-Aldrich S.r.l, Milan, Italy, and Phorbol 12-myristate 13-acetate (TPA) (CAT# P1585) from Merck Life Science S.r.l., Milan, Italy. Before the start of the experiments, DMBA and TPA were dissolved in acetone and stored at -20°C.

For the topical treatment with S6 and MDL-800, MEs loaded with the drugs were prepared as described in the Methods section.

Materials for protein extraction from cells.

Protease inhibitor PIC® Reagent A (CAT# WAT085101) was purchased from Waters S.p.A., Sesto San Giovanni, Italy, and 1:100 Phosphatase Inhibitor Cocktail 3 (CAT# P0044) was obtained from Sigma-Aldrich S.r.l, Milan, Italy.

Materials for mRNA extraction from skin tissues, retro transcription, and RT-PCR.

TRIzol (CAT# 15596018) and Invitrogen™ SuperScript™ VILO™ Master Mix (CAT# 11755.05) were purchased from Life Technologies Italia, Monza, Italy. All-In-One 5X RT MasterMix (CAT# G592) was supplied by Microtech Italia S.r.l., Saonara, Italy. iQ™ SYBR® Green Supermix (CAT# 1708882) was obtained from Bio-Rad Laboratories S.r.l., Segrate, Italy.

mRNA and tissue lysates of DS at different stages of skin carcinogenesis.

mRNA and protein samples obtained from DS of mice treated in a DMBA-TPA protocol and collected at different timepoints of carcinogenesis were kindly provided by Prof. Monica Dentice, Department of Clinical Medicine and Surgery, University of Naples Federico II. The samples' details can be found in (275). Of note: DS were harvested from mice at 0, 4, 12, 15, 20 and 30 weeks from the start of the DMBA treatment; at 15 weeks papillomas started arising and at 30 weeks SCCs replaced papillomas.

Antibodies for Western Blot and for Immunofluorescence.

The primary antibodies used in WB and IF analyses are listed in Table 21.

Secondary antibodies used in WB analyses were: anti-mouse IgG-HRP (CAT# 1706516) and anti-rabbit IgG-HRP (CAT# 1706515), purchased from Bio-Rad Laboratories S.r.l., Segrate, Italy; they were diluted 1:3000 in the blocking buffer used during the WB analysis. ECL kit for chemiluminescent detection was obtained from Merck Life Science S.r.l., Milan, Italy (CAT# WBKLS0500).

Secondary antibodies used in IF analyses were: anti-rabbit, and anti-rat conjugated to AlexaFluor488 (Molecular Probe, 1:300) and AlexaFluor594 (Molecular Probe, 1:300).

Table 21. List of antibodies used for WB and IF.

Antibody	Supplier	CAT#	Use and dilution
Mouse monoclonal anti- E-cadherin	BD Biosciences	610181	1:500 IF 1:1000 WB
Rabbit monoclonal anti-Vimentin	ABCAM	ab-92547	1:2000 WB 1:1000 IF
Rabbit polyclonal anti- α Tubulin	Santa Cruz Biotechnology	SC-5546	1:5000 WB
Rabbit polyclonal anti-cytokeratin 6	COVANCE	PRB-169P	1:1000 IF
Rat anti-cytokeratin 8 (TROMA 1)	Hybridoma bank	AB_531826	1:300 IF
Rabbit polyclonal anti-acetylated H3K9	Merck Life Science	H9286	1:10000 WB
Rabbit polyclonal anti-acetylated H3K56	Cell Signalling Technology	4243	1:1000 WB
Rabbit polyclonal anti-histone H3	Cell Signalling Technology	9715	1:5000 WB
Rabbit monoclonal anti-Sirt6	Cell Signalling Technology	12486	1:1000 WB
Rabbit polyclonal anti-keratin 1	Merck Life Science	SAB2101300	1:1000 WB
Rabbit polyclonal anti-vinculin	Cell Signalling Technology	E1E9V	1:1000 WB

Oligonucleotides used for RT-PCR.

Specific primers for each gene were designed to generate products of comparable sizes (about 200 bp for each amplification) (Table 22). Oligonucleotides were purchased from Merck Life Science S.r.l., Milan, Italy. They were stored at -20°C as powders or as water solutions.

Table 22. List of oligonucleotides used for RT-PCR.

Gene	Forward primer (5' → 3')	Reverse primer (5' → 3')
Cyclophilin A (CypA)	CGCCACTGTGCGTTTTTCG	AACTTTGTCTGCAAACAGCTC
Sirtuin 2 (Sirt2)	TGCAGGAGGCTCAGGATTCA	AGACGCTCCTTTGGGAACC

METHODS

CADD for SIRT-6 inhibitor identification.

The search of potential SIRT-6 inhibitors was pursued via CADD, and specifically through SBDD.

The chemical structure of the desired compounds was derived from the one of the SIRT-6 inhibitor S6 (described in Introduction, paragraph 2.2). In the hit-to-lead process, this compound is defined as the hit compound, while the novel structures identified are the potential lead compounds. With the aim of improving the solubility and the potency of S6, the functional groups believed to interact with SIRT-6 and the hydrophilic ones, such as the quinazoline-2,4(1H,3H)-dione building block and the sulphonamide (Figure 4), were kept as core structures of the novel inhibitors, while modifications were made on the right building block. First, in a database of more than 1 million compounds present on the platform available from www.mcule.com, all the compounds containing the desired S6 core structure were collected (212 compounds). Subsequently, a selection of the structures with improved water solubility compared to S6, but free of toxic or easily metabolized group was performed. These molecules were characterised by the following features: 1) not yet published as SIRT-6 inhibitors, 2) featuring maximum two chiral centres, 3) not presenting a bulky structure (MW<500kDa), 4) presenting features related to improved solubility, such as presence of polar functional groups, presence of double bonds or of functional groups that break a possible crystallisation process between molecules, low MW, logP lower than the one of S6, 5) few halogen atoms, 6) not rigid structure, 7) absence of toxicophores. In this step, 157 compounds were retained. Following this, a further screening of the compounds was made

in order to reduce the number of compounds, but still maximising the diversity of the different structures. 25 compounds were selected in this step.

Subsequently, through VS, the compounds' binding affinity to the active site of SIRT-6 was examined. The *in silico* evaluation of the potency of the compounds was achieved by computationally inserting each compound in the active site of SIRT-6 (PDB: 6HOY), using the docking programme Autodock Vina (276, 277). The compounds were screened on several parameters and the ones with the following features were selected: 1) few poses available (and preferentially just one), 2) high number of hydrogen bonds between molecule and active site, 3) absence of empty spaces in the pocket, 4) absence of collision in the electrostatic potential between molecule and enzyme, 5) a low-energy conformation of the molecule, 6) hydrophilic nature of the functional groups of the molecule that are outside the pocket and exposed to the solvent. Ten compounds were finally chosen in this last step; they are described in the Materials paragraph, and their chemical structure is depicted in Results and Discussion, paragraph 2.

CADD for SIRT-2 inhibitors identification.

The search of putative SIRT-2 inhibitors was pursued via CADD, and specifically through SBDD, by Prof. Elena Cichero, DIFAR, University of Genoa.

The process used for the discovery of potential modulators of this other sirtuin, was a hit identification one. In one first set of experiments, by exploiting the knowledge of SIRT-2 inhibition characteristics by compound SirReal2 (described in Introduction, paragraph 2.1), the core structure that was identified as promising and to seek in potential SIRT-2 inhibitors was the thiazole group. A wide library of compounds synthesised by several groups at DIFAR and DIMES, University of Genoa, and available for Prof. Cichero, was used for the screening of the compounds. The compounds featuring the desired backbone were docked into the active site of SIRT-2 (PDB: 4RMG) using Autodock Vina (276, 277) and 20 of them were selected. With a similar approach to the identification of thiazole SIRT-2 inhibitors, first thienopyrimidinones (272) and then indoles with a 3-cyclic structure (273), led to the identification of two pyrazolopyrimidines, and of two benzimidazoles, respectively. At this stage, 24 compounds were selected as putative SIRT-2 inhibitors and ready for *in vitro* testing. They are described in the Materials paragraph, and their chemical scaffold is depicted in Results and Discussion, paragraph 2.

Drug profile prediction of the putative SIRT-6 inhibitors.

All the putative SIRT-6 inhibitors were screened for a drug profile prediction evaluation, through software ACD/Percepta 14.0.0. The properties evaluated were: 1) physicochemical profiling: logP, MW, H-donors, H-acceptor, rotatable bonds, rings, Lipinski violations, lead-like, solubility; 2) ADME profiling: Caco-2 (*in vitro* model of the human small intestinal mucosa to predict the adsorption of orally administered drugs), plasma protein binding (PPB), CNS penetration properties, Human intestinal absorption (HIA); 3) metabolic stability; 4) drug safety profiling: P-gp substrates, cytochrome P450 inhibitor, Ames (assessment of the mutagenic potential of the compound) and hERG (evaluation of cardiotoxicity).

H3K9Ac and H3K9Palm peptide synthesis.

Peptides H3K9Ac and H3K9palm were synthesised using the standard 9-fluorenylmethoxycarbonyl (Fmoc) strategy of solid-phase peptide synthesis, as previously described (278).

The final products (Table 23) were judged to have a purity of 95% or higher, based on analytical HPLC/MS analysis. After lyophilisation, the peptides were stored as solid powders at -80°C. Alternatively, they were dissolved in DMSO and stored at -20°C.

Table 23. Detail of the peptides synthesised and reaction yield for both of them.

Name	Peptide of origin	Sequence	MW (g/mol)	Reaction yield
Pep-H3K9Ac	H3K9Ac	HOOC-WWGGTS(KAcetyl)IRATQK-NH ₂	1447.57	20% (8.1 mg)
Pep-H3K9Palm	H3K9Palm	HOOC-WWGGTS(KPalm)IRATQK-NH ₂	1643.38	46% (16.6 mg)

Recombinant SIRT-6 synthesis.

Recombinant SIRT-6 was synthesised as previously reported in (92). The purity of the recombinant protein was confirmed by electrophoresis. The pellet obtained was then dissolved in a glycerol/MQ water mixture (1.6 mL) with 20% glycerol. Final concentration of the protein was 68.8 μM.

Screening of different reaction conditions to evaluate the deacetylation of SIRT -2.

In a 30 μL reaction phosphate buffer, recombinant SIRT-2 was incubated with peptide H3K9Ac (240 μM), NAD⁺ (100 μM) and DMSO (1 μL) at 37°C. SIRT-2 concentration used was 195, 269 or 807 nM, and the reaction time was 10 or 20 min. The optimal reaction conditions (Table 11) were identified in the ones with a steady-linear correlation between reaction progression and time or SIRT-2 concentration. Moreover, different reaction buffers, such as 20 mM Tris pH 7.4, 20 mM phosphate buffer, and the buffer from the SIRT2 Direct Fluorescent Screening Assay Kit (50 mM Tris-HCl, pH 8.0, with 137 mM NaCl, 2.7 mM KCl, and 1 mM MgCl₂) were tested in the following way. A part from comparing the SIRT-2 activity in the different buffers, the solubility properties of one representative test compound (chosen among those further examined in the SIRT-2 inhibitor screening), namely Compound 15, was evaluated in the three buffers. Both in the SIRT-2-kit buffer and in Tris buffer the compound precipitated, while in the phosphate buffer it remained in higher portion in solution at 500 μM concentration. Compound 15 furthermore remained completely in solution at 200 μM concentration, thus defining this as the buffer to use in the future SIRT-2 reactions.

One other parameter taken into account while assaying SIRT-2 was the DMSO amount in the reaction mixture, which was fixed at max 5% of the reaction volume. The DMSO contribution to the 30 μL reaction mixture was given by the peptide H3K9Ac, which was dissolved in DMSO, and by 1 μL added to simulate the vehicle of the compounds later tested.

Screening of different reaction conditions to evaluate the deacetylation of SIRT -1 and -3.

In a 30 μL phosphate buffer, recombinant SIRT-1 was incubated with peptide H3K9Ac (240 μM), NAD⁺ and DMSO (1 μL) at 37°C. SIRT-1 concentration used was 17.3, 34.6 nM, NAD⁺ concentration was 100 or 500 μM, and the reaction time was 10, 20 min or 1 h.

In a 30 μL phosphate buffer, recombinant SIRT-3 (200 nM) was incubated with peptide H3K9Ac (200 μM), NAD⁺ (100 μM) and DMSO (1 μL) at 37°C for 10, 20 min and 2 h.

The optimal reaction conditions (Table 11) were identified in the ones with reaction progression linearly correlated with time and SIRT and NAD⁺ concentration.

One other parameter taken into account while assaying SIRT-1 and -3 was the DMSO amount in the reaction mixture, which was fixed at max 5% of the reaction volume. The DMSO contribution to the 30 μ L reaction mixture was given by the peptide H3K9Ac, which was dissolved in DMSO, and by 1 μ L added to simulate the vehicle of the compounds later tested.

Reaction conditions to assay SIRT-6 depalmitoylation.

Relying on previous knowledge of the lab regarding the SIRT-6 demyristoylation assay settings, the optimal reaction conditions for the depalmitoylation, which is also a deacylation, of SIRT-6 were identified (Table 11). Briefly, recombinant SIRT-6 (4.59 μ M), which had been previously synthesised, was incubated with peptide H3K9Palm (100 μ M), NAD⁺ (100 μ M) and DMSO (1 μ L) at 37°C for 30 min. The reaction was carried in 30 μ L of a 20 mM Tris 7.4 pH buffer, containing 4 mM MgCl₂ (Table 11). Along with the maximum DMSO amount in the reaction mixture, particular attention was paid also to the concentration also of glycerol, as the recombinant SIRT-6 stock solution (68.8 μ M) contained 20% glycerol; in the reaction mixture the amount of glycerol was approximately 1.3%.

Screening of different SIRT-6 activators to assay SIRT-6 deacetylation.

Recombinant SIRT-6 (4.59 μ M) was incubated with peptide H3K9Ac (240 μ M), NAD⁺ (500 μ M) and DMSO (1 μ L) at 37°C for 30 min, 1 and 2 h. The reaction was carried in 30 μ L of a 20 mM Tris 7.4 pH buffer, containing 4 mM MgCl₂. A decrease in the reagent level or an increase in the one of the product were not observed still after 2h, being SIRT-6 a weak deacetylase. Therefore, in order to investigate this enzymatic activity, SIRT-6 activators were added to the reaction mixture. Three known activators were screened: compound MDL-800, and the FAs palmitic acid and myristic acid; these activators have all been described in Introduction, paragraph 2.2. Briefly, at the same reaction conditions described above, either MDL-800 (100 μ M), palmitic acid (PA) (150, 300 μ M) or myristic acid (MA) (400, 500 μ M) were added.

On the one side, MDL-800 was stable and proved to activate potently SIRT-6 deacetylation. On the other side, comparing PA (300 μ M) and MA (500 μ M), PA activated SIRT-6 6-fold more potently than MA, even though it was less concentrated; moreover, they were both weaker activators than MDL-800 (Figure 37). PA was therefore the FA chosen to continue the studies. The concentration chosen for this activator was further adapted to 150 μ M, in order to use an amount well below the critical micellar concentration, avoiding thus completely the formation of micelles (7). In Table 11, the most suitable reaction conditions to assay SIRT-6 deacetylation either with MDL-800 or PA are reported. As for the previous reactions, particular attention was paid to the maximum DMSO amount in the reaction mixture, which was defined mainly by the contributions first of the peptide H3K9Ac dissolved in a DMSO solution, then of the DMSO representing the compound vehicle, and finally of MDL-800 or of PA, that are also dissolved in DMSO. Also the concentration of glycerol was monitored, as the recombinant SIRT-6 stock solution (68.8 μ M) contained 20% glycerol; in the reaction mixture the amount of glycerol was approximately 1.3%.

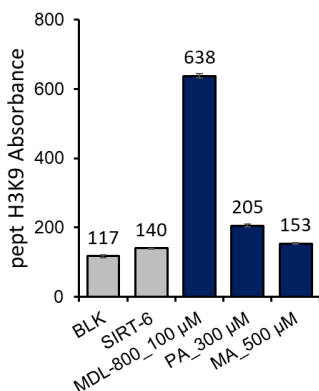


Figure 37. Amount of the deacetylated peptide H3K9 in a SIRT-6 deacetylation reaction activated either with MDL-800, palmitic acid or myristic acid. Abbreviation: PA, palmitic acid. MA, myristic acid.

Screening of different HPLC settings to evaluate the deacetylation/deacylation of sirtuins.

In order to obtain the best chromatographic separation of the reaction mixture components, different eluents A and B were screened: eluent A and B either H₂O + FoA 0.1%, and AcCN + FoA 0.1%, or H₂O + TFA 0.05%, and AcCN + TFA 0.02%, as well as different HPLC run gradients. In addition, for the detection of the different entities contained in the mixtures injected also different wavelengths were examined, such as 220, 254 and 280 nm. Optimal HPLC settings are the following. In an Agilent Technologies 1260 HPLC, with a ZORBAX® Eclipse Plus C18 3.5 µM, 4.6 mm × 10 mm column set on 25°C a fixed volume of 45 µL is injected. The reactions are monitored by quantifying the amount of deacetylated peptide H3K9 produced or of acetylated/palmitoylated peptides H3K9Ac and H3K9Palm consumed during the enzymatic reaction, at 220 nm. Optimal separation of substrate and product is obtained with two different HPLC methods for H3K9Ac/H3K9 and H3K9Palm/H3K9. For H3K9Ac/H3K9 the mobile phase consists of eluent A and B, with the following gradient of eluent B: 0 – 5 min 5%; 5 – 16 min, 5 – 25.1%; 16 – 20 min, 100%; 20 – 24 min, 100%; 24 – 24.1 min, 100 – 5%, at 1mL/min. Total run time is 24 minutes. Eluent A and B are H₂O + TFA 0.05%, and AcCN + TFA 0.02%, respectively.

For H3K9Palm/H3K9 the mobile phase consists of eluent A and B, with the following gradient of eluent B: 0 – 5 min 5%; 5 – 29 min, 5 – 49%; 29 – 35 min, 49 – 100%; 35 – 40 min, 100%; 40 – 40.1 min, 100 – 5%, at 1mL/min. Total run time is 40 minutes. Eluent A and B are H₂O + FoA 0.1%, and AcCN + FoA 0.1%, respectively.

Screening of different protocols to block the enzymatic reactions in the HPLC-based assay.

In the sirtuin enzymatic assay procedure, in order to block the reaction, different protocols were tested. Specifically, the experiments were carried not on the reaction mixture, but on a 20 mM Tris buffer pH 7.4 solution containing peptides H3K9Ac and H3K9Palm, evaluating thus the protein denaturation protocols' effects on the stability of the two peptides. In two first samples, to the peptide solutions, 3 volumes of either AcCN or of an acidic MeOH solution (200 mM HCl and 320 mM AcOH) were added; the 3rd sample, instead, was boiled at 83°C for 3 min and then diluted with 3 parts of the Tris buffer. All samples were then centrifuged at 16000 g for 3 min, and the supernatant was subjected to HPLC analysis.

Stability studies of the peptides H3K9, H3K9Ac and H3K9Palm in the quenching solvent.

In the sirtuin enzymatic assay procedure, after quenching the reaction in acidic MeOH, the supernatant is injected in the HPLC. However, considering that the samples are prepared contemporarily and that they are then injected in the HPLC in sequence, before being analysed one sample may lay in the vial for a period between 25 min to a few hours, since one H3K9Ac/H3K9 analysis takes 24 minutes, and one H3K9Palm/H3K9 analysis instead 40 minutes. The stabilities of the H3K9, H3K9Ac and H3K9Palm peptides in the quenching solvent were evaluated in several storage conditions, such as 2 h at 4°C, 32 h at RT, and 72 h at -20°C.

Screening of putative sirtuins' modulators by HPLC-based enzymatic assays.

Peptide H3K9Ac or H3K9Palm was incubated at 37°C with or without SIRT-1, -2, -3 or -6, with NAD⁺, and with the SIRT-6 activator MDL-800 or PA (if SIRT-6 deacetylation), and in the presence or absence of the compound to be tested. A brief reaction plan is depicted in Table 24. To be noted: each compound was pre-incubated for 5 min at RT with the recombinant sirtuin. The concentrations of the reagents, the reaction buffer and the reaction time are summarised for each type of reaction in Table 11. The compounds' final concentrations were 100 µM (SIRT-6 depalmitoylation), 150 µM (SIRT-1, -2, -3, and -6 deacetylation activated by MDL-800), or 300 µM (SIRT-6 activated by PA).

Along with the maximum DMSO amount in the reaction mixture, particular attention was paid also to the concentration also of glycerol, as the recombinant SIRT-6 stock solution (68.8 µM) contained 20% glycerol; in the reaction mixture the amount of glycerol was approximately 1.3%.

After quenching with 3 volumes of 200 mM HCl and 320 mM AcOH in MeOH, 45 µL of the supernatant was subjected to HPLC analysis, as described in the corresponding Method paragraph, and substrates or products were quantified. When the sirtuin was inhibited, the product H3K9 was less in the "SIRT + compound" sample compared to the "SIRT" one, whereas the acetylated or palmitoylated H3K9 decreased or remained at the "BLK" level (Figure 38). The opposite was observed if the sirtuin was activated. The "BLK + compound" sample was used as internal control of the reaction to verify that the compound's peak does not overlap with the one of the substrates or products, and also as internal standard of the reaction mixture.

Table 24. Overview of the composition of the reaction mixtures for evaluating the enzymatic modulation by a potential sirtuin modulator. In the table, the concentrations of the reactions referred to SIRT-2 are reported as example. Reactions were carried out at 37°C, in a total volume of 30 µL. Abbreviation: Pep, peptide. conc, concentration.

	BLK	SIRT-2	BLK + compound	SIRT-2 + compound
Sirtuin conc	-	0.269 µM	-	0.269 µM
NAD⁺ conc	100 µM	100 µM	100 µM	100 µM
Pep-H3K9Ac conc	240 µM	240 µM	240 µM	240 µM
DMSO	1 µL	-	1 µL	-
Compound	-	1 µL (150 µM)	-	1 µL (150 µM)
Reaction buffer	20mM NaH ₂ PO ₄	20mM NaH ₂ PO ₄	20mM NaH ₂ PO ₄	20mM NaH ₂ PO ₄
Reaction time	10 min	10 min	10 min	10 min

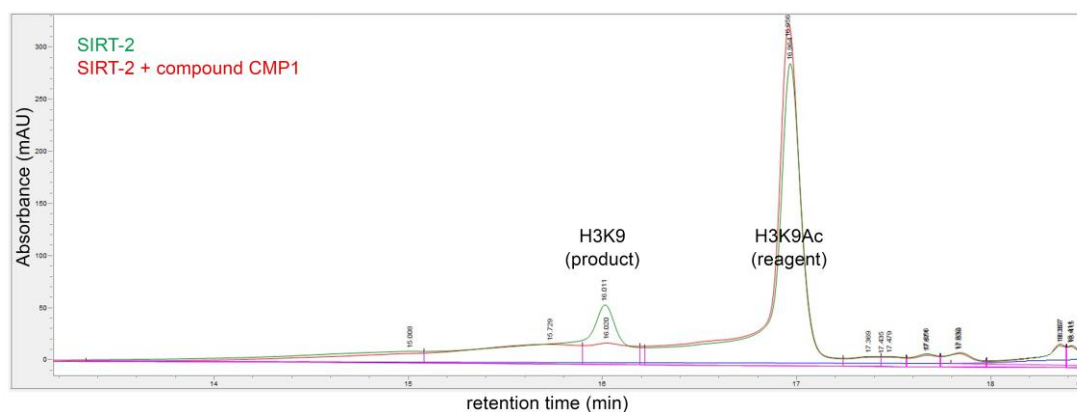


Figure 38. HPLC chromatograms of the deacetylation reaction mixture of SIRT-2 in absence (green) or in presence of the SIRT-2 inhibitor CMP1. Retention times of the deacetylated peptide H3K9, namely the product, and of the acetylated peptide H3K9, the reagent, are respectively 16 and 17 min. The amount of the deacetylated peptide produced is less when the reaction is performed in presence of the SIRT-2 inhibitor.

Determination of the IC_{50} of the SIRT-2 inhibitors by HPLC-based enzymatic assay.

Determination of the IC_{50} for SIRT-2 of several SIRT-2 inhibitors was assessed by monitoring the modulation of SIRT-2 at different concentrations of the compound (ranging from 10 to 150 μ M). By increasing the compound concentration, the amount of the H3K9 peptide produced increases; IC_{50} was obtained from the logarithmic nonlinear regression curves in GraphPad Prism (GraphPad Software, La Jolla, CA). Four independent IC_{50} measurements were determined for each compound.

MDL-800 chemical synthesis.

Compound MDL-800 was synthesised in a 3-step reaction process, adapted from (81) (Figure 39).

Reaction 1 + 2 \rightarrow 3: To a solution of 5-bromo-4-fluoro-2-methylaniline **1** (1 eq) in 2 mL pyridine was added methyl 2-(chlorosulfonyl)-5-nitrobenzoate **2** (1.2 eq) at 0 °C, and the reaction was continuously stirred at 0 °C for 20 min. Then, the reaction was moved to RT and stirred for another 5 - 6 h. The reaction was cooled to 0 °C, and the pH was adjusted to 4 with 2 N HCl. The precipitate formed was filtered and washed with water. The solid was dissolved in 3 mL of ethyl acetate and washed with water and dried over sodium sulfate. The organic layer was evaporated in vacuo and directly used in the next step without being purified.

Reaction 3 + Fe \rightarrow 4: Iron powder (2.9 eq) was added to crude compound **3** (1 eq) dissolved in acetic acid at T = 35 °C. Then, the reaction was stirred under the same conditions for 5 h and at RT O/N. The system was filtered, and the solvent was evaporated under reduced pressure. The solid was dissolved in 3 mL of ethyl acetate and washed with water and dried over sodium sulfate. The organic layer was evaporated in vacuo and directly used in the next step without being purified.

Reaction 4 + 5 \rightarrow MDL-800: To a solution of methyl 5-amino-2-(N-(5-bromo-4-fluoro-2-methylphenyl)sulfamoyl)benzoate **4** (1 eq) in 2 mL pyridine, 3,5-dichlorobenzene-1-sulfonyl chloride **5**, (2.4 eq) was added at 0 °C, and the reaction was stirred at the same temperature for 20 min. Then, the reaction was moved to RT and stirred for another 3 h and 30 min. The reaction was cooled to 0 °C, and the pH was adjusted to 4 with 2 N HCl. The precipitate formed was filtered and dried.

The crude product was purified with HPLC preparative to obtain the final product in 28% yield. The preparative HPLC was Agilent 1260 Infinity preparative HPLC; the column used for preparative chromatography was Phenomenex C18 Luna (21.2 × 250 mm, 15 μm). The mobile phase consisted of eluent A and B, with the gradient of eluent B as the following: 0 – 5 min 30 – 40%; 5 – 10 min, 40 – 50%; 10 – 35 min, 70%; 35 – 45 min, 70% – 90%; 45 – 60 min, 90 – 100%, at 20mL/min. Total run time was 60 minutes. Eluent A and B are H₂O + FoA 0.1%, and AcCN + FoA 0.1%, respectively.

The final product was judged to have a purity of 95% or higher, based on analytical HPLC/MS analysis.

The 3-step reaction process was repeated several times in order to obtain a bulk amount of MDL-800, needed for the preparation of MEs, to be then applied as topical formulations in mice studies. Therefore, a total of 970 mg of MDL-800 with at least 95% purity were synthesised. Test of effective modulation of SIRT-6 and comparison of the activation by the synthesised compound and the one purchased from Sigma-Aldrich S.r.l.

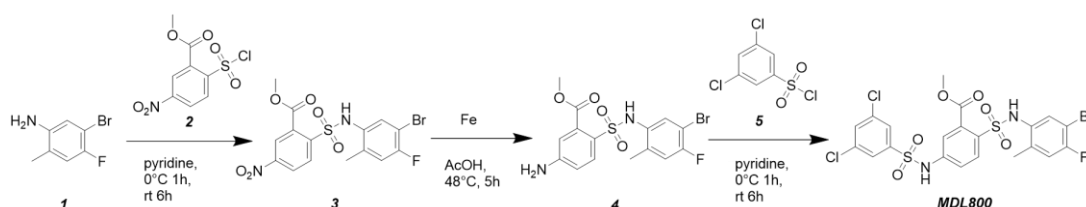


Figure 39. Reaction scheme of compound MDL-800.

Evaluation of solubility properties of S6 and MDL-800.

S6 and MDL-800 were added as solid compounds to several solvents or mixture of solvents, including purified water, EtOH and acetone and solubilisation was aided by heating the mixture; they were insoluble in all of them already at 3 mM concentration. Both compounds were able to dissolve instead in DMSO upon heating (50°C): S6 at 24 mg/mL (58.5 mM), and MDL-800 at 64 mg/mL (102 mM). S6 solubility in a DMSO/PBS solution was also further examined: a 50 mM S6 in DMSO was mixed with PBS in a 1:1 and 1:2 ratio. The compound remained dissolved in the 1:1 ratio solution, while it precipitated in the 1:2 one.

Preparation of lipogels.

Lipogel formulations were prepared by adding to syntesqual (10.2 g) DMSO (0.2 mL), which represents the APIs' vehicle, and different amounts of Lipogelag, followed by magnetic stirring for 2 min (Table 25).

Table 25. Composition of 8 lipogel formulations.

Formulation	Syntesqual	DMSO	Lipogelag
LG-1	10.2 g	0.2 mL	1% (0.1 g)
LG-2	10.2 g	0.2 mL	2% (0.2 g)
LG-3	10.2 g	0.2 mL	3% (0.3 g)
LG-4	10.2 g	0.2 mL	4% (0.4 g)
LG-5	10.2 g	0.2 mL	5% (0.6 g)
LG-6	10.2 g	0.2 mL	6% (0.6 g)
LG-7	10.2 g	0.2 mL	7% (0.7 g)
LG-10	10.2 g	0.2 mL	10% (1 g)

Preparation of O/W emulsions and MEs.

A total of 5 O/W emulsions and 25 O/W MEs were prepared by mixing purified water, oil, a surfactant, DMSO, and eventually a thickener (Table 26, Table 27).

Table 26. Composition of the O/W emulsion formulations.

Formulation	Water phase			Oil phase	
	O:W ratio	Water	Surfactant Tween 20	Oil IPM	DMSO
E-1	1 : 1	5 mL	2 gtt	5 mL	100 µL
E-2	4 : 1	1 mL	2 gtt	4 mL	100 µL
E-3	2.3 : 1	1.5 mL	2 gtt	3.5 mL	100 µL
E-4	4 : 1	1 mL	4 gtt	4 mL	100 µL
E-5	2.3 : 1	1.5 mL	4 gtt	3.5 mL	100 µL

Table 27. Composition of the O/W ME formulations.

ME	Water phase						Oil phase			
	O:W ratio	Water	Surfactant		Thickener		Oil		DMSO	
			Tween 20	Tween 80	PEG 7 GC	PEG 200	PEG 400	IPM	Synte-squal	DMSO
ME-1	1 : 1	5 mL	2 gtt					5 mL		0.1 mL
ME-2	4 : 1	1 mL	2 gtt					4 mL		0.1 mL
ME-3	4 : 1	0.5 mL	2 gtt						2 mL	0.2 mL
ME-4	2.3 : 1	1.5 mL	2 gtt					3.5 mL		0.1 mL
ME-5	4 : 1	1 mL	4 gtt					4 mL		0.1 mL
ME-6	4 : 1	0.5 mL	4 gtt						2 mL	0.2 mL
ME-7	2.3 : 1	1.5 mL	4 gtt					3.5 mL		0.1 mL
ME-8	3:1	1 mL	2 gtt		1 mL (20%)			3 mL		0.1 mL
ME-9	1.5 : 1	2 mL	2 gtt		0.5 mL (10%)			3 mL		0.1 mL
ME-10	8 : 1	0.5 mL	2 gtt		0.5 mL (10%)			4 mL		0.1 mL
ME-11	4 : 1	1 mL	2 gtt		0.5 mL (10%)			4 mL		0.1 mL
ME-12	4.7 : 1	0.75 mL	2 gtt		0.75 mL (15%)			3.5 mL		0.1 mL
ME-13	2.3 : 1	1.5 mL	2 gtt		0.5 mL (10%)			3.5 mL		0.1 mL
ME-14	3 : 1	1.25 mL	2 gtt					3.75 mL		0.1 mL
ME-15	2.8 : 1	1.25 mL	2 gtt		0.25 mL (5%)			3.5 mL		0.1 mL
ME-16	3.2 : 1	0.6 mL	2 gtt					1.9 mL		0.2 mL
ME-17	2.7 : 1	0.6 mL	2 gtt					1.6 mL		0.2 mL
ME-18	2.7 : 1	0.6 mL	2 gtt						1.6 mL	0.2 mL
ME-19	2.7 : 1	0.6 mL	2 gtt			0.3 mL (11%)		1.6 mL		0.2 mL
ME-20	3.2 : 1	0.6 mL	2 gtt			0.3 mL (10%)		1.9 mL		0.2 mL
ME-21	2.7 : 1	0.6 mL	2 gtt			0.3 mL (11%)			1.6 mL	0.2 mL
ME-22	3 : 1	0.6 mL	4 gtt			0.3 mL (10%)		1.8 mL		0.2 mL
ME-23	3 : 1	0.6 mL	4 gtt				0.3 mL (10%)	1.8 mL		0.2 mL
ME-24	3 : 1	0.6 mL		4 gtt				1.8 mL		0.2 mL
ME-25	4 : 1	0.4 mL	6 gtt					1.6 mL		0.4 mL

Emulsions were obtained by stirring the mixture in a beaker with a magnetic stirrer for 15 min, or by manual agitation of the mixture in a 10 mL corex glass tube (total volume: 5 – 10mL). On the other side, MEs were prepared by mixing in a 10 mL corex glass tube the excipients and by stirring them vigorously with the Ultra-Turrax® T18 Homogenizer (IKA®-Werke GmbH & Co. KG, Germany), which was set at speed 3 (16000 g/min), for approximately 2 min (total volume: 2.5 – 5 mL). In detail, in emulsions and MEs the main water phase component was purified water, while the main oil phase substance was either syntesqual or IPM. O:W ratio ranged from 1:1 to 8:1. The surfactants chosen were Tween 20 or Tween 80, 2 or 4 gtt. In the water phase, eventually also thickeners like PEG 7 GC, PEG 200 or PEG 400 were added. The different PEGs were added in different amounts in the range 5-20% V/V, according to the other excipients' amounts. Finally, in the oil phase, DMSO was added (100, 200 or 400 µL). To be noted that oils were added with a specific pipette for viscous liquids.

Stability studies of lipogels.

The physical stability of the lipogels was evaluated after 1-, 3-, and 7-days RT storage. The parameters assessed by visual inspection were fluidity of the mixture, phase separation and ability to reach again thermodynamical stability upon shaking.

Stability studies of emulsions and MEs.

The physical stability of the emulsions and of the MEs was evaluated after 1, 3 and 7 days. The formulations were further tested in accelerated stability studies, by storing them at RT for 2.5 months, which simulated the long-term 4°C storage condition of the subsequent *in vivo* study. The parameters assessed by visual inspection were fluidity of the mixture, ease of pipetting, phase separation and ability to reach again thermodynamical stability upon shaking (Table 17).

Plan of the dose of S6 and MDL-800 to apply in the in vivo studies.

The amount of S6 and of MDL-800 to deliver to the DS of mice treated in a DMBA-TPA protocol is described in Table 28. Specifically, in topical treatment studies, the dose to deliver to a mouse is not dependent on its weight, but it can be fixed to a certain value for all animals, considering that the skin has approximately the same extension for all the mice selected for the study. With respect to the physicochemical properties and to their known bioactive effects, the amounts of S6 and MDL-800 were defined respectively as 30 mg/kg and 80 mg/kg per dose. Considering an average mouse weight of 20 g, the desired amount of each compound was identified as 0.6 mg and 1.6 mg per dose. The application volume (ideally in the range of 80-200 µL) was fixed to 150 µL per dose.

Table 28. Amount of S6 and MDL-800 planned for 1 dose of treatment, and their concentration needed in the MEs.

Compound	Dose per mouse	Amount needed in 1 dose (150 µL of ME) (average mouse weight is 20 g)	Concentration needed in the ME
S6	30 mg/kg	0.6 mg	4 mg/mL (9.75 mM)
MDL-800	80 mg/kg	1.6 mg	10.67 mg/mL (17 mM)

Preparation of ME-25 loaded with S6 or MDL-800 or vehicle.

After selecting ME-25 as the most promising formulation, and after defining the dosage per mouse during the *in vivo* studies, the formulations containing S6 and MDL-800 were prepared. In detail, purified water (water phase), syntesqual (oil phase), Tween-20

(surfactant) and a solution of S6 or MDL800 in DMSO, were mixed with Ultra-Turrax® T18 Homogenizer at speed 3 (16000 g/min), according to Table 29 (total volume: 2.4 mL). A O/W ME containing the APIs' vehicle, namely DMSO, added in the same amount of the S6 and MDL-800-loaded MEs, was also prepared; this formulation was renamed "BLK". The container used for the emulsification was a 10 mL corex glass tube. In Table 30, the concentrations of S6 and of MDL-800 both in the DMSO stock solutions used to prepare the MEs, and in the final MEs are described.

Table 29. Composition of the O/W ME formulations containing S6, MDL-800 or their vehicle.

Formulation	Water phase			Oil phase		V prepared	
	O:W ratio	Water	Surfactant	Oil	API		Vehicle
			Tween 20	Syntesqual	S6 or MDL-800 DMSO solution	DMSO	
ME-BLK	4 : 1	0.4 mL	6 gtt	1.6 mL		0.4 mL	2.4 mL
ME-S6	4 : 1	0.4 mL	6 gtt	1.6 mL	0.4 mL (S6: 9.6mg)		2.4 mL
ME-MDL-800	4 : 1	0.4 mL	6 gtt	1.6 mL	0.4 mL (MDL-800: 25.6 mg)		2.4 mL

Table 30. Concentration of the compounds S6 and MDL-800 in the DMSO stock solution and in the MEs.

Compound	Concentration in the DMSO stock solution	Amount contained in 0.4 mL of stock solution transferred to the ME mix (2.4 mL)	Concentration in the ME
S6	24 mg/mL (58.2 mM)	9.6 mg	4 mg/mL (9.75 mM)
MDL-800	64 mg/mL (102.2 mM)	25.6 mg	10.67 mg/mL (17 mM)

Stability studies of drug-loaded MEs.

The physical stability of the API-loaded and vehicle MEs was evaluated after 1, 3 and 7 days. The formulations were further tested in stability studies: upon storage at 4°C for 6 months, they were examined periodically at 1, 3 and 6 months. The parameters assessed by visual inspection were fluidity of the mixture, ease of pipetting, phase separation and ability to reach again thermodynamical stability upon shaking.

Chemical stability of the compounds contained in the MEs was also determined. This was accomplished by HPLC analysis. In detail, S6- and MDL-800-loaded MEs were respectively 487- and 872-fold diluted in an acidic MeOH solution (200 mM HCl and 320 mM AcOH); following centrifugation at 16000 x g for 3 min, the supernatant was injected in HPLC. Analysis was performed in an Agilent Technologies 1260 HPLC, with a ZORBAX® Eclipse Plus C18 3.5 µM, 4.6 mm x 10 mm column, set on 25°C; injection volume was 45 µL. The mobile phase consisted of eluent A and B, with the following gradient of eluent B: 0 – 5 min 5%; 5 – 16 min, 5 – 25.1%; 16 – 20 min, 100%; 20 – 24 min, 100%; 24 – 24.1 min, 100 – 5%, at 1mL/min. Total run time is 24 minutes. Eluent A and B were H₂O + TFA 0.05%, and AcCN + TFA 0.02%, respectively. The whole absorbance profile at 220 nm was analysed. At the described HPLC conditions, S6 and MDL-800 retention times are respectively 17.65 min and 21.21 min.

Preparation of bulk quantities of drug-loaded MEs.

Since in ME preparation the correlation between different excipients is not linear, the scale-up process is not particularly straightforward. Therefore, the preparation of bulk quantities of the API-loaded MEs was chosen to be accomplished by repeating multiple times the protocol described previously.

Cell culture.

HaCaT and SCC13 cell lines were retained in Gibco™ Keratinocyte SFM 1X medium supplied with prequalified human recombinant Epidermal Growth Factor 1-53 (EGF 1-53) and Bovine Pituitary Extract (BPE). HEK293 cell lines were maintained in Dulbecco's Modified Eagle's Medium, high glucose, supplemented with 10% FBS, 50 IU/mL penicillin, and 50 µg/mL streptomycin. Cells were cultured in a humidified 5% CO₂ atm at 37 °C.

Constructs and viral infection: SIRT-6 silencing in SCC13 cells.

HEK293 (5×10^5) cells were plated in 4 ml of medium in 6-cm dishes and allowed to adhere for 24 h. Thereafter, cells were transfected with 4 µg of plasmid DNA using TransIT-293, according to the manufacturer's instructions. Plasmids used were empty pRETROSUPER (pRS) and pRS SIRT-6 sh1. Viral supernatants were harvested after 36, 48, and 60 h and used to infect SCC13 cells (5×10^5) in 10-cm dishes in the presence of 5 µg/ml protamine sulfate. Successfully infected cells were selected using 1.5 µg/ml puromycin.

Cell viability assay.

The effects of several compounds on SCC13 and HaCaT cell viability were assessed by sulphorhodamine (SRB) assay. Specifically, 24 h after seeding cells, these were incubated either in their regular medium supplemented with DMSO (control wells), or in the treatment medium containing increasing concentration of the tested compound dissolved in DMSO. Each condition was performed in triplicate and incubation was carried out for either 24, 48 or 72 h in 5% CO₂ atm at 37 °C. Afterwards, the culture plates were fixed with 10% trichloroacetic acid at 4 °C for 20 min, washed with cold water, and dried O/N. The plates were stained with 0.04% SRB in 1% AcOH and then washed with 1% AcOH and dried overnight. Lastly, a 10 mM Tris solution was added to each well, and cell viability was quantified by measuring absorbance at 540 nm on spectrophotometer CLARIOstar® Plus (BMG LabTech, Germany).

Co-treatment of SCC13 with sirtuins' modulators and 5-FU or Celecoxib.

In order to evaluate the synergic or additive effect of SIRTs' modulators on 5-FU and on Celecoxib, at first, the max concentration of each compound was screened: this was defined as the one giving at least 70% living cells. Several trials were performed in order to define the best incubation and concentration conditions. Treatments of SCC13 cells were performed for 24 and 72 h, at different ranges of concentrations of 5-FU, of Celecoxib, of the SIRT-6 modulators S6, MDL-800 and EAB1 to EAB10. The concentrations chosen for 5-FU and for Celecoxib were respectively 1.6 µM and 12.5 µM (Figure 40).

S6, EAB2, EAB3 and EAB5 were added to SCC13 cells at different concentrations in the ranges 0 – 100 µM, while MDL-800 in the range 1 – 10 µM, in co-treatment with either 5-FU or Celecoxib. After 72 h, cell viability was evaluated by SRB assay and the synergic or additive effect of the compounds was assessed. All compounds were dissolved in DMSO, therefore, appropriate control SCC13 cells, namely treated just with the DMSO vehicle, were also analysed.

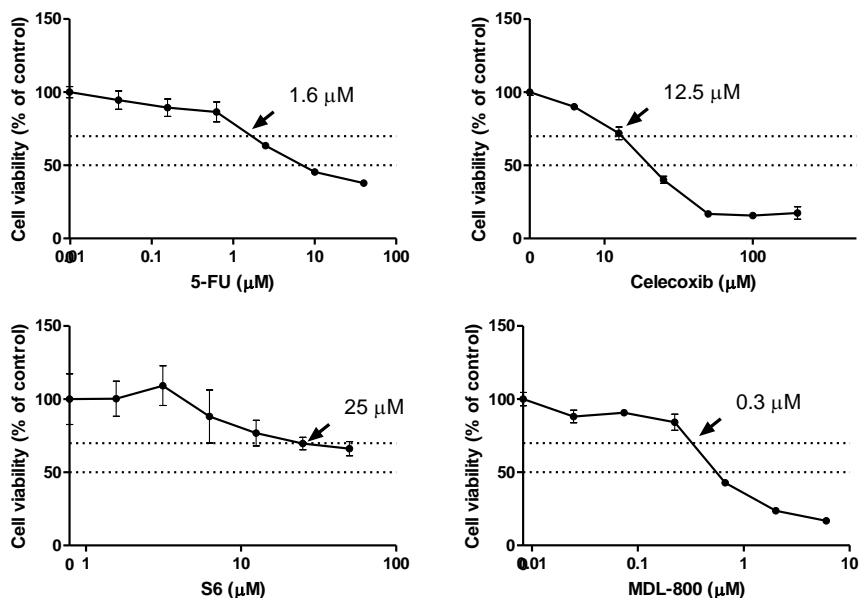


Figure 40. Transform curves of 5-FU, Celecoxib, S6 and MDL-800 after 48 h treatment of SCC13 cells with the compounds.

Cell treatment with the sirtuins' modulators for WB analyses.

SCC13 cells were treated with a selection of the SIRT-6 compounds that had been screened through VS. Specifically, SCC13 cells were incubated for 21 h with compounds S6, MDL-800, EAB2, EAB3 and EAB5 (50 μM), and with DMSO as control (max DMSO concentration was 0.1%).

Cutaneous chemical carcinogenesis and topical treatment with MEs.

DS of mice was subject to a two-time DMBA treatment (100 μL, 1 mg/mL in acetone), followed by TPA treatment twice a week (100 μL, 100 μM in acetone). The TPA treatment was continued on the DS until sacrifice (Table 31). Mice were shaved on their DS prior to DMBA treatment, and later as needed. Any palpable mass greater than 1 mm in size was considered a papilloma and recorded.

Mice were divided into three groups of approximately 18 mice, and each one was characterised by a different treatment plan with the MEs, which had been previously prepared, as described in Table 29. Specifically, topical application of MEs started in three different stages of skin carcinogenesis: for Group 1-mice, after papillomas arose on their skin; for Group 2-mice, at the promotion stage, together with TPA treatment; for Group 3-mice, 1 week prior to initiation with DMBA.

MEs were applied to DS of mice (150 μL) with a pipette for viscous liquids. For each group the MEs applied were ME-BLK, which contained the APIs' vehicle DMSO, ME-S6 and ME-MDL-800, that contained compounds S6 and MDL-800, respectively. Concentration of the MEs containing the APIs is described in Table 30.

DS of mice was treated topically with MEs named BLK, S6 and MDL-800, that contain either DMSO, the SIRT-6 inhibitor S6, or the SIRT-6 activator MDL-800. The starting date of the MEs treatment depended on the *in vivo* studies plan, while the end date corresponded to the mice sacrifice (Figure 41). Of note: treatment of Group 1-mice with the MEs was interrupted 7 weeks prior to sacrifice.

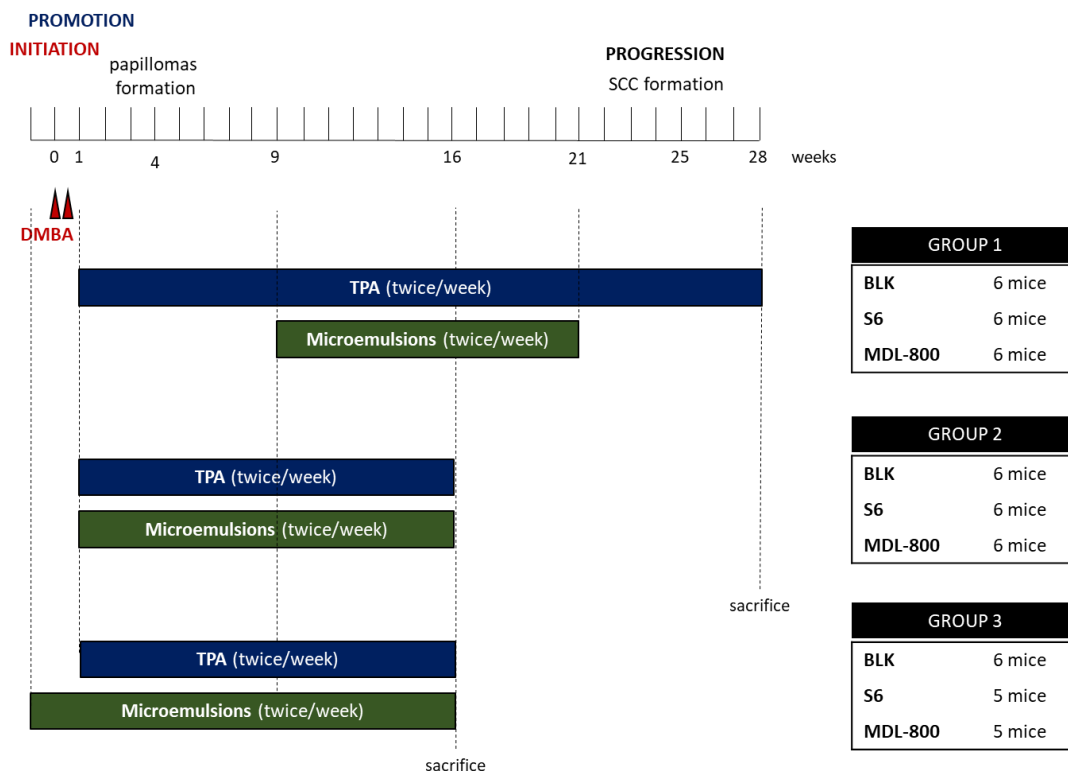


Figure 41. Detail of the treatment plan for the three different groups. Group 2 and 3 present a preventive approach, while Group 1 a therapeutic one.

Table 31. Detail of the weekly treatment plan for the 2-stage carcinogenesis protocol and for the topical treatment with MEs.

	Monday	Tuesday	Wednesday	Thursday	Friday	Saturday	Sunday
1st week	DMBA	-	-	DMBA	-	-	-
from 2nd week until sacrifice	TPA	-	-	TPA	-	-	-
starting date depending on the treatment group	-	MEs	-	-	MEs	-	-

Animal sacrifice and tissue collection.

At the termination of the carcinogenesis protocol, after shaving their DS, mice were sacrificed. Immediately, an image of the DS was taken and tissues were harvested. Specifically, DS was collected for further histological, WB and real-time PCR analyses.

Animal study approval.

All animal experiments were carried out in the animal facility of CEINGE-Biotecnologie Avanzate, Naples, Italy, in accordance with institutional guidelines.

Protein extraction from cells or DS tissues.

Cells were lysed in lysis buffer (50 mM Tris-HCl, pH 7.5, 150 mM NaCl, 1% NP40) enriched with 1:100 protease inhibitor PIC[®] Reagent A and 1:100 Phosphatase Inhibitor Cocktail 3.

Dorsal skin was removed from mice and immediately frozen at -80°C. 800 µL of Lysis Buffer (0.125 M Tris pH 8.6; 3% SDS, protease inhibitors including PMSF 1.0 mM and phosphatase

inhibitors) were added to all dorsal skin samples, which were then homogenised with TissueLyser II (QIAGEN, Hilden, Germany, 85300).

Western Blot analysis.

Total tissues protein was separated by 10 or 15% SDS-PAGE followed by Western Blot. The membrane was then blocked with 5% non-fat dry milk or BSA in TBS or PBS-0.2% Tween. It was then incubated with the primary antibodies for 1 h at RT or O/N at 4°C; the antibodies used and their dilutions are listed in Table 21. The following secondary antibodies were either anti-mouse IgG-HRP or anti-rabbit IgG-HRP. Band detection was achieved by chemiluminescence using an ECL kit. Loading control was monitored either with anti-vinculin, anti-tubulin or anti-H3 specific antibodies. Bands were quantified with ImageJ software (NIH Image, Bethesda, Maryland).

mRNA extraction from DS tissues and real-time PCR.

Messenger RNAs were extracted with TRIzol reagent, according to the manufacturer's protocol. Complementary DNAs (cDNAs) were prepared with VILO or ABM, as indicated by the manufacturer. The cDNAs were amplified by PCR in a CFX Connect Real-Time PCR Detection System (BioRad, Hercules, California, USA, 1855201) with the fluorescent double-stranded DNA-binding dye SYBR Green. Specific primers for each gene were designed to work under the same cycling conditions (95°C for 10 min followed by 40 cycles at 95°C for 15 sec and 60°C for 1 min), thereby generating products of comparable sizes (about 200-300 bp for each amplification). Primer sequences are listed in Table 22. For each reaction, standard curves for reference genes were constructed based on six four-fold serial dilutions of cDNA. All samples were run in triplicate. The template concentration was calculated from the cycle number when the amount of PCR product passed a threshold established in the exponential phase of the PCR. The relative amounts of gene expression were normalised to CyA expression and calculated with $N^{\Delta\Delta Ct} = 2^{(\Delta Ct_{\text{sample}} - \Delta Ct_{\text{calibrator}})}$.

Histology and Immunostaining of DS tissues.

Dorsal skin from CD-1 mice treated with BLK, S6 and MDL-800 MEs was embedded in paraffin and cut into 15.0 µm sections; slides were then baked at 37°C. Sections were then stained with Haematoxylin & Eosin (H&E). Alternatively, for immunostaining, they were deparaffinised by xylene, dehydrated with ethanol, rehydrated in PBS, and permeabilised by placing them in 0.2% Triton X-100 in PBS. Antigens were retrieved by incubation in 0.1 M citrate buffer pH 6.0 at 95°C for 5 min. Sections were blocked in 1% BSA/0.02% Tween/PBS for 1 h at RT. Primary antibodies were incubated O/N at 4°C in blocking buffer and washed in 0.2% Tween/PBS. Secondary antibodies were incubated at RT for 1 h and washed in 0.2% Tween/PBS. At last, sections were incubated with 4',6-diamidino-2-phenylindole (DAPI) for nuclei staining and washed with PBS. Details of the antibodies used are reported in the Materials paragraph. Images were acquired with a Leica DMI8 microscope using the Leica Application Suite LAS X Imaging Software.

ACKNOWLEDGMENTS

This work was supported by the European Union's Horizon 2020 research and innovation programme under the Marie Skłodowska-Curie grant agreement No 671881 (INTEGRATA).

REFERENCES

1. Min J, Landry J, Sternglanz R, Xu R-M. Crystal structure of a SIR2 homolog–NAD complex. *Cell*. 2001;105(2):269-79.
2. North BJ, Verdin E. Sirtuins: Sir2-related NAD-dependent protein deacetylases. *Genome biology*. 2004;5(5):224.
3. Imai S, Armstrong CM, Kaeberlein M, Guarente L. Transcriptional silencing and longevity protein Sir2 is an NAD-dependent histone deacetylase. *Nature*. 2000;403(6771):795-800.
4. Verdin E, Dequiedt F, Fischle W, Frye R, Marshall B, North B. Measurement of mammalian histone deacetylase activity. *Methods in enzymology*. 2004;377:180-96.
5. Chalkiadaki A, Guarente L. The multifaceted functions of sirtuins in cancer. *Nature reviews Cancer*. 2015;15(10):608-24.
6. Tanny JC, Dowd GJ, Huang J, Hilz H, Moazed D. An enzymatic activity in the yeast Sir2 protein that is essential for gene silencing. *Cell*. 1999;99(7):735-45.
7. Feldman JL, Baeza J, Denu JM. Activation of the protein deacetylase SIRT6 by long-chain fatty acids and widespread deacylation by mammalian sirtuins. *The Journal of biological chemistry*. 2013;288(43):31350-6.
8. Haigis MC, Mostoslavsky R, Haigis KM, Fahie K, Christodoulou DC, Murphy AJ, et al. SIRT4 inhibits glutamate dehydrogenase and opposes the effects of calorie restriction in pancreatic beta cells. *Cell*. 2006;126(5):941-54.
9. Mao Z, Hine C, Tian X, Van Meter M, Au M, Vaidya A, et al. SIRT6 promotes DNA repair under stress by activating PARP1. *Science*. 2011;332(6036):1443-6.
10. Van Meter M, Kashyap M, Rezazadeh S, Geneva AJ, Morello TD, Seluanov A, et al. SIRT6 represses LINE1 retrotransposons by ribosylating KAP1 but this repression fails with stress and age. *Nature communications*. 2014;5:5011.
11. Yuan H, Marmorstein R. Structural basis for sirtuin activity and inhibition. *The Journal of biological chemistry*. 2012;287(51):42428-35.
12. Mei Z, Zhang X, Yi J, Huang J, He J, Tao Y. Sirtuins in metabolism, DNA repair and cancer. *Journal of experimental & clinical cancer research : CR*. 2016;35(1):182.
13. Michishita E, Park JY, Burneskis JM, Barrett JC, Horikawa I. Evolutionarily conserved and nonconserved cellular localizations and functions of human SIRT proteins. *Molecular biology of the cell*. 2005;16(10):4623-35.
14. Villalba JM, Alcain FJ. Sirtuin activators and inhibitors. *BioFactors*. 2012;38(5):349-59.
15. Luo G, Jian Z, Zhu Y, Zhu Y, Chen B, Ma R, et al. Sirt1 promotes autophagy and inhibits apoptosis to protect cardiomyocytes from hypoxic stress. *International journal of molecular medicine*. 2019;43(5):2033-43.
16. Raynes R, Brunquell J, Westerheide SD. Stress Inducibility of SIRT1 and Its Role in Cytoprotection and Cancer. *Genes & cancer*. 2013;4(3-4):172-82.
17. Oberdoerffer P, Michan S, McVay M, Mostoslavsky R, Vann J, Park SK, et al. SIRT1 redistribution on chromatin promotes genomic stability but alters gene expression during aging. *Cell*. 2008;135(5):907-18.
18. North BJ, Verdin E. Interphase nucleo-cytoplasmic shuttling and localization of SIRT2 during mitosis. *PloS one*. 2007;2(8):e784.
19. Jing E, Gesta S, Kahn CR. SIRT2 regulates adipocyte differentiation through FoxO1 acetylation/deacetylation. *Cell metabolism*. 2007;6(2):105-14.

20. Dryden SC, Nahhas FA, Nowak JE, Goustin AS, Tainsky MA. Role for human SIRT2 NAD-dependent deacetylase activity in control of mitotic exit in the cell cycle. *Molecular and cellular biology*. 2003;23(9):3173-85.
21. Onyango P, Celic I, McCaffery JM, Boeke JD, Feinberg AP. SIRT3, a human SIR2 homologue, is an NAD-dependent deacetylase localized to mitochondria. *Proceedings of the National Academy of Sciences of the United States of America*. 2002;99(21):13653-8.
22. Ahn BH, Kim HS, Song S, Lee IH, Liu J, Vassilopoulos A, et al. A role for the mitochondrial deacetylase Sirt3 in regulating energy homeostasis. *Proceedings of the National Academy of Sciences of the United States of America*. 2008;105(38):14447-52.
23. Bell EL, Emerling BM, Ricoult SJ, Guarente L. Sirt3 suppresses hypoxia inducible factor 1alpha and tumor growth by inhibiting mitochondrial ROS production. *Oncogene*. 2011;30(26):2986-96.
24. Tao R, Coleman MC, Pennington JD, Ozden O, Park SH, Jiang H, et al. Sirt3-mediated deacetylation of evolutionarily conserved lysine 122 regulates MnSOD activity in response to stress. *Molecular cell*. 2010;40(6):893-904.
25. Huang JY, Hirschev MD, Shimazu T, Ho L, Verdin E. Mitochondrial sirtuins. *Biochimica et biophysica acta*. 2010;1804(8):1645-51.
26. Wang Y, Chen H, Zha X. Overview of SIRT5 as a potential therapeutic target: Structure, function and inhibitors. *European journal of medicinal chemistry*. 2022;236:114363.
27. Khan RI, Nirzhor SSR, Akter R. A Review of the Recent Advances Made with SIRT6 and its Implications on Aging Related Processes, Major Human Diseases, and Possible Therapeutic Targets. *Biomolecules*. 2018;8(3).
28. Grob A, Roussel P, Wright JE, McStay B, Hernandez-Verdun D, Sirri V. Involvement of SIRT7 in resumption of rDNA transcription at the exit from mitosis. *Journal of cell science*. 2009;122(Pt 4):489-98.
29. Ford E, Voit R, Liszt G, Magin C, Grummt I, Guarente L. Mammalian Sir2 homolog SIRT7 is an activator of RNA polymerase I transcription. *Genes & development*. 2006;20(9):1075-80.
30. Csibi A, Fendt SM, Li C, Poulogiannis G, Choo AY, Chapski DJ, et al. The mTORC1 pathway stimulates glutamine metabolism and cell proliferation by repressing SIRT4. *Cell*. 2013;153(4):840-54.
31. Tasselli L, Xi Y, Zheng W, Tennen RI, Odrowaz Z, Simeoni F, et al. SIRT6 deacetylates H3K18ac at pericentric chromatin to prevent mitotic errors and cellular senescence. *Nature structural & molecular biology*. 2016;23(5):434-40.
32. Wang WW, Zeng Y, Wu B, Deiters A, Liu WR. A Chemical Biology Approach to Reveal Sirt6-targeted Histone H3 Sites in Nucleosomes. *ACS chemical biology*. 2016;11(7):1973-81.
33. Wang W, Li J, Cai L. Research progress of sirtuins in renal and cardiovascular diseases. *Current opinion in nephrology and hypertension*. 2021;30(1):108-14.
34. Kitada M, Ogura Y, Monno I, Koya D. Sirtuins and Type 2 Diabetes: Role in Inflammation, Oxidative Stress, and Mitochondrial Function. *Frontiers in endocrinology*. 2019;10:187.
35. Jurkowska K, Szymanska B, Knysz B, Kuzniarski A, Piwowar A. Sirtuins as Interesting Players in the Course of HIV Infection and Comorbidities. *Cells*. 2021;10(10).
36. Zhao E, Hou J, Ke X, Abbas MN, Kausar S, Zhang L, et al. The Roles of Sirtuin Family Proteins in Cancer Progression. *Cancers*. 2019;11(12).
37. Leite JA, Ghirotto B, Targhetta VP, de Lima J, Camara NOS. Sirtuins as pharmacological targets in neurodegenerative and neuropsychiatric disorders. *British journal of pharmacology*. 2022;179(8):1496-511.

38. Chen Y, Fu LL, Wen X, Wang XY, Liu J, Cheng Y, et al. Sirtuin-3 (SIRT3), a therapeutic target with oncogenic and tumor-suppressive function in cancer. *Cell death & disease*. 2014;5(2):e1047.
39. Bosch-Presegue L, Vaquero A. The dual role of sirtuins in cancer. *Genes & cancer*. 2011;2(6):648-62.
40. Kitada M, Koya D. SIRT1 in Type 2 Diabetes: Mechanisms and Therapeutic Potential. *Diabetes & metabolism journal*. 2013;37(5):315-25.
41. Song J, Yang B, Jia X, Li M, Tan W, Ma S, et al. Distinctive Roles of Sirtuins on Diabetes, Protective or Detrimental? *Frontiers in endocrinology*. 2018;9:724.
42. Mostoslavsky R, Chua KF, Lombard DB, Pang WW, Fischer MR, Gellon L, et al. Genomic instability and aging-like phenotype in the absence of mammalian SIRT6. *Cell*. 2006;124(2):315-29.
43. Zhong L, D'Urso A, Toiber D, Sebastian C, Henry RE, Vadysirisack DD, et al. The histone deacetylase Sirt6 regulates glucose homeostasis via Hif1alpha. *Cell*. 2010;140(2):280-93.
44. Garcia-Peterson LM, Guzman-Perez G, Krier CR, Ahmad N. The sirtuin 6: An overture in skin cancer. *Experimental dermatology*. 2020;29(2):124-35.
45. Abbotto E, Scarano N, Piacente F, Millo E, Cichero E, Bruzzone S. Virtual Screening in the Identification of Sirtuins' Activity Modulators. *Molecules*. 2022;27(17).
46. Ehrenberg AJ, Khatun A, Coomans E, Betts MJ, Capraro F, Thijssen EH, et al. Relevance of biomarkers across different neurodegenerative diseases. *Alzheimer's research & therapy*. 2020;12(1):56.
47. Gu Q, Zhou P, Xu X, Fang W, Jia S, Liu W, et al. Benzothiazole derivatives upregulate SIRT1 and relevant genes in high-fat fed C57BL/6J mice. *Medicinal Chemistry Research*. 2015;24:2454-60.
48. Liu P, Feng T, Zuo X, Wang X, Luo J, Li N, et al. A novel SIRT1 activator E6155 improves insulin sensitivity in type 2 diabetic KKA(y) mice. *Biochemical and biophysical research communications*. 2018;498(3):633-9.
49. Lee AY, Christensen SM, Duong N, Tran QA, Xiong HM, Huang J, et al. Sirt3 Pharmacologically Promotes Insulin Sensitivity through PI3/AKT/mTOR and Their Downstream Pathway in Adipocytes. *International journal of molecular sciences*. 2022;23(7).
50. Hong JY, Fernandez I, Anmangandla A, Lu X, Bai JJ, Lin H. Pharmacological Advantage of SIRT2-Selective versus pan-SIRT1-3 Inhibitors. *ACS chemical biology*. 2021;16(7):1266-75.
51. Arora A, Dey CS. SIRT2 negatively regulates insulin resistance in C2C12 skeletal muscle cells. *Biochimica et biophysica acta*. 2014;1842(9):1372-8.
52. Parenti MD, Grozio A, Bauer I, Galeno L, Damonte P, Millo E, et al. Discovery of novel and selective SIRT6 inhibitors. *Journal of medicinal chemistry*. 2014;57(11):4796-804.
53. Sun W, Chen X, Huang S, Li W, Tian C, Yang S, et al. Discovery of 5-(4-methylpiperazin-1-yl)-2-nitroaniline derivatives as a new class of SIRT6 inhibitors. *Bioorganic & medicinal chemistry letters*. 2020;30(16):127215.
54. Sanders BD, Jackson B, Marmorstein R. Structural basis for sirtuin function: what we know and what we don't. *Biochimica et biophysica acta*. 2010;1804(8):1604-16.
55. Wawruszak A, Luszczki J, Czerwonka A, Okon E, Stepulak A. Assessment of Pharmacological Interactions between SIRT2 Inhibitor AGK2 and Paclitaxel in Different Molecular Subtypes of Breast Cancer Cells. *Cells*. 2022;11(7).
56. Spiegelman NA, Price IR, Jing H, Wang M, Yang M, Cao J, et al. Direct Comparison of SIRT2 Inhibitors: Potency, Specificity, Activity-Dependent Inhibition, and On-Target Anticancer Activities. *ChemMedChem*. 2018;13(18):1890-4.
57. She DT, Wong LJ, Baik SH, Arumugam TV. SIRT2 Inhibition Confers Neuroprotection by Downregulation of FOXO3a and MAPK Signaling Pathways in Ischemic Stroke. *Molecular neurobiology*. 2018;55(12):9188-203.

58. Outeiro TF, Kontopoulos E, Altmann SM, Kufareva I, Strathearn KE, Amore AM, et al. Sirtuin 2 inhibitors rescue alpha-synuclein-mediated toxicity in models of Parkinson's disease. *Science*. 2007;317(5837):516-9.
59. Tatum PR, Sawada H, Ota Y, Itoh Y, Zhan P, Ieda N, et al. Identification of novel SIRT2-selective inhibitors using a click chemistry approach. *Bioorganic & medicinal chemistry letters*. 2014;24(8):1871-4.
60. Rumpf T, Schiedel M, Karaman B, Roessler C, North BJ, Lehotzky A, et al. Selective Sirt2 inhibition by ligand-induced rearrangement of the active site. *Nature communications*. 2015;6:6263.
61. Funato K, Hayashi T, Echizen K, Negishi L, Shimizu N, Koyama-Nasu R, et al. SIRT2-mediated inactivation of p73 is required for glioblastoma tumorigenicity. *EMBO reports*. 2018;19(11).
62. Rotili D, Tarantino D, Nebbioso A, Paolini C, Huidobro C, Lara E, et al. Discovery of salermide-related sirtuin inhibitors: binding mode studies and antiproliferative effects in cancer cells including cancer stem cells. *Journal of medicinal chemistry*. 2012;55(24):10937-47.
63. Yang H, Chen Y, Jiang Y, Wang D, Yan J, Zhou Z. TP53 mutation influences the efficacy of treatment of colorectal cancer cell lines with a combination of sirtuin inhibitors and chemotherapeutic agents. *Experimental and therapeutic medicine*. 2020;20(2):1415-22.
64. Taylor DM, Balabadra U, Xiang Z, Woodman B, Meade S, Amore A, et al. A brain-permeable small molecule reduces neuronal cholesterol by inhibiting activity of sirtuin 2 deacetylase. *ACS chemical biology*. 2011;6(6):540-6.
65. Zhang Y, Au Q, Zhang M, Barber JR, Ng SC, Zhang B. Identification of a small molecule SIRT2 inhibitor with selective tumor cytotoxicity. *Biochemical and biophysical research communications*. 2009;386(4):729-33.
66. Liu PY, Xu N, Malyukova A, Scarlett CJ, Sun YT, Zhang XD, et al. The histone deacetylase SIRT2 stabilizes Myc oncoproteins. *Cell death and differentiation*. 2013;20(3):503-14.
67. Kudo N, Ito A, Arata M, Nakata A, Yoshida M. Identification of a novel small molecule that inhibits deacetylase but not defatty-acylase reaction catalysed by SIRT2. *Philosophical transactions of the Royal Society of London Series B, Biological sciences*. 2018;373(1748).
68. Farooqi AS, Hong JY, Cao J, Lu X, Price IR, Zhao Q, et al. Novel Lysine-Based Thioureas as Mechanism-Based Inhibitors of Sirtuin 2 (SIRT2) with Anticancer Activity in a Colorectal Cancer Murine Model. *Journal of medicinal chemistry*. 2019;62(8):4131-41.
69. Jing H, Hu J, He B, Negron Abril YL, Stupinski J, Weiser K, et al. A SIRT2-Selective Inhibitor Promotes c-Myc Oncoprotein Degradation and Exhibits Broad Anticancer Activity. *Cancer cell*. 2016;29(3):297-310.
70. Seifert T, Malo M, Kokkola T, Engen K, Friden-Saxin M, Wallen EA, et al. Chroman-4-one- and chromone-based sirtuin 2 inhibitors with antiproliferative properties in cancer cells. *Journal of medicinal chemistry*. 2014;57(23):9870-88.
71. Moniot S, Forgione M, Lucidi A, Hailu GS, Nebbioso A, Carafa V, et al. Development of 1,2,4-Oxadiazoles as Potent and Selective Inhibitors of the Human Deacetylase Sirtuin 2: Structure-Activity Relationship, X-ray Crystal Structure, and Anticancer Activity. *Journal of medicinal chemistry*. 2017;60(6):2344-60.
72. Shah AA, Ito A, Nakata A, Yoshida M. Identification of a Selective SIRT2 Inhibitor and Its Anti-breast Cancer Activity. *Biological & pharmaceutical bulletin*. 2016;39(10):1739-42.
73. Yang LL, Wang HL, Zhong L, Yuan C, Liu SY, Yu ZJ, et al. X-ray crystal structure guided discovery of new selective, substrate-mimicking sirtuin 2 inhibitors that exhibit activities against non-small cell lung cancer cells. *European journal of medicinal chemistry*. 2018;155:806-23.

74. Yeong KY, Khaw KY, Takahashi Y, Itoh Y, Murugaiyah V, Suzuki T. Discovery of gamma-mangostin from *Garcinia mangostana* as a potent and selective natural SIRT2 inhibitor. *Bioorganic chemistry*. 2020;94:103403.
75. McCarthy AR, Sachweh MC, Higgins M, Campbell J, Drummond CJ, van Leeuwen IM, et al. Tenovin-D3, a novel small-molecule inhibitor of sirtuin Sirt2, increases p21 (CDKN1A) expression in a p53-independent manner. *Molecular cancer therapeutics*. 2013;12(4):352-60.
76. Kozako T, Mellini P, Ohsugi T, Aikawa A, Uchida YI, Honda SI, et al. Novel small molecule SIRT2 inhibitors induce cell death in leukemic cell lines. *BMC cancer*. 2018;18(1):791.
77. Carafa V, Rotili D, Forgione M, Cuomo F, Serrettiello E, Hailu GS, et al. Sirtuin functions and modulation: from chemistry to the clinic. *Clinical epigenetics*. 2016;8:61.
78. Fiorentino F, Mai A, Rotili D. Emerging Therapeutic Potential of SIRT6 Modulators. *Journal of medicinal chemistry*. 2021;64(14):9732-58.
79. Huang Z, Zhao J, Deng W, Chen Y, Shang J, Song K, et al. Identification of a cellularly active SIRT6 allosteric activator. *Nature chemical biology*. 2018;14(12):1118-26.
80. Shang J, Zhu Z, Chen Y, Song J, Huang Y, Song K, et al. Small-molecule activating SIRT6 elicits therapeutic effects and synergistically promotes anti-tumor activity of vitamin D(3) in colorectal cancer. *Theranostics*. 2020;10(13):5845-64.
81. Shang JL, Ning SB, Chen YY, Chen TX, Zhang J. MDL-800, an allosteric activator of SIRT6, suppresses proliferation and enhances EGFR-TKIs therapy in non-small cell lung cancer. *Acta pharmacologica Sinica*. 2021;42(1):120-31.
82. Jiang X, Yao Z, Wang K, Lou L, Xue K, Chen J, et al. MDL-800, the SIRT6 Activator, Suppresses Inflammation via the NF-kappaB Pathway and Promotes Angiogenesis to Accelerate Cutaneous Wound Healing in Mice. *Oxidative medicine and cellular longevity*. 2022;2022:1619651.
83. Zhang J, Li Y, Liu Q, Huang Y, Li R, Wu T, et al. Sirt6 Alleviated Liver Fibrosis by Deacetylating Conserved Lysine 54 on Smad2 in Hepatic Stellate Cells. *Hepatology*. 2021;73(3):1140-57.
84. Wu X, Liu H, Brooks A, Xu S, Luo J, Steiner R, et al. SIRT6 Mitigates Heart Failure With Preserved Ejection Fraction in Diabetes. *Circulation research*. 2022;131(11):926-43.
85. Chen Y, Chen J, Sun X, Yu J, Qian Z, Wu L, et al. The SIRT6 activator MDL-800 improves genomic stability and pluripotency of old murine-derived iPS cells. *Aging cell*. 2020;19(8):e13185.
86. Jin J, Li W, Wang T, Park BH, Park SK, Kang KP. Loss of Proximal Tubular Sirtuin 6 Aggravates Unilateral Ureteral Obstruction-Induced Tubulointerstitial Inflammation and Fibrosis by Regulation of beta-Catenin Acetylation. *Cells*. 2022;11(9).
87. You W, Rotili D, Li TM, Kambach C, Meleshin M, Schutkowski M, et al. Structural Basis of Sirtuin 6 Activation by Synthetic Small Molecules. *Angewandte Chemie*. 2017;56(4):1007-11.
88. Iachettini S, Trisciuglio D, Rotili D, Lucidi A, Salvati E, Zizza P, et al. Pharmacological activation of SIRT6 triggers lethal autophagy in human cancer cells. *Cell death & disease*. 2018;9(10):996.
89. Chen X, Sun W, Huang S, Zhang H, Lin G, Li H, et al. Discovery of Potent Small-Molecule SIRT6 Activators: Structure-Activity Relationship and Anti-Pancreatic Ductal Adenocarcinoma Activity. *Journal of medicinal chemistry*. 2020;63(18):10474-95.
90. Del Rio A, Barbosa AJ, Caporuscio F, Mangiatordi GF. CoCoCo: a free suite of multiconformational chemical databases for high-throughput virtual screening purposes. *Molecular bioSystems*. 2010;6(11):2122-8.

91. Pan PW, Feldman JL, Devries MK, Dong A, Edwards AM, Denu JM. Structure and biochemical functions of SIRT6. *The Journal of biological chemistry*. 2011;286(16):14575-87.
92. Sociali G, Galeno L, Parenti MD, Grozio A, Bauer I, Passalacqua M, et al. Quinazolinone SIRT6 inhibitors sensitize cancer cells to chemotherapeutics. *European journal of medicinal chemistry*. 2015;102:530-9.
93. Damonte P, Sociali G, Parenti MD, Soncini D, Bauer I, Boero S, et al. SIRT6 inhibitors with salicylate-like structure show immunosuppressive and chemosensitizing effects. *Bioorganic & medicinal chemistry*. 2017;25(20):5849-58.
94. Ferrara G, Benzi A, Sturla L, Marubbi D, Frumento D, Spinelli S, et al. Sirt6 inhibition delays the onset of experimental autoimmune encephalomyelitis by reducing dendritic cell migration. *Journal of neuroinflammation*. 2020;17(1):228.
95. Mishra S, Cosentino C, Tamta AK, Khan D, Srinivasan S, Ravi V, et al. Sirtuin 6 inhibition protects against glucocorticoid-induced skeletal muscle atrophy by regulating IGF/PI3K/AKT signaling. *Nature communications*. 2022;13(1):5415.
96. Sociali G, Magnone M, Ravera S, Damonte P, Vigliarolo T, Von Holtey M, et al. Pharmacological Sirt6 inhibition improves glucose tolerance in a type 2 diabetes mouse model. *FASEB journal : official publication of the Federation of American Societies for Experimental Biology*. 2017;31(7):3138-49.
97. Cea M, Cagnetta A, Adamia S, Acharya C, Tai YT, Fulciniti M, et al. Evidence for a role of the histone deacetylase SIRT6 in DNA damage response of multiple myeloma cells. *Blood*. 2016;127(9):1138-50.
98. Yang J, Li Y, Zhang Y, Fang X, Chen N, Zhou X, et al. Sirt6 promotes tumorigenesis and drug resistance of diffuse large B-cell lymphoma by mediating PI3K/Akt signaling. *Journal of experimental & clinical cancer research : CR*. 2020;39(1):142.
99. Liu Y, Xie QR, Wang B, Shao J, Zhang T, Liu T, et al. Inhibition of SIRT6 in prostate cancer reduces cell viability and increases sensitivity to chemotherapeutics. *Protein & cell*. 2013;4(9):702-10.
100. Yu W, MacKerell AD, Jr. Computer-Aided Drug Design Methods. *Methods in molecular biology*. 2017;1520:85-106.
101. Kore PP, Mutha MM, Antre RV, Oswal RJ, Kshirsagar SS. Computer-aided drug design: an innovative tool for modeling. 2012.
102. Rahnasto-Rilla M, Lahtela-Kakkonen M, Moaddel R. Sirtuin 6 (SIRT6) Activity Assays. *Methods in molecular biology*. 2016;1436:259-69.
103. Lambeth DO, Muhonen WW. High-performance liquid chromatography-based assays of enzyme activities. *Journal of chromatography B, Biomedical applications*. 1994;656(1):143-57.
104. Hong JY, Zhang X, Lin H. HPLC-Based Enzyme Assays for Sirtuins. *Methods in molecular biology*. 2018;1813:225-34.
105. Feldman JL, Dittenhafer-Reed KE, Kudo N, Thelen JN, Ito A, Yoshida M, et al. Kinetic and Structural Basis for Acyl-Group Selectivity and NAD(+) Dependence in Sirtuin-Catalyzed Deacylation. *Biochemistry*. 2015;54(19):3037-50.
106. Teng YB, Jing H, Aramsangtienchai P, He B, Khan S, Hu J, et al. Efficient demyristoylase activity of SIRT2 revealed by kinetic and structural studies. *Scientific reports*. 2015;5:8529.
107. Pacholec M, Bleasdale JE, Chrunyk B, Cunningham D, Flynn D, Garofalo RS, et al. SRT1720, SRT2183, SRT1460, and resveratrol are not direct activators of SIRT1. *The Journal of biological chemistry*. 2010;285(11):8340-51.
108. Eckert RL, Rorke EA. Molecular biology of keratinocyte differentiation. *Environmental health perspectives*. 1989;80:109-16.
109. Moll R, Divo M, Langbein L. The human keratins: biology and pathology. *Histochemistry and cell biology*. 2008;129(6):705-33.

110. Candi E, Schmidt R, Melino G. The cornified envelope: a model of cell death in the skin. *Nature reviews Molecular cell biology*. 2005;6(4):328-40.
111. Marshall D, Hardman MJ, Nield KM, Byrne C. Differentially expressed late constituents of the epidermal cornified envelope. *Proceedings of the National Academy of Sciences of the United States of America*. 2001;98(23):13031-6.
112. Sandilands A, Sutherland C, Irvine AD, McLean WH. Filaggrin in the frontline: role in skin barrier function and disease. *Journal of cell science*. 2009;122(Pt 9):1285-94.
113. Eckhart L, Lippens S, Tschachler E, Declercq W. Cell death by cornification. *Biochimica et biophysica acta*. 2013;1833(12):3471-80.
114. Bahri OA, Naldaiz-Gastesi N, Kennedy DC, Wheatley AM, Izeta A, McCullagh KJA. The panniculus carnosus muscle: A novel model of striated muscle regeneration that exhibits sex differences in the mdx mouse. *Scientific reports*. 2019;9(1):15964.
115. Waldman A, Schmults C. Cutaneous Squamous Cell Carcinoma. *Hematology/oncology clinics of North America*. 2019;33(1):1-12.
116. Lefort K, Brooks Y, Ostano P, Cario-Andre M, Calpini V, Guinea-Viniegra J, et al. A miR-34a-SIRT6 axis in the squamous cell differentiation network. *The EMBO journal*. 2013;32(16):2248-63.
117. Krutmann J, Bouloc A, Sore G, Bernard BA, Passeron T. The skin aging exposome. *Journal of dermatological science*. 2017;85(3):152-61.
118. Gordon R. Skin cancer: an overview of epidemiology and risk factors. *Seminars in oncology nursing*. 2013;29(3):160-9.
119. Wenande E, Togsverd-Bo K, Hastrup A, Lei U, Philipsen PA, Haedersdal M. Skin cancer development is strongly associated with actinic keratosis in solid organ transplant recipients: a Danish cohort study. *Dermatology*. 2023.
120. Stratigos AJ, Garbe C, Dessinioti C, Lebbe C, Bataille V, Bastholt L, et al. European interdisciplinary guideline on invasive squamous cell carcinoma of the skin: Part 2. Treatment. *European journal of cancer*. 2020;128:83-102.
121. Ou-Yang Y, Zheng Y, Mills KE. Photodynamic therapy for skin carcinomas: A systematic review and meta-analysis. *Frontiers in medicine*. 2023;10:1089361.
122. Mirali S, Tang E, Drucker AM, Turchin I, Gooderham M, Levell N, et al. Follow-up of Patients With Keratinocyte Carcinoma: A Systematic Review of Clinical Practice Guidelines. *JAMA dermatology*. 2023;159(1):87-94.
123. Nagarajan P, Asgari MM, Green AC, Guhan SM, Arron ST, Proby CM, et al. Keratinocyte Carcinomas: Current Concepts and Future Research Priorities. *Clinical cancer research : an official journal of the American Association for Cancer Research*. 2019;25(8):2379-91.
124. Ryu TH, Kye H, Choi JE, Ahn HH, Kye YC, Seo SH. Features Causing Confusion between Basal Cell Carcinoma and Squamous Cell Carcinoma in Clinical Diagnosis. *Annals of dermatology*. 2018;30(1):64-70.
125. Iyer PV, Leong AS. Poorly differentiated squamous cell carcinomas of the skin can express vimentin. *Journal of cutaneous pathology*. 1992;19(1):34-9.
126. Compton LA, Murphy GF, Lian CG. Diagnostic Immunohistochemistry in Cutaneous Neoplasia: An Update. *Dermatopathology*. 2015;2(1):15-42.
127. Santos M, Paramio JM, Bravo A, Ramirez A, Jorcano JL. The expression of keratin k10 in the basal layer of the epidermis inhibits cell proliferation and prevents skin tumorigenesis. *The Journal of biological chemistry*. 2002;277(21):19122-30.
128. Lefort K, Dotto GP. Notch signaling in the integrated control of keratinocyte growth/differentiation and tumor suppression. *Seminars in cancer biology*. 2004;14(5):374-86.

129. Yilmaz M, Christofori G. EMT, the cytoskeleton, and cancer cell invasion. *Cancer metastasis reviews*. 2009;28(1-2):15-33.
130. Riihila P, Nissinen L, Kahari VM. Matrix metalloproteinases in keratinocyte carcinomas. *Experimental dermatology*. 2021;30(1):50-61.
131. Pogorzelska-Dyrbus J, Szepietowski JC. Adhesion Molecules in Non-melanoma Skin Cancers: A Comprehensive Review. *In vivo*. 2021;35(3):1327-36.
132. Kuburich NA, den Hollander P, Pietz JT, Mani SA. Vimentin and cytokeratin: Good alone, bad together. *Seminars in cancer biology*. 2022;86(Pt 3):816-26.
133. Jolly MK, Ware KE, Gilja S, Somarelli JA, Levine H. EMT and MET: necessary or permissive for metastasis? *Molecular oncology*. 2017;11(7):755-69.
134. Brabletz T, Jung A, Spaderna S, Hlubek F, Kirchner T. Opinion: migrating cancer stem cells - an integrated concept of malignant tumour progression. *Nature reviews Cancer*. 2005;5(9):744-9.
135. Hanahan D, Weinberg RA. The hallmarks of cancer. *Cell*. 2000;100(1):57-70.
136. Leedham SJ, Wright NA. Expansion of a mutated clone: from stem cell to tumour. *Journal of clinical pathology*. 2008;61(2):164-71.
137. Pitot HC, Dragan YP. Facts and theories concerning the mechanisms of carcinogenesis. *FASEB journal : official publication of the Federation of American Societies for Experimental Biology*. 1991;5(9):2280-6.
138. Klein EA. Can prostate cancer be prevented? *Nature clinical practice Urology*. 2005;2(1):24-31.
139. Bornstein S, Hoot K, Han GW, Lu SL, Wang XJ. Distinct roles of individual Smads in skin carcinogenesis. *Molecular carcinogenesis*. 2007;46(8):660-4.
140. Zhang J, Bowden GT. Targeting Bcl-X(L) for prevention and therapy of skin cancer. *Molecular carcinogenesis*. 2007;46(8):665-70.
141. Kim DJ, Chan KS, Sano S, Digiovanni J. Signal transducer and activator of transcription 3 (Stat3) in epithelial carcinogenesis. *Molecular carcinogenesis*. 2007;46(8):725-31.
142. Yuspa SH. The pathogenesis of squamous cell cancer: lessons learned from studies of skin carcinogenesis--thirty-third G. H. A. Clowes Memorial Award Lecture. *Cancer research*. 1994;54(5):1178-89.
143. Verma AK, Wheeler DL, Aziz MH, Manoharan H. Protein kinase Cepsilon and development of squamous cell carcinoma, the nonmelanoma human skin cancer. *Molecular carcinogenesis*. 2006;45(6):381-8.
144. Kemp CJ. Multistep skin cancer in mice as a model to study the evolution of cancer cells. *Seminars in cancer biology*. 2005;15(6):460-73.
145. Hennings H, Glick AB, Lowry DT, Krsmanovic LS, Sly LM, Yuspa SH. FVB/N mice: an inbred strain sensitive to the chemical induction of squamous cell carcinomas in the skin. *Carcinogenesis*. 1993;14(11):2353-8.
146. DiGiovanni J, Slaga TJ, Boutwell RK. Comparison of the tumor-initiating activity of 7,12-dimethylbenz[a]anthracene and benzo[a]pyrene in female SENCAR and CS-1 mice. *Carcinogenesis*. 1980;1(5):381-9.
147. Aldaz CM, Conti CJ, Larcher F, Trono D, Roop DR, Chesner J, et al. Sequential development of aneuploidy, keratin modifications, and gamma-glutamyltransferase expression in mouse skin papillomas. *Cancer research*. 1988;48(11):3253-7.
148. Gimenez-Conti I, Aldaz CM, Bianchi AB, Roop DR, Slaga TJ, Conti CJ. Early expression of type I K13 keratin in the progression of mouse skin papillomas. *Carcinogenesis*. 1990;11(11):1995-9.
149. Nischt R, Roop DR, Mehrel T, Yuspa SH, Rentrop M, Winter H, et al. Aberrant expression during two-stage mouse skin carcinogenesis of a type I 47-kDa keratin, K13,

normally associated with terminal differentiation of internal stratified epithelia. *Molecular carcinogenesis*. 1988;1(2):96-108.

150. Roop DR, Krieg TM, Mehrel T, Cheng CK, Yuspa SH. Transcriptional control of high molecular weight keratin gene expression in multistage mouse skin carcinogenesis. *Cancer research*. 1988;48(11):3245-52.

151. Diaz-Guerra M, Haddow S, Bauluz C, Jorcano JL, Cano A, Balmain A, et al. Expression of simple epithelial cytokeratins in mouse epidermal keratinocytes harboring Harvey ras gene alterations. *Cancer research*. 1992;52(3):680-7.

152. Navarro P, Gomez M, Pizarro A, Gamallo C, Quintanilla M, Cano A. A role for the E-cadherin cell-cell adhesion molecule during tumor progression of mouse epidermal carcinogenesis. *The Journal of cell biology*. 1991;115(2):517-33.

153. Kundu JK, Shin YK, Surh YJ. Resveratrol modulates phorbol ester-induced pro-inflammatory signal transduction pathways in mouse skin in vivo: NF-kappaB and AP-1 as prime targets. *Biochemical pharmacology*. 2006;72(11):1506-15.

154. DiGiovanni J. Modification of multistage skin carcinogenesis in mice. *Progress in experimental tumor research*. 1991;33:192-229.

155. Benjamin CL, Ananthaswamy HN. p53 and the pathogenesis of skin cancer. *Toxicology and applied pharmacology*. 2007;224(3):241-8.

156. Hennings H, Spangler EF, Shores R, Mitchell P, Devor D, Shamsuddin AK, et al. Malignant conversion and metastasis of mouse skin tumors: a comparison of SENCAR and CD-1 mice. *Environmental health perspectives*. 1986;68:69-74.

157. Abel EL, Angel JM, Kiguchi K, DiGiovanni J. Multi-stage chemical carcinogenesis in mouse skin: fundamentals and applications. *Nature protocols*. 2009;4(9):1350-62.

158. Garcia-Peterson LM, Wilking-Busch MJ, Ndiaye MA, Philippe CGA, Setaluri V, Ahmad N. Sirtuins in Skin and Skin Cancers. *Skin pharmacology and physiology*. 2017;30(4):216-24.

159. Benavente CA, Schnell SA, Jacobson EL. Effects of niacin restriction on sirtuin and PARP responses to photodamage in human skin. *PloS one*. 2012;7(7):e42276.

160. Spallotta F, Cencioni C, Straino S, Nanni S, Rosati J, Artuso S, et al. A nitric oxide-dependent cross-talk between class I and III histone deacetylases accelerates skin repair. *The Journal of biological chemistry*. 2013;288(16):11004-12.

161. Bai XZ, Liu JQ, Yang LL, Fan L, He T, Su LL, et al. Identification of sirtuin 1 as a promising therapeutic target for hypertrophic scars. *British journal of pharmacology*. 2016;173(10):1589-601.

162. Thandavarayan RA, Garikipati VN, Joladarashi D, Suresh Babu S, Jeyabal P, Verma SK, et al. Sirtuin-6 deficiency exacerbates diabetes-induced impairment of wound healing. *Experimental dermatology*. 2015;24(10):773-8.

163. Ming M, Soltani K, Shea CR, Li X, He YY. Dual role of SIRT1 in UVB-induced skin tumorigenesis. *Oncogene*. 2015;34(3):357-63.

164. Ming M, Han W, Zhao B, Sundaresan NR, Deng CX, Gupta MP, et al. SIRT6 promotes COX-2 expression and acts as an oncogene in skin cancer. *Cancer research*. 2014;74(20):5925-33.

165. Dong K, Pelle E, Yarosh DB, Pernodet N. Sirtuin 4 identification in normal human epidermal keratinocytes and its relation to sirtuin 3 and energy metabolism under normal conditions and UVB-induced stress. *Experimental dermatology*. 2012;21(3):231-3.

166. Ouyang W. Distinct roles of IL-22 in human psoriasis and inflammatory bowel disease. *Cytokine & growth factor reviews*. 2010;21(6):435-41.

167. Fan X, Yan K, Meng Q, Sun R, Yang X, Yuan D, et al. Abnormal expression of SIRT6 in psoriasis: Decreased expression of SIRT 1-5 and increased expression of SIRT 6 and 7. *International journal of molecular medicine*. 2019;44(1):157-71.

168. Rasheed H, El-Komy M, Hegazy RA, Gawdat HI, AlOrbani AM, Shaker OG. Expression of sirtuins 1, 6, tumor necrosis factor, and interferon-gamma in psoriatic patients. *International journal of immunopathology and pharmacology*. 2016;29(4):764-8.
169. Li N, Liu Y. LARP7 alleviates psoriasis symptoms in mice by regulating the SIRT1/NF-kappaB signaling pathway. *Allergologia et immunopathologia*. 2023;51(1):140-5.
170. Lee JH, Moon JH, Lee YJ, Park SY. SIRT1, a Class III Histone Deacetylase, Regulates LPS-Induced Inflammation in Human Keratinocytes and Mediates the Anti-Inflammatory Effects of Hinokitiol. *The Journal of investigative dermatology*. 2017;137(6):1257-66.
171. Eid AA, Aly RG, Elkholy SAE, Sorour OA. Influence of narrow-band ultraviolet B therapy on sirtuin 1 expression in lesional skin of patients with chronic plaque psoriasis: Relation to clinical improvement and interferon-gamma expression. *Photodermatology, photoimmunology & photomedicine*. 2022;38(6):555-63.
172. D'Amico F, Costantino G, Salvatorelli L, Ramondetta A, De Pasquale R, Sortino MA, et al. Inverse correlation between the expression of AMPK/SIRT1 and NAMPT in psoriatic skin: A pilot study. *Advances in medical sciences*. 2022;67(2):262-8.
173. Wang Y, Huo J, Zhang D, Hu G, Zhang Y. Chemerin/ChemR23 axis triggers an inflammatory response in keratinocytes through ROS-sirt1-NF-kappaB signaling. *Journal of cellular biochemistry*. 2019;120(4):6459-70.
174. Liu A, Zhang B, Zhao W, Tu Y, Wang Q, Li J. Catalpol ameliorates psoriasis-like phenotypes via SIRT1 mediated suppression of NF-kappaB and MAPKs signaling pathways. *Bioengineered*. 2021;12(1):183-95.
175. Qiong H, Han L, Zhang N, Chen H, Yan K, Zhang Z, et al. Glycyrrhizin improves the pathogenesis of psoriasis partially through IL-17A and the SIRT1-STAT3 axis. *BMC immunology*. 2021;22(1):34.
176. Xu F, Xu J, Xiong X, Deng Y. Salidroside inhibits MAPK, NF-kappaB, and STAT3 pathways in psoriasis-associated oxidative stress via SIRT1 activation. *Redox report : communications in free radical research*. 2019;24(1):70-4.
177. Hao L, Park J, Jang HY, Bae EJ, Park BH. Inhibiting Protein Kinase Activity of Pyruvate Kinase M2 by SIRT2 Deacetylase Attenuates Psoriasis. *The Journal of investigative dermatology*. 2021;141(2):355-63 e6.
178. Yanli M, Yu W, Yuzhen L. Elevated SIRT3 Parkin-dependently activates cell mitophagy to ameliorate TNF-alpha-induced psoriasis-related phenotypes in HaCaT cells through deacetylating FOXO3a for its activation. *Archives of dermatological research*. 2022.
179. Wang C, He D, Shi C. SIRT5 reduces the inflammatory response and barrier dysfunction in IL-17A-induced epidermal keratinocytes. *Allergologia et immunopathologia*. 2023;51(1):30-6.
180. Strub T, Ghiraldini FG, Carcamo S, Li M, Wroblewska A, Singh R, et al. SIRT6 haploinsufficiency induces BRAF(V600E) melanoma cell resistance to MAPK inhibitors via IGF signalling. *Nature communications*. 2018;9(1):3440.
181. Su S, Ndiaye M, Singh CK, Ahmad N. Mitochondrial Sirtuins in Skin and Skin Cancers. *Photochemistry and photobiology*. 2020;96(5):973-80.
182. Temel M, Koc MN, Ulutas S, Gogebakan B. The expression levels of the sirtuins in patients with BCC. *Tumour biology : the journal of the International Society for Oncodevelopmental Biology and Medicine*. 2016;37(5):6429-35.
183. Garcia-Peterson LM, Ndiaye MA, Singh CK, Chhabra G, Huang W, Ahmad N. SIRT6 histone deacetylase functions as a potential oncogene in human melanoma. *Genes & cancer*. 2017;8(9-10):701-12.
184. Sun R, Guo M, Fan X, Meng Q, Yuan D, Yang X, et al. MicroRNA-148b Inhibits the Malignant Biological Behavior of Melanoma by Reducing Sirtuin 7 Expression Levels. *BioMed research international*. 2020;2020:9568976.

185. Lu RH, Xiao ZQ, Zhou JD, Yin CQ, Chen ZZ, Tang FJ, et al. MiR-199a-5p represses the stemness of cutaneous squamous cell carcinoma stem cells by targeting Sirt1 and CD44/ICD cleavage signaling. *Cell cycle*. 2020;19(1):1-14.
186. Liu T, Jiang F, Yu LY, Wu YY. Lidocaine represses proliferation and cisplatin resistance in cutaneous squamous cell carcinoma via miR-30c/SIRT1 regulation. *Bioengineered*. 2022;13(3):6359-70.
187. Wang SH, Zhou JD, He QY, Yin ZQ, Cao K, Luo CQ. MiR-199a inhibits the ability of proliferation and migration by regulating CD44-Ezrin signaling in cutaneous squamous cell carcinoma cells. *International journal of clinical and experimental pathology*. 2014;7(10):7131-41.
188. Senbanjo LT, Chellaiah MA. CD44: A Multifunctional Cell Surface Adhesion Receptor Is a Regulator of Progression and Metastasis of Cancer Cells. *Frontiers in cell and developmental biology*. 2017;5:18.
189. Okamoto I, Kawano Y, Murakami D, Sasayama T, Araki N, Miki T, et al. Proteolytic release of CD44 intracellular domain and its role in the CD44 signaling pathway. *The Journal of cell biology*. 2001;155(5):755-62.
190. Tysnes BB. Tumor-initiating and -propagating cells: cells that we would like to identify and control. *Neoplasia*. 2010;12(7):506-15.
191. Ming M, Qiang L, Zhao B, He YY. Mammalian SIRT2 inhibits keratin 19 expression and is a tumor suppressor in skin. *Experimental dermatology*. 2014;23(3):207-9.
192. Kugel S, Mostoslavsky R. Chromatin and beyond: the multitasking roles for SIRT6. *Trends in biochemical sciences*. 2014;39(2):72-81.
193. Dominy JE, Jr., Lee Y, Jedrychowski MP, Chim H, Jurczak MJ, Camporez JP, et al. The deacetylase Sirt6 activates the acetyltransferase GCN5 and suppresses hepatic gluconeogenesis. *Molecular cell*. 2012;48(6):900-13.
194. Jiang H, Khan S, Wang Y, Charron G, He B, Sebastian C, et al. SIRT6 regulates TNF- α secretion through hydrolysis of long-chain fatty acyl lysine. *Nature*. 2013;496(7443):110-3.
195. Liszt G, Ford E, Kurtev M, Guarente L. Mouse Sir2 homolog SIRT6 is a nuclear ADP-ribosyltransferase. *The Journal of biological chemistry*. 2005;280(22):21313-20.
196. Lombard DB, Schwer B, Alt FW, Mostoslavsky R. SIRT6 in DNA repair, metabolism and ageing. *Journal of internal medicine*. 2008;263(2):128-41.
197. Sebastian C, Satterstrom FK, Haigis MC, Mostoslavsky R. From sirtuin biology to human diseases: an update. *The Journal of biological chemistry*. 2012;287(51):42444-52.
198. Tennen RI, Chua KF. Chromatin regulation and genome maintenance by mammalian SIRT6. *Trends in biochemical sciences*. 2011;36(1):39-46.
199. Toiber D, Erdel F, Bouazoune K, Silberman DM, Zhong L, Mulligan P, et al. SIRT6 recruits SNF2H to DNA break sites, preventing genomic instability through chromatin remodeling. *Molecular cell*. 2013;51(4):454-68.
200. McCord RA, Michishita E, Hong T, Berber E, Boxer LD, Kusumoto R, et al. SIRT6 stabilizes DNA-dependent protein kinase at chromatin for DNA double-strand break repair. *Aging*. 2009;1(1):109-21.
201. Gao Y, Tan J, Jin J, Ma H, Chen X, Leger B, et al. SIRT6 facilitates directional telomere movement upon oxidative damage. *Scientific reports*. 2018;8(1):5407.
202. Michishita E, McCord RA, Berber E, Kioi M, Padilla-Nash H, Damian M, et al. SIRT6 is a histone H3 lysine 9 deacetylase that modulates telomeric chromatin. *Nature*. 2008;452(7186):492-6.
203. Michishita E, McCord RA, Boxer LD, Barber MF, Hong T, Gozani O, et al. Cell cycle-dependent deacetylation of telomeric histone H3 lysine K56 by human SIRT6. *Cell cycle*. 2009;8(16):2664-6.

204. Kouzarides T. Chromatin modifications and their function. *Cell*. 2007;128(4):693-705.
205. Kawahara TL, Michishita E, Adler AS, Damian M, Berber E, Lin M, et al. SIRT6 links histone H3 lysine 9 deacetylation to NF-kappaB-dependent gene expression and organismal life span. *Cell*. 2009;136(1):62-74.
206. Sundareshan NR, Vasudevan P, Zhong L, Kim G, Samant S, Parekh V, et al. The sirtuin SIRT6 blocks IGF-Akt signaling and development of cardiac hypertrophy by targeting c-Jun. *Nature medicine*. 2012;18(11):1643-50.
207. Elhanati S, Kanfi Y, Varvak A, Roichman A, Carmel-Gross I, Barth S, et al. Multiple regulatory layers of SREBP1/2 by SIRT6. *Cell reports*. 2013;4(5):905-12.
208. van Riggelen J, Yetil A, Felsher DW. MYC as a regulator of ribosome biogenesis and protein synthesis. *Nature reviews Cancer*. 2010;10(4):301-9.
209. Choi JE, Sebastian C, Ferrer CM, Lewis CA, Sade-Feldman M, LaSalle T, et al. A unique subset of glycolytic tumour-propagating cells drives squamous cell carcinoma. *Nature metabolism*. 2021;3(2):182-95.
210. Smith ML, Fornace AJ, Jr. p53-mediated protective responses to UV irradiation. *Proceedings of the National Academy of Sciences of the United States of America*. 1997;94(23):12255-7.
211. Dotto GP, Karine L. miR-34a/SIRT6 in squamous differentiation and cancer. *Cell cycle*. 2014;13(7):1055-6.
212. Chun KS, Akunda JK, Langenbach R. Cyclooxygenase-2 inhibits UVB-induced apoptosis in mouse skin by activating the prostaglandin E2 receptors, EP2 and EP4. *Cancer research*. 2007;67(5):2015-21.
213. Fischer SM, Pavone A, Mikulec C, Langenbach R, Rundhaug JE. Cyclooxygenase-2 expression is critical for chronic UV-induced murine skin carcinogenesis. *Molecular carcinogenesis*. 2007;46(5):363-71.
214. Yamaguchi K, Mitsui T, Aso Y, Sugibayashi K. Structure-permeability relationship analysis of the permeation barrier properties of the stratum corneum and viable epidermis/dermis of rat skin. *Journal of pharmaceutical sciences*. 2008;97(10):4391-403.
215. Pham QD, Biatry B, Gregoire S, Topgaard D, Sparr E. Solubility of Foreign Molecules in Stratum Corneum Brick and Mortar Structure. *Langmuir : the ACS journal of surfaces and colloids*. 2023.
216. Prausnitz MR, Langer R. Transdermal drug delivery. *Nature biotechnology*. 2008;26(11):1261-8.
217. Walters KA. *Dermatological and transdermal formulations*: CRC Press; 2002.
218. Naik A, Kalia YN, Guy RH. Transdermal drug delivery: overcoming the skin's barrier function. *Pharmaceutical science & technology today*. 2000;3(9):318-26.
219. Park D, Park H, Seo J, Lee S. Sonophoresis in transdermal drug delivery. *Ultrasonics*. 2014;54(1):56-65.
220. Hmingthansanga V, Singh N, Banerjee S, Manickam S, Velayutham R, Natesan S. Improved Topical Drug Delivery: Role of Permeation Enhancers and Advanced Approaches. *Pharmaceutics*. 2022;14(12).
221. Gorukanti SR, Li L, Kim KH. Transdermal delivery of antiparkinsonian agent, benzotropine. I. Effect of vehicles on skin permeation. *International journal of pharmaceutics*. 1999;192(2):159-72.
222. Wallace SM, Barnett G. Pharmacokinetic analysis of percutaneous absorption: evidence of parallel penetration pathways for methotrexate. *Journal of pharmacokinetics and biopharmaceutics*. 1978;6(4):315-25.
223. Kuo P-C, Liu J-C, Chang S-F, Chien YW. In-vitro transdermal permeation of oxycodone:(I) effect of PH, delipidization and skin stripping. *Drug Development and Industrial Pharmacy*. 1989;15(8):1199-215.

224. Kushla GP, Zatz JL. Influence of pH on lidocaine penetration through human and hairless mouse skin in vitro. *International journal of pharmaceutics*. 1991;71(3):167-73.
225. Ahmed EM. Hydrogel: Preparation, characterization, and applications: A review. *Journal of advanced research*. 2015;6(2):105-21.
226. Cascone S, Lamberti G. Hydrogel-based commercial products for biomedical applications: A review. *International journal of pharmaceutics*. 2020;573:118803.
227. Egito EST, Amaral-Machado L, Alencar EN, Oliveira AG. Microemulsion systems: from the design and architecture to the building of a new delivery system for multiple-route drug delivery. *Drug delivery and translational research*. 2021;11(5):2108-33.
228. Souto EB, Cano A, Martins-Gomes C, Coutinho TE, Zielinska A, Silva AM. Microemulsions and Nanoemulsions in Skin Drug Delivery. *Bioengineering*. 2022;9(4).
229. Sintov AC. Transdermal delivery of curcumin via microemulsion. *International journal of pharmaceutics*. 2015;481(1-2):97-103.
230. Ali A, Mekhloufi G, Huang N, Agnely F. beta-lactoglobulin stabilized nanemulsions--Formulation and process factors affecting droplet size and nanoemulsion stability. *International journal of pharmaceutics*. 2016;500(1-2):291-304.
231. Burguera JL, Burguera M. Analytical applications of emulsions and microemulsions. *Talanta*. 2012;96:11-20.
232. Ryu KA, Park PJ, Kim SB, Bin BH, Jang DJ, Kim ST. Topical Delivery of Coenzyme Q10-Loaded Microemulsion for Skin Regeneration. *Pharmaceutics*. 2020;12(4).
233. Das S, Lee SH, Chia VD, Chow PS, Macbeath C, Liu Y, et al. Development of microemulsion based topical ivermectin formulations: Pre-formulation and formulation studies. *Colloids and surfaces B, Biointerfaces*. 2020;189:110823.
234. Kreilgaard M, Pedersen EJ, Jaroszewski JW. NMR characterisation and transdermal drug delivery potential of microemulsion systems. *Journal of controlled release : official journal of the Controlled Release Society*. 2000;69(3):421-33.
235. Peira E, Scolari P, Gasco MR. Transdermal permeation of apomorphine through hairless mouse skin from microemulsions. *International journal of pharmaceutics*. 2001;226(1-2):47-51.
236. Mei Z, Chen H, Weng T, Yang Y, Yang X. Solid lipid nanoparticle and microemulsion for topical delivery of triptolide. *European journal of pharmaceutics and biopharmaceutics : official journal of Arbeitsgemeinschaft fur Pharmazeutische Verfahrenstechnik eV*. 2003;56(2):189-96.
237. Alvarez-Figueroa MJ, Blanco-Mendez J. Transdermal delivery of methotrexate: iontophoretic delivery from hydrogels and passive delivery from microemulsions. *International journal of pharmaceutics*. 2001;215(1-2):57-65.
238. Dalmora ME, Dalmora SL, Oliveira AG. Inclusion complex of piroxicam with beta-cyclodextrin and incorporation in cationic microemulsion. In vitro drug release and in vivo topical anti-inflammatory effect. *International journal of pharmaceutics*. 2001;222(1):45-55.
239. Peltola S, Saarinen-Savolainen P, Kiesvaara J, Suhonen TM, Urtti A. Microemulsions for topical delivery of estradiol. *International journal of pharmaceutics*. 2003;254(2):99-107.
240. Rhee YS, Choi JG, Park ES, Chi SC. Transdermal delivery of ketoprofen using microemulsions. *International journal of pharmaceutics*. 2001;228(1-2):161-70.
241. Zhao X, Liu JP, Zhang X, Li Y. Enhancement of transdermal delivery of theophylline using microemulsion vehicle. *International journal of pharmaceutics*. 2006;327(1-2):58-64.
242. Chen H, Chang X, Weng T, Zhao X, Gao Z, Yang Y, et al. A study of microemulsion systems for transdermal delivery of triptolide. *Journal of controlled release : official journal of the Controlled Release Society*. 2004;98(3):427-36.

243. Osborne DW, Ward AJ, O'Neill KJ. Microemulsions as topical drug delivery vehicles: in-vitro transdermal studies of a model hydrophilic drug. *The Journal of pharmacy and pharmacology*. 1991;43(6):450-4.
244. Trotta M, Pattarino F, Gasco MR. Influence of counter ions on the skin permeation of methotrexate from water--oil microemulsions. *Pharmaceutica acta Helvetiae*. 1996;71(2):135-40.
245. Gupta RR, Jain SK, Varshney M. AOT water-in-oil microemulsions as a penetration enhancer in transdermal drug delivery of 5-fluorouracil. *Colloids and surfaces B, Biointerfaces*. 2005;41(1):25-32.
246. Djordjevic L, Primorac M, Stupar M, Krajsnik D. Characterization of caprylocaproyl macroglycerides based microemulsion drug delivery vehicles for an amphiphilic drug. *International journal of pharmaceutics*. 2004;271(1-2):11-9.
247. Gallarate M, Carlotti ME, Trotta M, Bovo S. On the stability of ascorbic acid in emulsified systems for topical and cosmetic use. *International journal of pharmaceutics*. 1999;188(2):233-41.
248. Yuan Y, Li SM, Mo FK, Zhong DF. Investigation of microemulsion system for transdermal delivery of meloxicam. *International journal of pharmaceutics*. 2006;321(1-2):117-23.
249. Escribano E, Calpena AC, Queralt J, Obach R, Domenech J. Assessment of diclofenac permeation with different formulations: anti-inflammatory study of a selected formula. *European journal of pharmaceutical sciences : official journal of the European Federation for Pharmaceutical Sciences*. 2003;19(4):203-10.
250. Paolino D, Ventura CA, Nistico S, Puglisi G, Fresta M. Lecithin microemulsions for the topical administration of ketoprofen: percutaneous adsorption through human skin and in vivo human skin tolerability. *International journal of pharmaceutics*. 2002;244(1-2):21-31.
251. Spiclin P, Gasperlin M, Kmetec V. Stability of ascorbyl palmitate in topical microemulsions. *International journal of pharmaceutics*. 2001;222(2):271-9.
252. Valenta C, Schultz K. Influence of carrageenan on the rheology and skin permeation of microemulsion formulations. *Journal of controlled release : official journal of the Controlled Release Society*. 2004;95(2):257-65.
253. Deng J, Cai W, Jin F. A novel oil-in-water emulsion as a potential adjuvant for influenza vaccine: development, characterization, stability and in vivo evaluation. *International journal of pharmaceutics*. 2014;468(1-2):187-95.
254. Lee J, Lee Y, Kim J, Yoon M, Choi YW. Formulation of microemulsion systems for transdermal delivery of aceclofenac. *Archives of pharmacal research*. 2005;28(9):1097-102.
255. Effendy I, Maibach HI. Surfactants and experimental irritant contact dermatitis. *Contact dermatitis*. 1995;33(4):217-25.
256. Kogan A, Garti N. Microemulsions as transdermal drug delivery vehicles. *Advances in colloid and interface science*. 2006;123-126:369-85.
257. Baby AR, Lacerda AC, Velasco MV, Lopes PS, Kawano Y, Kaneko TM. Evaluation of the interaction of surfactants with stratum corneum model membrane from *Bothrops jararaca* by DSC. *International journal of pharmaceutics*. 2006;317(1):7-9.
258. Shokri J, Nokhodchi A, Dashbolaghi A, Hassan-Zadeh D, Ghafourian T, Barzegar Jalali M. The effect of surfactants on the skin penetration of diazepam. *International journal of pharmaceutics*. 2001;228(1-2):99-107.
259. Vaddi HK, Wang LZ, Ho PC, Chan SY. Effect of some enhancers on the permeation of haloperidol through rat skin in vitro. *International journal of pharmaceutics*. 2001;212(2):247-55.

260. Bu N, Huang L, Cao G, Pang J, Mu R. Stable O/W emulsions and oleogels with amphiphilic konjac glucomannan network: preparation, characterization, and application. *Journal of the science of food and agriculture*. 2022;102(14):6555-65.
261. Mudshinge SR, Deore AB, Patil S, Bhalgat CM. Nanoparticles: Emerging carriers for drug delivery. *Saudi pharmaceutical journal : SPJ : the official publication of the Saudi Pharmaceutical Society*. 2011;19(3):129-41.
262. Rane SS, Anderson BD. What determines drug solubility in lipid vehicles: is it predictable? *Advanced drug delivery reviews*. 2008;60(6):638-56.
263. Sanna V, Pintus G, Roggio AM, Punzoni S, Posadino AM, Arca A, et al. Targeted biocompatible nanoparticles for the delivery of (-)-epigallocatechin 3-gallate to prostate cancer cells. *Journal of medicinal chemistry*. 2011;54(5):1321-32.
264. Siddiqui IA, Adhami VM, Bharali DJ, Hafeez BB, Asim M, Khwaja SI, et al. Introducing nanochemoprevention as a novel approach for cancer control: proof of principle with green tea polyphenol epigallocatechin-3-gallate. *Cancer research*. 2009;69(5):1712-6.
265. Abu-Huwaij R, Al-Assaf SF, Hamed R. Recent exploration of nanoemulsions for drugs and cosmeceuticals delivery. *Journal of cosmetic dermatology*. 2022;21(9):3729-40.
266. Lv X, Liu T, Ma H, Tian Y, Li L, Li Z, et al. Preparation of Essential Oil-Based Microemulsions for Improving the Solubility, pH Stability, Photostability, and Skin Permeation of Quercetin. *AAPS PharmSciTech*. 2017;18(8):3097-104.
267. Gokhale JP, Mahajan HS, Surana SJ. Quercetin loaded nanoemulsion-based gel for rheumatoid arthritis: In vivo and in vitro studies. *Biomedicine & pharmacotherapy = Biomedecine & pharmacotherapie*. 2019;112:108622.
268. Zhu W, Yu A, Wang W, Dong R, Wu J, Zhai G. Formulation design of microemulsion for dermal delivery of penciclovir. *International journal of pharmaceutics*. 2008;360(1-2):184-90.
269. Kreilgaard M. Influence of microemulsions on cutaneous drug delivery. *Advanced drug delivery reviews*. 2002;54 Suppl 1:S77-98.
270. M El Maghraby G. Microemulsions as transdermal drug delivery systems. *Current Nanoscience*. 2012;8(4):504-11.
271. He B, Hu J, Zhang X, Lin H. Thiomyristoyl peptides as cell-permeable Sirt6 inhibitors. *Organic & biomolecular chemistry*. 2014;12(38):7498-502.
272. Sundriyal S, Moniot S, Mahmud Z, Yao S, Di Fruscia P, Reynolds CR, et al. Thienopyrimidinone Based Sirtuin-2 (SIRT2)-Selective Inhibitors Bind in the Ligand Induced Selectivity Pocket. *Journal of medicinal chemistry*. 2017;60(5):1928-45.
273. Rumpf T, Gerhardt S, Einsle O, Jung M. Seeding for sirtuins: microseed matrix seeding to obtain crystals of human Sirt3 and Sirt2 suitable for soaking. *Acta crystallographica Section F, Structural biology communications*. 2015;71(Pt 12):1498-510.
274. Yuan S, Liao G, Zhang M, Zhu Y, Xiao W, Wang K, et al. Multiomics interrogation into HBV (Hepatitis B virus)-host interaction reveals novel coding potential in human genome, and identifies canonical and non-canonical proteins as host restriction factors against HBV. *Cell discovery*. 2021;7(1):105.
275. Miro C, Di Cicco E, Ambrosio R, Mancino G, Di Girolamo D, Cicatiello AG, et al. Thyroid hormone induces progression and invasiveness of squamous cell carcinomas by promoting a ZEB-1/E-cadherin switch. *Nature communications*. 2019;10(1):5410.
276. Eberhardt J, Santos-Martins D, Tillack AF, Forli S. AutoDock Vina 1.2.0: New Docking Methods, Expanded Force Field, and Python Bindings. *Journal of chemical information and modeling*. 2021;61(8):3891-8.
277. Trott O, Olson AJ. AutoDock Vina: improving the speed and accuracy of docking with a new scoring function, efficient optimization, and multithreading. *Journal of computational chemistry*. 2010;31(2):455-61.

278. Sociali G, Liessi N, Grozio A, Caffa I, Parenti MD, Ravera S, et al. Differential modulation of SIRT6 deacetylase and deacylase activities by lysine-based small molecules. *Molecular diversity*. 2020;24(3):655-71.